**Title**
Development and Simulation of Increased Generation on a Secondary Circuit of a Microgrid



**Author**
Reyes, Karina

**Publication Date**
2014

Peer reviewed|Thesis/dissertation

UNIVERSITY OF CALIFORNIA,
IRVINE

# Development and Simulation of Increased Generation on a Secondary Circuit of a Microgrid

THESIS

submitted in partial satisfaction of the requirements
for the degree of

MASTER OF SCIENCE

in Civil and Environmental Engineering

by

Karina Reyes

Thesis Committee:
Professor Scott Samuelsen, Chair
Professor Jack Brouwer
Professor Sunny Jiang

2014

## DEDICATION

I would like to dedicate my thesis to my family for always believing in me and pushing me

## TABLE OF CONTENTS

# LIST OF FIGURES

# LIST OF TABLES

# LIST OF EQUATIONS

# LIST OF ACRONYMS

| | |
|---|---|
| AC | alternating current |
| A | Ampere, amp |
| AIRB | Anteater Instruction & Research Building |
| BESS | Battery Energy Storage System |
| CT | current transformer |
| DER | distributed energy resource |
| DC | direct current |
| DG | distributed generation |
| DRI | demand response inverter |
| ETAP | Electrical transient and analysis program |
| EPS | electric power system |
| EV | electric vehicle |
| kWh | kilowatt-hour |
| kV | Kilovolt |
| kVA | kilovolt-Amperes |
| MW | Megawatt |
| MATLAB | Matrix Laboratory |
| PV | photovoltaic |
| PEV | plug-in electric vehicle |
| PHEV | plug-in hybrid electric vehicle |
| PLS | Permanent load shifting |

| | |
|---|---|
| PMU | Phasor Measurement Unit |
| PPS | Princeton Power Systems |
| SCE | Southern California Edison |
| SQL | Structured Query Language |
| V | Volt |
| WAMS | Wide Area Monitoring Systems |

# ACKNOWLEDGEMENTS

I would like to thank my graduate advisor, Professor Scott Samuelsen for believing in me and allowing me the opportunity to pursue this degree. I would also like to thank Professor Jack Brouwer for accepting me into the lab four years ago. The APEP lab has always been so welcoming and friendly and it has really become a family to me. I also am very thankful for all of my lab mates in ELF as well as the staff there, they became very good friends.

I also want to thank ETAP for helping me with the first steps to creating the model and the countless debugging meetings with Derek Dean and Luyang Sun. I would never have been able to finish my model without the data, reports, and diagrams received from Daryl Coleman of Southern California Edison as well as Matt Gudorf, and so I thank them.

# ABSTRACT OF THE THESIS


Development and Simulation of Increased Distributed Generation on a Secondary Circuit of a Microgrid

By

Karina Reyes

Masters of Science in Civil and Environmental Engineering

University of California, Irvine, 2014

Professor G. Scott Samuelsen, Chair

As fossil fuels are depleted and their environmental impacts remain, other sources of energy must be considered to generate power. Renewable sources, for example, are emerging to play a major role in this regard. In parallel, electric vehicle (EV) charging is evolving as a major load demand. To meet reliability and resiliency goals demanded by the electricity market, interest in microgrids are growing as a distributed energy resource (DER). In this thesis, the effects of intermittent renewable power generation and random EV charging on secondary microgrid circuits are analyzed in the presence of a controllable battery in order to characterize and better understand the dynamics associated with intermittent power production and random load demands in the context of the microgrid paradigm.

For two reasons, a secondary circuit on the University of California, Irvine (UCI) Microgrid serves as the case study. First, the secondary circuit (UC-9) is heavily loaded and an integral component of a highly characterized and metered microgrid. Second, a unique “next-generation” distributed energy resource has been deployed at the end of the circuit that integrates photovoltaic power generation, battery storage, and EV charging.

In order to analyze this system and evaluate the impact of the DER on the secondary circuit, a model was developed to provide a real-time load flow analysis. The research develops a power management system applicable to similarly integrated systems. The model is verified by metered data obtained from a network of high resolution electric meters and estimated load data for the buildings that have unknown demand. An increase in voltage is observed when the amount of photovoltaic power generation is increased. To mitigate this effect, a constant power factor is set. Should the real power change dramatically, the reactive power is changed to mitigate voltage fluctuations.

# 1 INTRODUCTION

In 2010, the United States (US) consumed 13.3 MWH, the second largest energy consumer in the world (Barr 2011). The major sources used for power generation in the United States are fossil fuels (natural gas, petroleum, and coal), nuclear, and renewable energy (Energy in Brief 2013). Most of the energy comes from fossil fuels (82%) with 8% coming from nuclear and 9% from renewable sources (Center for Sustainable Systems 2013).

In order for the percentage of renewable sourced energy to increase, the US electric power system needs to be modernized by implementing a smart grid (i.e., a grid that uses information and communications technology to improve efficiency and produce electricity in a sustainable manner). The evolution to smart technology will require the combined effort of many stakeholders, such as: utilities, policy makers, educational institutions, think tanks, entrepreneurs, and governmental agencies in order to realize the goals that smart grid technology portends.

The University of California, Irvine (UCI) is home to many types of buildings, such as research laboratories, classrooms and lecture halls, faculty and administrative offices, athletic facilities, and on-campus housing. These buildings require an extensive amount of reliable power to meet the goals of the university. The campus electrical point of interconnection with the local utility, Southern California Edison (SCE) occurs at the UCI Substation that is serviced by an incoming 66 kV line from SCE, steps down the voltage to 12 kV, and then feeds 10 high voltage 12 kV circuits. The 12 kV circuits are connected to secondary distribution transformers which reduce the voltage to 120 V or 480 V to support the electrical loads throughout the UCI campus. Most building transformers are connected to a main 12kV circuit through a closed (conducting) switch and a separate 12 kV circuit through an open (non-conducting) switch. This combination of switches allows a building to be moved to a different circuit should a major failure occur on the main power connection. The substation and all outgoing 12 kV cables with associated transformers are owned by UCI, while the incoming 66 kV line belongs to SCE.

UCI generates the majority of its power locally through on-campus generation that consists of a 13MW gas turbine generator, a 6MW steam generator, and 1MW of distributed solar photovoltaic of which 113kW is concentrated photovoltaic (PV). The balance of generation is supplied to the campus from the SCE interconnection and managed though an agreement between UCI and SCE which allows a minimum “inadvertent” export of power.

Microgrids are emerging to meet the growing demand for reliability and resiliency in the electricity market. Similar to the utility grid, microgrids face challenges of the intermittency associated with a high-penetration of renewable power generation (e.g., PV) and randomly occurring loads associated with electric vehicle (EV) charging. Characterizing and understanding the dynamics of these challenges are required in order to establish the smart controls and other distributed energy resources (DER) that will be required for microgrids to remain stable.

At UCI, a unique next-generation DER has been established as part of a U.S. Department of Energy “Irvine Smart Grid Demonstration” project. On the roof of a parking structure, 48kW of PV panels have been deployed. On the first floor of the structure, 20 monitored EV chargers have been installed. Outside but immediately adjacent to the parking structure, a 100kW battery energy storage system (BESS) has been integrated into a combined system. The system has an internal inverter that converts the photovoltaic power from direct current to alternating current. A Princeton Power Systems (PPS) site controller switches the inverter between two control modes: the demand response mode and the distributed generation mode. The modes determine to which control signals the inverter responds while the other modes contain the algorithms for overall system behavior. The demand response mode allows the control of the BESS minimum state of charge. This means that if the battery is at or below this set-point, no further discharge can occur. The distributed generation mode allows the use of PV power without curtailment. The BESS immediately charges the battery using either PV or grid power.

The battery has four different control modes. The first is a demand response event mode that allows the system to operate at a specified power until the battery limit is reached. The second is a peak shaver mode that causes the BESS to charge and discharge in order to bring the power imported from the microgrid to a specified level. In the third mode, a PV smoother algorithm uses the battery system to lower the fluctuation in the PV power output. In the fourth mode, the chargers are powered from the UCI Microgrid for power when energy is not available from the BESS.

In this thesis, the effects of intermittent renewable power generation and random EV charging on secondary microgrid circuits are analyzed in the presence of a controllable battery in order to characterize and better understand the dynamics associated with intermittent power production and random load demands in the context of the microgrid paradigm.

## 1.1 GOAL

The goal of this research is to characterize an integrated solar PV, battery energy storage, and electric vehicle charging system, and assess the impact of the system on the secondary microgrid circuits.

## 1.2 OBJECTIVES

In order to meet the goal of the research, four objectives are required:

**Objective 1:** Develop a steady-state model to simulate the addition of distributed generation from the Car Shade project.

**Objective 2:** Obtain EV charging data, PV generation, BESS energy data, and grid power from an experimental platform as inputs into the model.

**Objective 3:** Verify the model using data comparisons as well as a state load estimator.

**Objective 4:** Create scenarios to establish the maximum and minimum amounts of distributed generation that the current circuits can manage.

# 2 BACKGROUND

## 2.1 ELECTRIC POWER

The first power system consisted of a generator connected to an appropriately matched load. In the early 1990s, these isolated systems started to interconnect with each other ultimately becoming an expansive synchronous grid. This led to the following three separate alternating systems in the United States:  the Western United States, Texas, and the Eastern United States.

### 2.1.1 Circuit Fundamentals

An electrical circuit is a network that produces a flow of current driven by a voltage difference. A closed loop circuit provides a return path for the current.  A breaker in the circuit can open and thereby cause the current flow to cease.

#### 2.1.1.1 Voltage Drop

In a circuit, the difference in voltages across the wire is referred to as the voltage drop. Equation 1 represents Ohm's Law and it shows how the voltage is proportional to the current multiplied by the resistance. The voltage drop is important for this research because the high demand and associated current results in a high voltage drop.

$$V = IR$$

Equation 1: Ohm's Law (Meier 2006)

The power dissipated of a circuit can be calculated using Equation 2. P represents the power, I represents the current and V the voltage. The real power is a result of resistive components. This formula comes into use when referring to transmission voltage and resistive losses.

$$Real\ Power = P = IV = I^2R$$

Equation 2 : Power Formula (Meier 2006)

In purely resistive circuits, P=S as there is no reactive component. The reactive components, in addition to a time dependent voltage or current, necessitate the use of the apparent power equation (Equation 3) where the apparent power, a combination of the real and reactive power, is described as S. The phase angle is the angle from unity with the sign indicating if it is leading or lagging from the reference value. The sign does not appear for a power factor since cos(x)=cos(-x). The cosine of this phase angle is known as the power factor which can be obtained by using Equation 4Equation 5. The lower the power factor, the lower the operating efficiency. The reactive power, shown in Equation 5 and known as Q, is obtained by using the average current and voltage along with the power factor. A power factor of zero means that there is no reactive power. The reactive power is a result of capacitive and inductive components. The reactive power is important in order to ensure that the apparent power output from a system is enough to supply the load (Meier 2006).

$$S = I * V$$

**Equation 3: Apparent Power (Meier 2006)**

$$Power\ factor = \frac{Real\ Power}{Apparent\ Power}$$

**Equation 4: Power Factor (Meier 2006)**

$$Q = Irms * Vrms * sin\emptyset$$

Equation 5: Reactive Power (Meier 2006)

An increasing power factor is associated with minimizing losses and maximizing the capacity of the equipment. The line losses refer to real power losses and are internal impedances inherent to the materials. Reactive losses refer to the difference between the consumed loads and the reactive power supplied by the generators.

## 2.2 GRID STRUCTURE

A power system is divided into three electrical subsystems (Figure 1): a generation subsystem, a transmission subsystem, and a distribution subsystem. This division depends on the voltage levels (Meier 2006). Transmission is the transfer of electrical energy to a high-voltage substation. At this point, the distribution subsystem conveys the electricity to customers. The design of the system takes into account economic factors and network safety. Certain components such as power lines, cables, switches and transformers are used to account for these factors. In order to operate at different voltages, transformers are used to step up or step down the voltage.

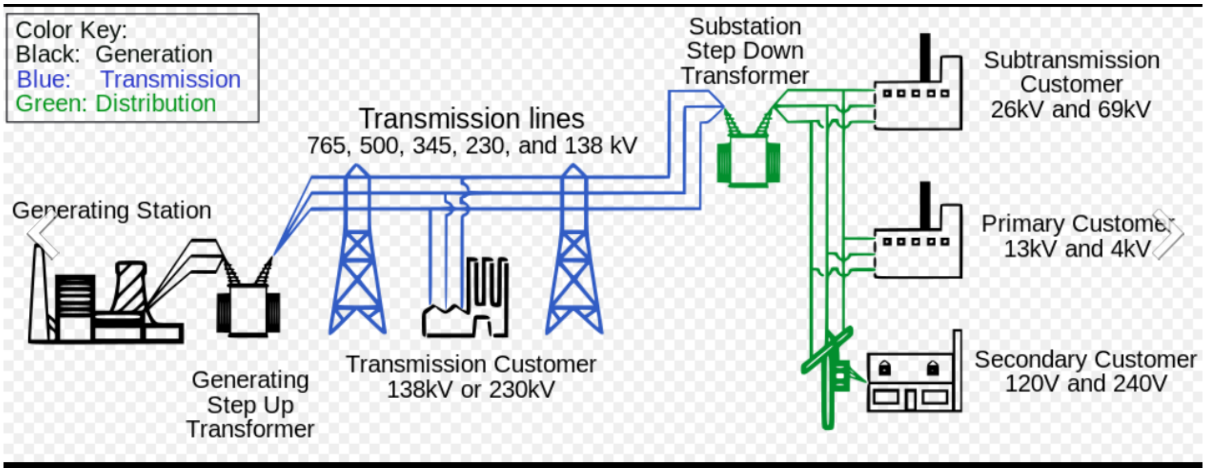


Figure 1: Electric Grid ( U.S.-Canada Power System Outage Task Force 2014)

A transmission system covers long distances at voltages that typically range between 60 and 500kV. The transmission system is broken down into a sub transmission which operates on average of about 100kV. The distribution system operates typically at 66kV with circuits local to the load operating at 12kV to 480V.

The transmission system and distribution system are the backbone of an integrated power system. Transmission and distribution lines must tolerate dynamic changes in load and current flow in both directions. There are different strategies involved such as dynamic optimal power flow, real-time stability assessment, reliability and market simulation. The real-time information is gathered most of the time from Phasor Measurement Unit (PMU), state estimator sensors, and different communication technologies (J. Mamoh 2012).

### 2.2.1 Distribution System

A distribution system is broken down into primary and secondary distribution systems. The secondary distribution systems connect to small commercial customers and households at voltages in the 120V range. The distribution system begins at the substation where it receives power from the transmission lines and provides the power through distribution feeders.

#### 2.2.1.1 Primary distribution system

A typical primary distribution system consists of feeders that come from the substation and supplies power to the secondary distribution systems. The feeders send the power from the substation to the loads in one direction. These systems have higher voltage ranges which allows for less voltage drop, decreased losses, and operation over long distances. Usually in residential neighborhoods the system is radial and in more populated areas it is a looped system. The differences between a loop system as well as other types are described below.

##### 2.2.1.1.1 Radial distribution system

The radial distribution system is typically the least expensive to build. A major disadvantage is loss of power over the entire circuit in the event of a “fault (i.e., short-circuit).

##### 2.2.1.1.2 Loop System

This system is tied to two power sources and it loops through the service area and returns to its original point. Placing switches in the system allows for the utility to supply power in either direction. If one power source fails, the switches on the circuit can be configured to provide power from the second source. It has more continuous service than the radial system and, in the event of a power failure, the utility isolates the fault and switches to a different power source until repairs are completed. The loop system is more expensive that the radial system due to the additional switches and conductors.

##### 2.2.1.1.3 Network System

A network system is an interlocking loop system. The system uses various power sources which increase reliability as well as price. If one of the sources fails, the power can flow from one of the other sources. A network system is typically found in higher loaded areas such as a metropolitan area. A network does not have a downstream or upstream direction, so any point in the system can be either receiving or giving power from either side (Sivanagaraju 2008).

#### 2.2.1.1.4 Power Island

A power island is a section of circuits that are separate from the larger system. A distributed generator is located on the island in order to provide power independent from the electric utility.  In the event of a utility grid outage, a power island can island and remain in operation. (Sivanagaraju 2008).

### 2.2.1.2 Secondary distribution system

The secondary distribution system branches out from the main feeder. It has a lower voltage than the primary distribution system with a range that typically varies from 120/208 V or 277/480 V for three phase systems. For a single phase system, the voltage is typically 120/240 V.   The secondary distribution system feeds the loads. If any changes are made to the loads then the secondary distribution is a point of interest. For the research herein, the secondary distribution is the focus. The sections below describe switching, transformers, and 3 phase transmission.

#### 2.2.1.2.1 Switching

Switching connections among high-voltage circuits is used to increase system efficiency as well as manage overloads and other grid upsets. For example, if a transformer is overheating, the circuit can be switched to a different transformer. Loads can also be switched to other transformers to balance the loads (Meier 2006).

#### 2.2.1.2.2 Three-Phase Transmission

An alternating current circuit has three separate phases, each of which is out of phase with the others by 120 or 240 degrees. Three phase transmission uses less wire, ultimately making it more economical.

#### 2.2.1.2.3 Transformers

A transformer either increases or decreases the voltage and is comprised of two conductor coils that connect through magnetic flux. The magnetic flux is the magnetomotive force divided by the reluctance (Equation 6). The magnetomotive force (mmf) is the product of the number of turns in the coil and current. The alternating current from one coil sets up an alternating current in the other coil. The current and voltage on each of the coils depend on the number of turns in each coil. The primary side of the transformer connects to the power source and drops down the voltage to the secondary side which connects to the load. There are a few losses associated with the transmission of power across the transformer. Overloading the distribution line may lead to heating that can limit the function of the transformer..

$$\Phi = \frac{\mathrm{mmf}}{\mathscr{R}}$$

Equation 6: Magnetic Flux (Meier 2006)

## 2.3 SMART GRID

### 2.3.1 History

The Public Utility Regulatory Policies Act (PURPA) of 1978 spurred research on new environmentally friendly technologies that use wind and solar power to produce electricity. The goal of Congress was to reduce the amount of foreign oil that the U.S. bought by promoting those alternative energy sources. The intent of PURPA was to promote new sources of electricity as an alternative to the norm of generation facilities. These new facilities had to meet Federal Energy Regulatory Commission (FERC) rules on fuel, efficiency, and reliability in order to be recognized as small power producers. The small power producers had a maximum power range of 80 megawatts and were required to use renewable sources such as solar or wind as their primary fuel. The Energy Policy Act of 1992 allowed for the increased development of these facilities by allowing FERC to order transmission owners to carry power for other parties (Itron Inc Jan.2010). The Energy Policy Act of 2005 changed the US energy policy by providing tax incentives to help with the growing energy crisis. The 2005 Policy Act sets federal reliability standards regulating the electrical grid. The Energy Independence and Security Act of 2007 was adopted to " to move the United States toward greater energy independence and security, to increase the production of clean renewable fuels, to protect consumers, to increase the efficiency of products, buildings, and vehicles, to promote research on and deploy greenhouse gas capture and storage options, and to improve the energy performance of the Federal Government, and for other purposes (Energy Independence and Security Act of 2007 2007)."

The Energy Independence and Security Act of 2007 was the key legislation that catalyzed the smart grid movement. The Act provided funding for utilities and consumers to build smart grids, and more acts were passed that benefited the evolution of smart grid technology. For example, the American Recovery and Reinvestment Act of 2009 allocated $11 billion for smart grid research.

The term “smart grid” has come far from where it first originated, namely the discovery of electricity in the $16^{th}$ century. Thomas Edison invented the incandescent light bulb, a few years later he flipped the switch on the first electric grid in lower Manhattan. The pull of an electromagnet against a spring opened or closed contacts that were represented by an illumination of a red lamp when the line voltage rose and a blue lamp when it dropped.

These lamp colors helped determine the control that would be needed in the electromagnetic field in order for the generators to match the output to the load. In order for Edison to measure the electricity used, he created a meter consisting of an electrolyte and two electrodes. The meter was based on Faraday’s law of electrolytic deposition wherein a current passing through the meter caused metal to be removed from one electrode and deposited on the other. By weighting both electrodes, the electricity used by the customer was established.

In 1872, Samuel Gardiner patented the first electric meter. After Gardiner there were others who contributed to the development of the meter. In 1883, Hermann Aron patented a recording meter that showed the energy consumed on a series of clock dials (A. P. Johnson 2010).

It was not until 1889 that the recording wattmeter was introduced by Elihu Thomson to measure the amount of electricity provided to the customer. The watt-meters were not particularly effective and utilities would disconnect customers during peak times and reconnect them during low demand in order to lower customer charges.

In the 1970s, automatic meters were introduced into the grid. These meters collected consumption and status data from energy metering devices. This technology was a necessary foundation for creating a more reliable and efficient electricity distribution network. The first devices were used to measure consumption.  Today, two-way metering technology can turn appliances on and off according to demand and off-peak electricity prices (Smart Grid, Building on the Grid 2011).

The electric grid has developed since the first meter was patented over one hundred years ago. The first smart grid was completed in 2005 by ENEL S.P.A of Italy with an integration of electronic meters that communicate through satellites and LV concentrators in every substation. The LV concentrators manage the communication in both directions, through the remote metering central system and the electronic meters. While the smart grid has been around for less than 10 years, remarkable progress has been made to the obstacles that were faced in the late 1800s.

### 2.3.2 Technology

The core duties of the smart grid are to maintain stability and reliably monitor and control performance, prevent theft of electricity. There are a variety of technologies involved in order to achieve the desired outcome. Different types of subsystems can be distinguished for the sake of easier implementing of all the technology needed in the grid.

### 2.3.3 Monitoring and Control Systems

A variety of monitoring and control systems are required to keep the lights on. Smart grid requires even greater control and visibility of the system to manage all the complex technologies involved. Examples of some of the systems that will likely be employed are described in this section.

#### 2.3.3.1 Wide Area Monitoring Systems (WAMS)

Wide area monitoring systems are designed for optimal capacity of the transmission grid and to prevent spread of disturbances. WAMS provide real-time information to the operator, monitor current system state, ensure operating safety margins, give early warnings for disturbances, and attempt to prevent and mitigate blackouts.

#### 2.3.3.2 Phasor Measurement Unit (PMU) Systems

Phasor Measurement Units are high speed sensors that provide phasor information in real time. PMU systems measure the three-phase current and angle at different spots throughout the utility grid network. GPS satellites are used to synchronize and gather PMU measurements in what are dubbed "Synchro-Phasor" measurements. Microprocessor-based instrumentation is used, such as protection relays and Disturbance Fault Recorders (DFRs). A specific data recording and communication protocol standard has been established to transfer the data to repositories. PMUs can be used for high accuracy measurement of 3-phase voltage and current at a rate of 288 kHz, and calculate real and reactive power, frequency, and phase 12 times per minute for 60 Hz grid (J. Mamoh 2012). Effective use of the PMU is useful in reducing blackouts and in observing the real time behavior of the power system (Bindeshwar Singh 2011).

#### 2.3.3.3 Smart Meters

Smart meters provide energy usage information to the consumer, and send data to the utility. The data sent are used for load factor control, peak-load requirements, and price development strategies. This allows for the consumers to switch on/off their appliances to the grid in a remote manner (Commonwealth Edison Company 2013). Smart meters are also used for automated meter reading and billing, which reduces costs. Finally, smart meters are usually the communications gateway for smart electric appliances and smart devices that can be manipulated and/or controlled behind the meter (PG&E 2014).

##### 2.3.3.4 Smart Appliances

Smart appliances are new generation home appliances that allow consumers to voluntarily take part in programs that can save them money if they allow automatic and smart control of the appliance power consumption. Such appliances include air-conditioners, TVs, space heaters, water heaters, refrigerators, washers, dryers, etc. They have an internal communications, sensing and computing power which can communicate with the utility and/or sense disturbances in the grid and respond appropriately (e.g., switch off the device for a couple of minutes) until such action is no longer desired or needed.

#### 2.3.4 Advantages

Smart grid technology is a pathway, in principle, to reducing the consumer cost of electricity. A recent study, however, suggests that simple and relatively low-price energy meters can achieve the same goals. Energy Insight, an affiliate of IT research firm IDC, conducted a survey which confirms what most people would expect: consumers are screaming for more information on their electric usage (LaMonica 2008). This is not surprising given the increasing costs of electricity in many regions of the U.S. and growing environmental concerns. Rather than access the information presented on PCs, most of people said that they'd prefer an "in-home display" that would look something like a thermostat which is programmable. There are stripped-down devices on the market. They cost between 100 and 300 dollars and could reduce electric consumption by 10 percent. Devices which are simpler than others are enough to some consumers, regarding to one of the report's authors. Some consumers are willing to have some devices that display on a television or dashboard touch screen

One of the biggest sources of pollution and a major health threat is burning fossil fuels to generate electricity. Harmful air increases asthma and lung disease, especially among the elderly and children. Since a smart grid is able to adjust demand to match sporadic wind and solar supplies, it will enable customers to rely far more heavily on clean, renewable energy in the U.S. A smart grid will also facilitate the switch to electric vehicles, making it available to smart-charge at night when wind power is sufficient and inexpensive (EPA 2013).

The gathering of a number of smart grid technologies can make for huge improvements in economics. Advanced Metering Infrastructure with smart meters and duplex communication capability will provide real-time price signals that are linked to retail prices to consumers. This information will make the incentive for consumers to respond to prices just as they do for most of other products they purchase. Reducing the peak demand and the associated prices for electricity expected to this response (Environmental Defense Fund 2011).

Systems for customers will offer the benefits that consumers expect when they participate with the smart grid. Even though “simple” from the customer’s perspective, these systems will be able to conduct complicated transactions such as demand response combined with “smart rate designs” and thereby create new markets that will stimulate the US economy (National Energy Technology Laboratory 2010).

### 2.3.5 **Challenges**

#### 2.3.5.1 Customer Engagement

The Smart Grid Consumer Collaborative recently released its 2013 State of the Smart Grid Consumer Report which collects and summarizes not-for-profit research groups' results for the previous year. Their findings reveal that utilities have more work to do when it comes to spreading the word about smart grid and its many advantages. Fifty-four percent of utility customers questioned said that they were not familiar with the term "smart grid." Twenty-one percent revealed that they had heard the term, but were not sure what it means, while only 17 percent claimed to have an introductory understanding, and 7 percent were confident that they knew exactly what the movement entailed (GreenTech Media 2013).

Research published by the DOE suggests that consumers will more likely be engaged in smart grid so long as it is easy to use and does not interfere with their daily lives (U.S. Department of Energy, Office of Electricity Delivery & Energy Reliability 2008). As a result, the potential exists for innovators to create tools for consumers at the industrial, business, and residential level to optimize their energy use and minimize their financial exposure. Financial savings in the form of lower energy bills are the best motivator for increased energy efficiency awareness.

#### 2.3.5.2 Technology Integration

Grid modernization will evolve incrementally over time and need to accommodate a yet to be determined number of new products and services while it continues to operate. Ensuring that all these new products and services interact positively with each other requires special attention by key smart grid stakeholders.

Information and automation technologies will play a critical role in the success of the smart grid. Information, operational, and automation systems will need to be modified or designed from scratch to accommodate emerging smart grid technologies. Visualization of system loads and generation capabilities will be required to allow for effective demand response and distributed energy resource allocation. Metering, communications, utility assets, supervisory control and data acquisition (SCADA), feeder & substation automation, scheduling & dispatch, forecasting, planning, engineering, billing & accounting, and customer service systems will be required to support intermittent renewable energy resources, additional demand from electric vehicles, and accommodate bidirectional power flow (A. Ipakchi and F. Albuyeh 2009).

Today, these systems operate independently of each other. The smart grid paradigm requires that information be stored, shared, and coordinated across all systems. Spatial information, synchronized in time using geographic information systems (GIS) techniques and technologies, is a key requirement to successfully integrate utility systems. The data needed to conduct business within each organization need to be stored securely and accessed quickly. Capabilities enabled by the cloud will allow integration and access to all of the data over the web. Large data servers will be required to house the massive amounts of data that will be stored. Use of the Web as information technology platform will enable new and existing systems to access and store as needed (A. Ipakchi and F. Albuyeh 2009). With these systems in place, the system can be visualized with greater detail and operated more efficiently.

Interoperability capabilities between existing utility systems and new technologies are evolving through the development of standards and best practices. These standards and best practices will help to build an open architecture, apply existing internet protocol approaches, and define plug-and-play requirements. The effort is managed by National Institute of Standards and Technology (NIST), an agency of the U.S. Department of Commerce. NIST was empowered to lead and coordinate standards development by EISA of 2007 (Energy Independence and Security Act of 2007 2007). Lack of agreement on the details of the standards between stakeholders and who should issue the standards have slowed the implementation of smart grid technology.

#### 2.3.5.3 Intermittent Resources

Wind and solar power generation as sources of power generation are gaining in popularity due to their sustainability potential and regulatory drivers, such as Renewable Portfolio Standards (R. Wiser 2007). As technology improves, their economic viability becomes more appealing. While solar power systems can be sited at a location near or at where the load is centered wind farms are typically located far from the load and require expensive transmission infrastructure investments. Integrating high penetrations of intermittent resources such as wind and solar will require advanced energy management systems, the ability to store excess generation, and strategies for addressing power production variability. The traditional flow of power from a central power plant to the load is transitioning to a system with many smaller sites of distributed power. Protection schemes and control strategies will need to be modified to reflect the new power flows. The management of these intermittencies needs to occur dynamically and knowledge of behavior of other parts of the system (through communications) makes sensing and system visualization all the more critical.

#### 2.3.5.4 Power Quality and Reliability

Utilities are expected to supply high quality electric power electricity reliably to its users. Installation of DER, including renewable resources, need be designed to operate in a manner that complements the grid. Islanding of these resources requires that the islanded systems be safe for line workers and that the process of islanding does not negatively impact grid operation and power quality. Voltage levels need to remain within the ranges specified by American National Standards Institute (ANSI) since introduction of DER can cause voltage levels to rise locally and downstream of the circuit (American National Standards Institute (ANSI) 2007).

Intermittent resources can cause transient voltages and excessive harmonic distortions. Protection schemes also need to be examined for their effectiveness and ability to protect the circuit and ensure line worker safety during outages and repairs. System stability will need to be closely watched. These issues create additional support for the need to better measure, sense, control and visualize the system. DER introduces the potential for bidirectional power flow on a system design for power to flow one way: from generator to user. Demand growth and the large load introduced on the grid by electric vehicles likewise need to be considered (A. E. Auld 2010).

## 2.4 MICROGRID

### 2.4.1 What is a microgrid?

A microgrid is a dedicated local distribution system with (1) one or more connection points to the utility grid, (2) on-site power generation, and (3) the capability island. A microgrid will also typically require the ability to store excess electrical power that it can be used later to balance the generation and load, particularly when islanding and operating under the islanding mode.

A microgrid, with the appropriate policy, can in principle elect to purchase electricity from the grid (Lawrence Berkeley National Laboratory 2014), or generate dispatchable power on-site based on pricing.

### 2.4.2 Challenges

#### 2.4.2.1 Islanding

A safety concern from the utility perspective is the islanding of a microgrid during a grid outage. It can be dangerous to utility workers since they may be unaware that the circuit still has power. Islanding can also prevent automatic reconnection of devices to the grid (PricewaterhouseCoopers 2012).

### 2.4.3 Advantages

#### 2.4.3.1 Reliability

Microgrids increase their reliability by integrating redundant distribution, smart switches, automation, power generation, power storage, and other smart technologies. Local power generation and storage allow for parts of the grid to operate independently of the electric grid and thereby maintain services to the community local to the microgrid. Technologies such as smart switches and sensors automatically fix power disturbances. Currently, switches have to be reset manually in case of an outage. Redundant sources ensure that power continues to flow when storms, ice, or other events cause interruptions in the power system. Microgrids can back up the power grid when power demand is at its highest by supplying ancillary services.

#### 2.4.3.2 Economic Growth

Microgrids are envisioned to improve the economy by increasing the reliability of power to the customer base, creating a new market for a wide portfolio of products, and increasing the job market. Microgrids increase financial investment through the financing of energy efficiency, grid improvements, and the integration of distributed energy. With the development of a microgrid, more efficient electricity business models will evolve that are more environmentally friendly and better suited for future technologies (Galvin Electricity Initiative 2014).

#### 2.4.3.3 Lower Emissions

A benefit of a microgrid is the potential for a positive environmental impact. Microgrids are able to accommodate environmentally sensitive power generators such as solar and fuel cells, and the ability to operate with complementary DER (e.g., batteries) in a manner to minimize pollutant emissions and operating costs. It allows for consumers to generate their own power making it easier for them to meet their electricity needs. Microgrids offer the ability to increase the effectiveness of renewable energy and to help implement net-zero buildings (Dohn 2011).

### 2.4.4 Examples

#### 2.4.4.1 U.S. Army Fort Bragg

Fort Bragg, a U.S. Army base in North Carolina, has one of the world's largest microgrids. The microgrid covers over 100 square miles with a dedicated electric distribution network. Fort Bragg has a total of 15 diesel generators that represent over 8MW, one 5kW fuel cell and a 5MW gas turbine.  It uses a full parallel interface to reduce any losses from the power flow and the generator uses the system to export power to other loads. The diesel generators were installed to provide electricity during a power outage (Joshua Meyer 2003).

The microgrid has a central energy management center that is able to monitor and dispatch multiple generators that are dependent on the utility availability and load requirements. The management system is connected to the generation technologies through a fiber optic network. The base starts to save money when the self-generated power is less than the grid power, and island from the main grid in the event of a grid outage. Fort Bragg has enhanced its energy reliability as well as its overall energy savings due to its microgrid distribution system (Joshua Meyer 2003).

#### 2.4.4.2 Beach Cities Microgrid Project

This microgrid project, located in San Diego, is utilizing information based technologies and distributed generation to increase asset utilization and reliability. The goal of the project is to design and demonstrate a smart microgrid that incorporates sophisticated sensors, controls, and communications. The system has incorporated solar power generators in homes and businesses, biodiesel-fueled generators, energy storage devices, and smart meters. The microgrid hopes to ultimately reduce peak loads by more than 15 percent (Galvin Power 2014).

#### 2.4.4.3 University of California, Irvine Microgrid

The UCI Microgrid serves over 30,000 students and staff. It is comprised of different building types such as classrooms, research centers, offices, and housing facilities. The UCI Microgrid circuit is powered by a variety of sources that include on-campus generation consisting of a 13MW gas turbine generator, a 5MW steam power plant, and 857kW of peak solar roof-mounted generation distributed throughout the campus. The power is also provided by two dual-axis concentrated photovoltaic panels that produce a combined peak power of 153kW. The microgrid is comprised of ten 12 kV circuits (UC 1-10) that originate from the interconnection with the utility grid, a Southern California Edison 66kV source, at the UCI Substation. On an average day the campus demand is approximately 21MW with an average of 0.5MW imported from Southern California Edison. There are currently expansion plans that include the addition of 3MW of peak solar PV along with installation of a 2.0 MW 500 kWh battery system (Brendan P. Shaffer 2013).

## 2.5 DISTRIBUTED GENERATION

Distributed generation is electric power generation that is distributed across the grid. A few common types of distributed generation include photovoltaic panels, wind turbines, and fuel cells.

### 2.5.1 Solar Power

The term solar power refers to the conversion of light into electricity by using photovoltaics or concentrated solar power. A few solar energy technologies include solar heating, solar photovoltaics, and solar thermal electricity. These solar technologies are categorized as either passive solar or active solar depending on the way they capture, convert, and give out the solar energy.

#### 2.5.1.1 Passive Solar

Passive solar includes using sunlight to heat a building and to promote airflow through a structure. It does not involve the use of mechanical and electrical devices to help this energy transfer.

#### 2.5.1.2 Active Solar

Active solar technologies convert solar energy into a useful form of energy by utilizing electrical or mechanical equipment. A benefit of active solar is that controls can be used to maximize the effectiveness of the system.

##### 2.5.1.2.1 Photovoltaic

A solar cell or photovoltaic cell, converts the concentrated sunlight into electricity using semiconductors that demonstrate the photoelectric effect.  The photoelectric effect absorbs protons of light and releases electrons.

##### 2.5.1.2.2 Concentrated Solar Power

Sunlight can be indirectly converted into electricity through concentrated solar power. Concentrating solar power (CSP) technologies use mirrors and tracking systems to concentrate sunlight onto receivers that collect and convert the solar energy to heat or electricity. Electrical power is produced when the light is converted to heat or electrons. There are a wide range of concentrating technologies such as the parabolic trough, concentrating Fresnel lens, and the solar power tower. The solar power tower generates electric power by using sun-tracking mirrors to focus sunlight on a receiver at the top of the tower. Parabolic-trough collectors use mirrored surfaces curved in a linearly extended parabolic shape to focus sunlight on a dark surfaced absorber tube running the length of the trough. A mixture of water and antifreeze or other heat transfer fluid is pumped through the absorber tube to pick up the solar heat, and then through heat exchangers to heat potable water or a thermal storage tank. Because the trough mirrors will reflect only direct-beam sunlight, parabolic-trough systems use single-axis tracking systems to keep them facing the sun (Federal Energy Management Program 1998) .

### 2.5.2 Wind Power

Wind power technology generates electricity using wind. Wind power is a renewable source that can be used as an alternative to using fossil fuel.

Wind is caused by heat from the sun; the solar radiation unevenly heats the surface of the Earth at different speeds. These surfaces release heat at different rates causing the Earth to get warmer in the day and colder in the night. This ultimately causes hot air to rise, reducing the atmospheric pressure and drawing in the cooler air to replace it.

A wind turbine, comprised of long blades (air foils) and housed on a high tower facing the wind, converts the kinetic energy in the wind to electrical energy.

### 2.5.3 Energy Storage

Renewable technologies are expected to require energy storage in order to balance the generation with the load demand. Wind and solar renewable energy sources are intermittent and do not produce energy exactly when the load demand is present. As a result, storing and releasing the energy will preclude curtailing the generation when the load is absent, and using the energy with the load is present. Simply stated, energy storage allows charging when there is excess of energy and discharging when there is a lack of energy.

#### 2.5.3.1 Pumped Hydro Storage Method

In the case where excess power is generated (e.g., during non-peak hours), the excess power is used to pump water uphill from a lower to a higher reservoir. When power is required to serve loads, the water is released to flow downhill, drive a generator, and thereby produce electricity. This is the most popular and most efficient way of storing energy and encompasses 99% of the worldwide storage capacity (127,000 MW) (The Economist 2012). It is widely used for energy storage because of the relatively low cost, the ability to stabilize frequency, and the extent of reserve capacity.

#### 2.5.3.2 Flow Batteries

Flow Batteries are similar to lead-acid batteries. The electrolyte flows in this type of battery and is then stored in an external container. Then it is circulated back through the battery cell stack to the original reservoir. The electrical storage capacity depends on the size of the container. The system requires replacement of the fluid every 3 to 5 years (J. Mamoh 2012).

#### 2.5.3.3 Super Capacitor

A super capacitor is an electronic device with characteristics similar to a simple capacitor or electrochemical battery with the difference that there is no chemical reaction. Super capacitors charge rapidly, have low impedance, and virtually unlimited life cycles. The major challenge with super capacitors is the low energy density (J. Mamoh 2012).

#### 2.5.3.4 Super Conducting Magnetic Energy Storage

This is energy stored in the magnetic field created by the flow of direct current in a coil of superconducting material that has been cryogenically cooled. The high voltage output power is available almost instantaneously. While the efficiency can exceed 70% (Hyper-Librarian 1997), the technology is limited in energy density (J. Mamoh 2012).

#### 2.5.3.5 Flywheels

Flywheels are cylindrical devices that store rotational energy. They can charge and discharge rapidly, are not affected from the surrounding temperature, and require relatively little space. (J. Mamoh 2012) (Green Optimistic 2009).

#### 2.5.3.6 Compressed Air Energy Storage

The compressed air energy storage pumps air under very high pressure into ground cavities using electricity at off-peak hours. The energy is recovered by the generation of power through gas turbines (J. Mamoh 2012) (Energy Tower 2014).

### 2.5.4 Challenges with the Penetration of Distributed Generation

Power generated from solar resources at the distribution level varies temporally, experiences intermittencies, and is neither guaranteed nor dispatchable. The current grid, as a result, can face voltage and frequency challenges with a high penetration of intermittent renewables (Guohung Wu n.d.). In order for the grid to accommodate an increase in intermittent renewables, the structural design of the electricity sectors needs to be altered.

Distributed generation can also be sourced from dependable resources such as gas turbines, microturbine generators, and fuel cells. A few of the technical issues causes by distributed generation are listed below.

Adding distributed generators at the distribution level can impact the amount of power to be handled by the cables, lines, and transformers. In order to avoid overload problems, upgrades need to be made to the infrastructure. The transformers are the most important part when it comes to upgrading. Transformers convert high voltage to medium voltage or medium voltage to low voltage. If too much power is generated the power flow of the transformers will go in the opposite direction. The transformer has to be able to handle this and so when there is an increase in DG, an upgrade may be required for the transformer.

DG can increase the voltage locally, the extent to which depends on the amount of DG on the circuit. The deployment can, at some level, have a negative impact on the network should the voltage rise above specifications (Kakigano, DC Micro-grid for Super High Quality Distribution-System Configuration and Control of Distributed Generations and Energy Storage Devices- 2006).

When using DG, additional protection systems are required to avoid faults and accommodate islanding (Jenkins, Embedded Generation 1995). Islanding occurs when the DG continues to power a location when the circuit is disconnected from the utility grid. Islanding poses a danger to utility staff should power be inadvertently returned to the grid. It is common today for the distributed generator to detect the loss of grid power and anti-island (i.e., drop off line).

Renewables such as PV and wind power cannot supply constant power in order to fulfill the power demand. A combination of renewables along fuel cells, microturbine generators, gas turbines, and energy storage is adopted to accommodate this challenge. The majority of the energy storage and DG components are DC based requiring an inverter-based interface to connect to the grid. When the AC side of the microgrid is connected to the grid, the frequency and voltage are fixed and the DG works in synchronization with the grid (Dan Wu, Coordinated Primary and Secondary Control with Frequency-Bus-Signaling for Distributed Generation and Storage in Islanded Microgrids 2013).

## 2.6 SUMMARY

The current utility grid infrastructure is aging and reaching the end of its design life. The microgrid paradigm will allow future load growth as well as smart, renewable, and efficient grid technologies. New energy resources will need to be deployed at all levels of the grid to buffer the intermittencies introduced by solar and wind power production. As a result, the infrastructure must interact with existing technologies as well as incorporate new energy technologies over time. While distributed generation can reduce network losses and improve the stability of the network, many challenges remain (e.g., interconnection designs and costs). In the near future, these renewable technologies will eventually lead to easier and faster integration of distributed generation and significant growth in distributed generating capacity.

Research has been conducted on the effects of adding different types of DG to the microgrid such as rooftop solar or electric vehicles. There is limited research on the impact of a combination of all these generation sources and loads on the microgrid. This thesis focuses on the challenges associated by interconnecting and accommodating solar power, energy storage, and electric vehicle charging in a microgrid.

# 3 APPROACH

## 3.1 TASK 1: Develop the secondary circuit, UC-9 real time model

This task addresses (1) the development of a steady-state model to simulate the effect of adding rooftop solar panels, a battery energy storage system, and electric vehicle charging on a secondary circuit, (2) the adoption of a simulation code, and (3) the identification of an experimental verification platform.

## 3.2 TASK 2: Verification of the model

This task addresses the verification of the model. One of the legacy metering databases for the UCI Microgrid, the ION network, which contains the real and reactive power for the entire microgrid for April 17, 2011. Initially, the strategy for verifying the model was to compare the known legacy data to the simulated data. Recently, 40 high-resolution meters have been installed with data ported to a SQL managed database. This combination of legacy and high-resolution data provides a rich resource for model verification.

## 3.3 TASK 3: Analyze data received from Experimental Platform

This task addresses the analysis and verification of data from the experimental platform in order to establish the quality and suitability of the data. Ideally the data will include rooftop solar power, EV charging for each vehicle, and battery storage performance in 5 minute intervals.

### 3.4 TASK 4: Create and analyze scenarios with additional distributed generation

The last step involves applying the model to various generation and load scenarios in order to meet the goal of the research. The primary scenarios will include the characterization of an integrated solar PV, battery energy storage bank, and electric vehicle charging system, along with the assessment of the impact the system has on the secondary microgrid circuits.

## 4 TASK 1: DEVELOP THE SECONDARY CIRCUIT, UC-9 REAL TIME MODEL

### 4.1 EXPERIMENTAL PLATFORM

The experimental platform selected for the study is the “Car Shade” project, the unique resource installed on the UCI Microgrid as part of the “Irvine Smart Grid Demonstration”. As described in the Introduction (Section 1.0) and illustrated in Figure 2, the Car Shade is located on the UCI Anteater Parking Structure and comprised of:

- 48kW of rooftop PV panel
- 20 monitored EV chargers
- A 100kW smart battery energy storage system (BESS)
- A Princeton Power Systems (PPS) site controller

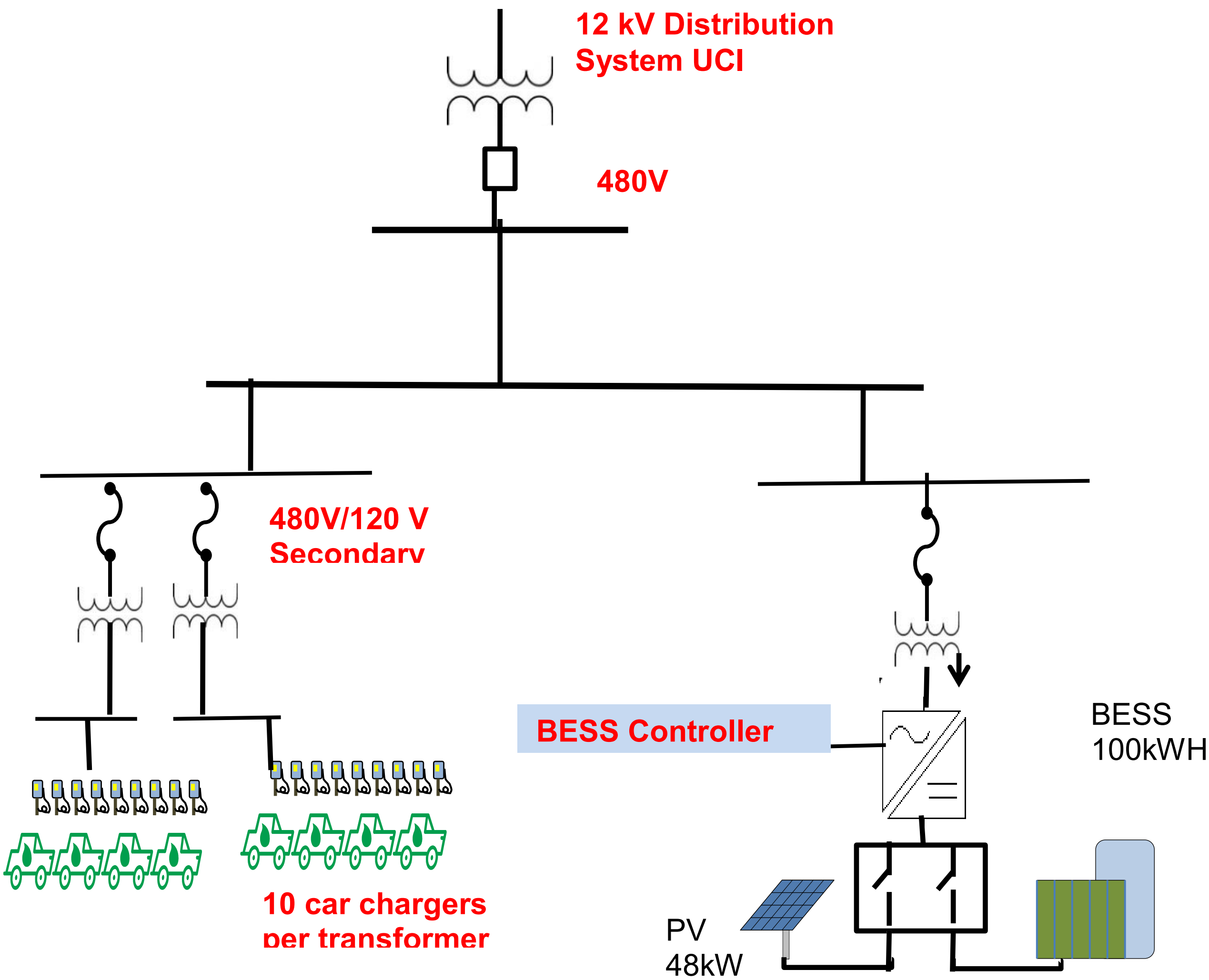

Figure 2: Car Shade Project One-line diagram representation

The UCI Microgrid is supplied by a 66kV line from the MacArthur substation. A transformer steps down the voltage from 66kV to 12kV for 10 different circuits as seen in Figure 3 and Figure 4. Each one of those circuits (known as UC-1 through UC-10) has a 12kV to 480V step down transformer. The UC-9 circuit is the focus of the research herein.

UC-9 is connected to the UCI East Substation and is broken down into 6 different circuits labeled ES-2 through ES-8. UC-9 has most of the engineering buildings on campus as well as some of the on-campus housing.  For the Car Shade, the transformers of interest are located on circuit ES-5.  ES-5 encompasses 12 transformers and 7 buses. Once the voltage has been switched down from 12kV to a 480V bus, it is split up into two circuits, one for the Anteater Parking Structure and one for the Car Shade elements.

For the Car Shade, a DC bus is connected to the rooftop solar PV and the BESS. The AC bus feeds power from the DC side through an inverter to the power grid. The AC voltage is established by the power grid.

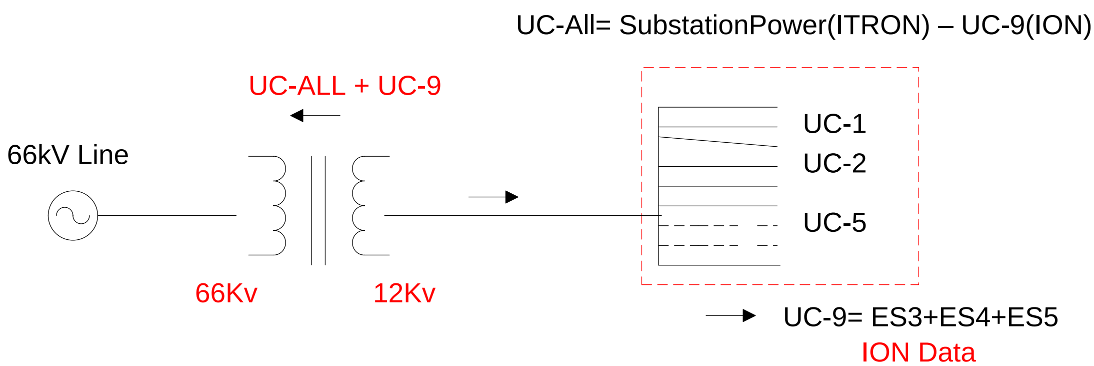


Figure 3: Substation voltage drop

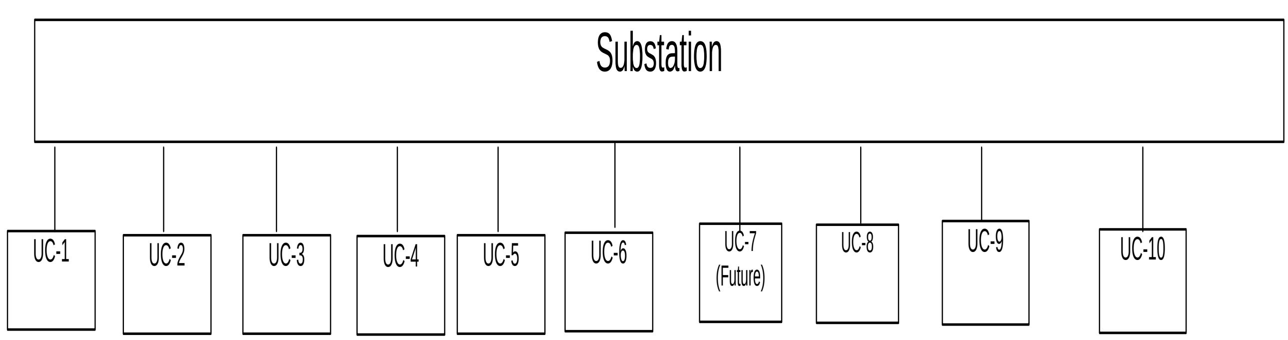


Figure 4: Primary Circuits of the UCI Microgrid

### 4.1.1 BATTERY ENERGY STORAGE SYSTEM

The purpose of the BESS (Figure 5) is to reduce the amount of power needed from the grid to charge the electric vehicles by storing and discharging the PV energy.

The system contains a 100kWh Samsung battery and a PPS Demand Response Inverter (DRI). The inverter has two DC inputs for the PV and the battery, and a 480V three-phase delta connected AC interface for connection to the grid.

Figure 5: Battery Energy Storage System (Coleman 2013)

The BESS site controller has four different operating modes that contain the algorithms for overall system behavior:

1. A demand response event mode which allows the system to operate at the given power level until the battery limits are reached. The power level from or to the battery is determined in response to SCE signals (demands) via the demand response program of SCE.
2. A peak shaver mode that causes the BESS to charge and discharge in order to bring the power imported from the microgrid to a specified level. This ultimately reduces the site demand with the purpose to reduce 15 minute customer demand charges.
3. Another peak shaver mode that, instead of specifying a certain threshold, adjusts the threshold based on historical data.
4. A PV smoother algorithm uses the battery system to lower the fluctuation in the PV power output by limiting the ramping rate at any given point in time by either charging or discharging the battery.

### 4.1.2 INVERTER

The inverter converts the power from direct current to alternating current. Alternating current is used to interconnect power of the grid to that from a DC source such as a battery or photovoltaic array. The PPS inverter used in this project is an internal inverter that is a part of the battery system. The inverter has two operating modes that determine to which signals the inverter responds.

#### 4.1.2.1 Demand Response Mode

In order for the inverter to respond to the controller modes described in the previous section, it must be in the demand response mode. The controller can then control the inverter by changing the power levels. An "Inverter Policy Manager" is used to manage the BESS (e.g., controlling the BESS minimum state of charge). If the battery is at or below that set-point, then no further discharge can occur. The inverter manager is used to enable or disable export of PV or battery power by preventing reverse power flow at the AC interface.

#### 4.1.2.2 Distributed Generation Mode

In order to use the PV power without curtailment, the inverter must be in this mode. In this mode the BESS immediately charges the battery using either PV or grid power.

### 4.1.3 Rooftop Photovoltaic Panels

The E20 series rooftop solar panels are manufactured by Sunpower (Figure 6). E20 solar panels have the highest efficiency currently on the market. The cell technology includes a thick copper foundation that adds strength, no grid lines on the front of the cell which helps to absorb more sunlight, and thick connectors to help with strain relief. Each of the 128 panels has a peak power of 327W and a rated voltage of 54.7 V.

Figure 6: Rooftop solar PV for car shade project (Reyes 2014)

### 4.1.4 ELECTRIC VEHICLES

An EVSE (Electric Vehicle Supply Equipment) is used to connect between the vehicle and the electricity source also known as the charging station. The charging station has 3 different levels of operation. Level 1 charging where the power supply operates at 120V and provides between 1-1.5 kW of power (typically used in residential charging or in other locations where only 120V power is available). Level 2 charging provides the power from a 240V supply at 3-7 kW. The level 3 charger is known as a “fast charger” provides power levels up to 90 kW. The charger used in the Car Shade project is shown in Figure 7.

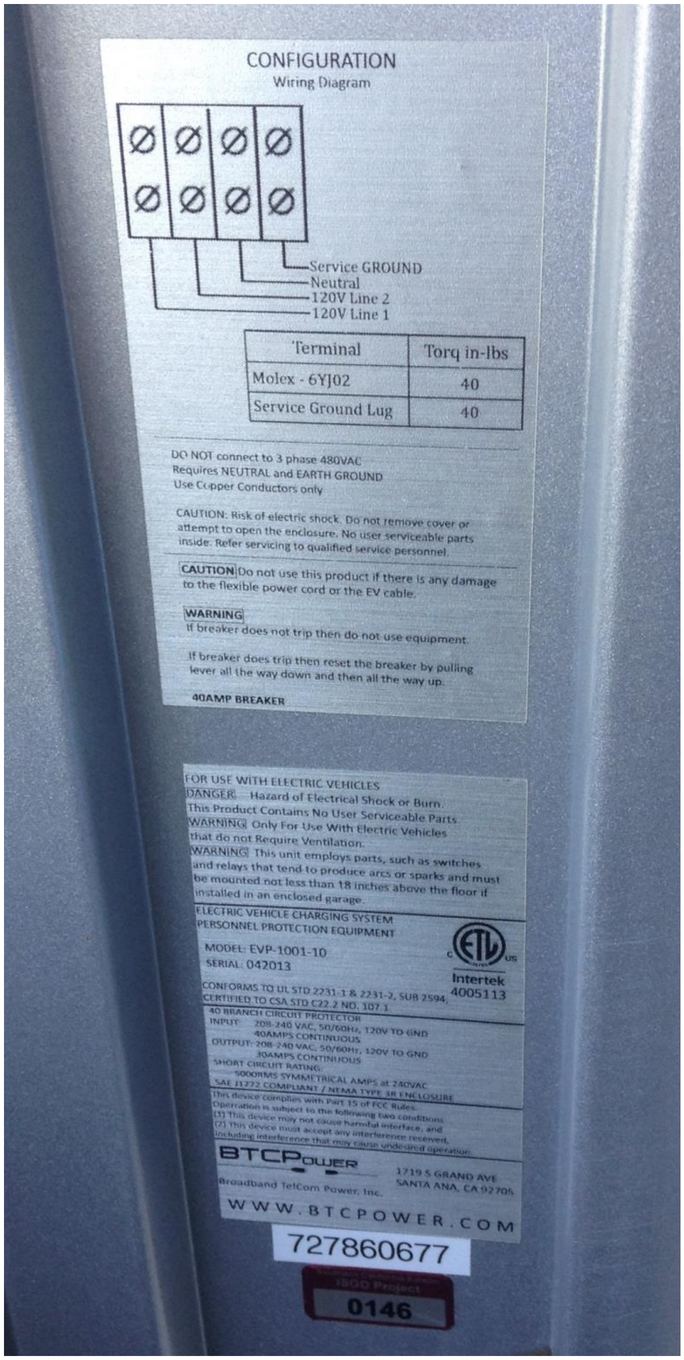


Figure 7: EVSE Charger (Reyes, 2014)

The electric vehicle charging data were recorded at 15 minute intervals to provide the load profiles used in the model. The 100kW battery stores any excess rooftop solar PV generation that has not been used during the day. This energy is then used to charge the electric vehicles during the evening. The battery has a demand response inverter that allows for the integration of rooftop solar PV, trimming back loads during the grid's peak usage time, energy storage, as well as voltage and frequency regulations. The battery has been running on PLS (Permanent load-shifting) mode.

## 4.2 MODEL

The UCI model was developed using the Electrical Transient and Analysis Program (ETAP). The model uses the known information to account for any unknown factors using the state load estimator (SLE). The estimator uses any given data such as power measurements in order to estimate the angles and magnitudes of bus voltages in the system. From that point, the state load estimator checks the data for any major errors and creates artificial measurements for the unknown loads. Another feature that the state load estimator gives is the comparison of the measured data versus the estimated data.

The model needs to include (1) the UCI Substation which transitions a 66Kv line into ten 12kV lines that are named UC-1 to UC-10, (2) a transformer, located in the Anteater Parking Structure, that reduces the voltage of UC-9 from 12kV to 480V, (3) a 48kW rooftop solar array made up of 8 modules per string with a total of 18 strings that are fed to a PPS DRI inverter, and (4) a 100kVA battery energy storage system (BESS) that is connected to the DC part of the inverter. The BESS has an internal transformer that drops the voltage from 480V/208V which is connected to the AC side of the inverter. This transformer then connects to a main bus that has 480V. That bus has a connection to another bus which is broken down into two cables with two transformers that are each 75kVA and drop the voltage from 480V/208V. Each transformer is connected to 10 electric vehicle chargers that have a max power of 6.6kW each. Each of the components modeled have real power, reactive power, voltage, and current data for 24 hours that will be modeled in 15 minute intervals.

The model uses photovoltaic, inverter, and battery specifications received from SCE. The data inputted and outputted from the model are in 15 minute increments in order to see the types of factors that will be attributed to increasing the generation already in place by different orders of magnitude.

Figure 8 shows a detailed view of the UC-9 circuit which includes the 5 branches that run throughout the east side of campus as well as the transformer numbers and the name of the bus.

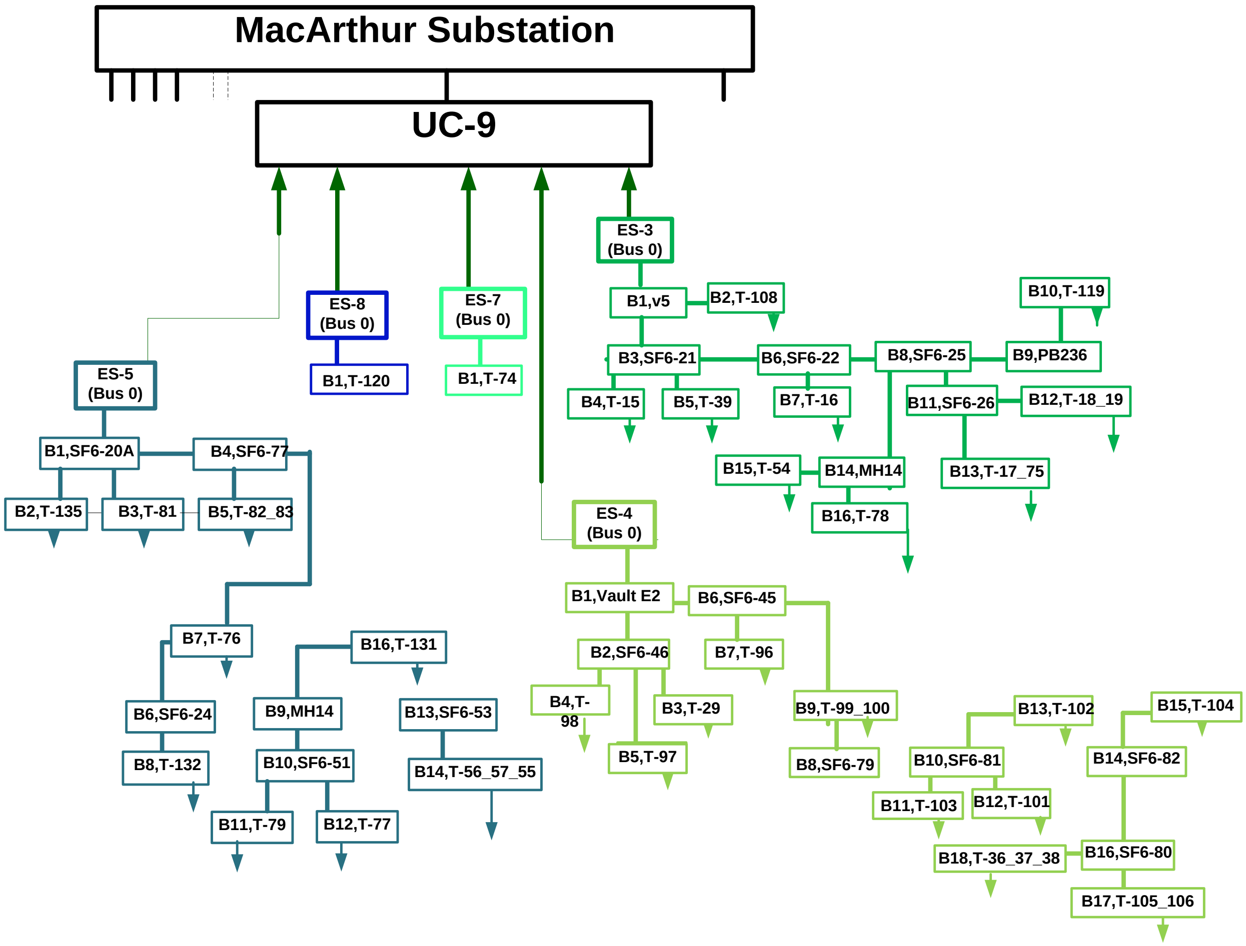


Figure 8: Detailed View of UC-9

A model of the UC-9 circuit was run in MATLAB that contained load information from the ITRON network, SunEdison data, and estimated loads for the unknown buildings, and a varying power factor. The same was procedure was conducted in ETAP one point in time (the point selected according to the time with the maximum power) and at a power factor of 0.96 that was calculated in the program. The results of these two program simulations are compared to metered UC-9 data from the ION network in Table 1: Simulation Comparisons to the Ion Network at 8pmTable 1.

| | MATLAB/Simulink | ETAP | ION | Error for MATLAB | Error for ETAP |
|---|---|---|---|---|---|
| Reactive Power | 1308.473 kVAR | 1588 | 1,650.80 | 20.73% under | 3.6763% under |
| Real Power | 5161.654 kW | 5149 | 5130.14 | 0.614% over | .368% over |

Table 1: Simulation Comparisons to the Ion Network at 8pm

Figure 9 and Figure 10 show a bar graph comparison of the real and the reactive power for the simulated data in ETAP and MATLAB as well as the measured ION data. These data were simulated and measured for the time of 8:00pm since the ETAP software simulates one point in time. The ETAP measurement revealed a better power factor calculated through the software SLE feature.

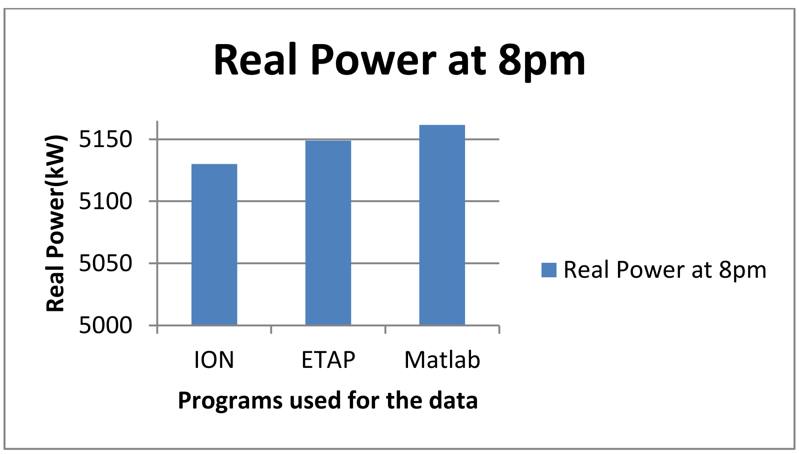


Figure 9: Real Power Comparisons

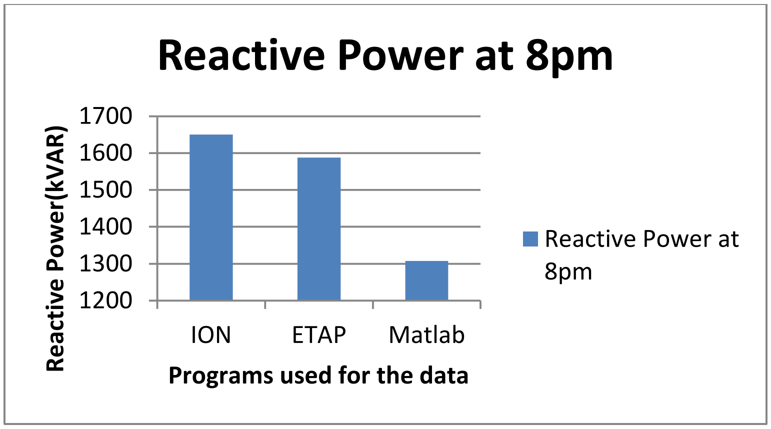


Figure 10: Reactive Power Comparisons

The ETAP calculated power factors were used in MATLAB. The results shown in Table 2, Figure 10, and Figure 11, show the real and reactive power vs. ION metered data. Note that the simulated data better corresponds to the measured data in this case.

| | MATLAB/Simulink | ETAP | ION | Error for MATLAB | Error for ETAP |
|---|---|---|---|---|---|
| Reactive Power | **1600.157kVAR** | 1588 | 1,650.80 | **3.07% under** | 3.6763% under |
| Real Power | **5162.443kW** | 5149 | 5130.14 | **0.6296% over** | .368% over |

Table 2: Updated Program Comparisons

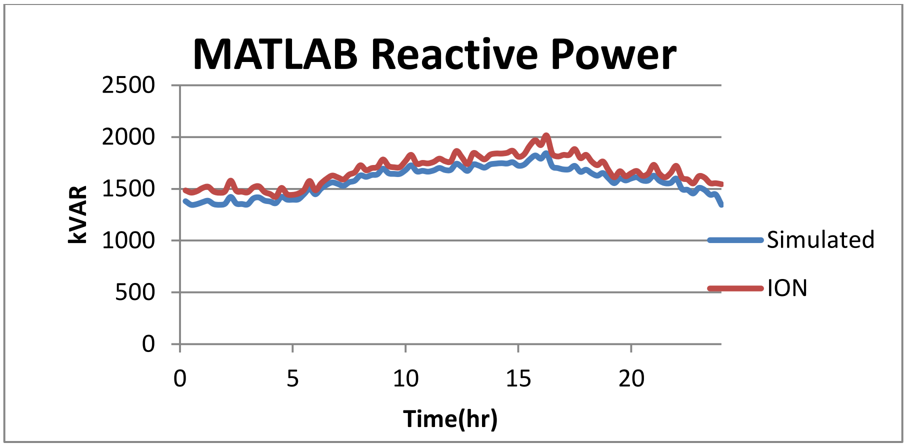


Figure 11: Reactive Power with new power factor

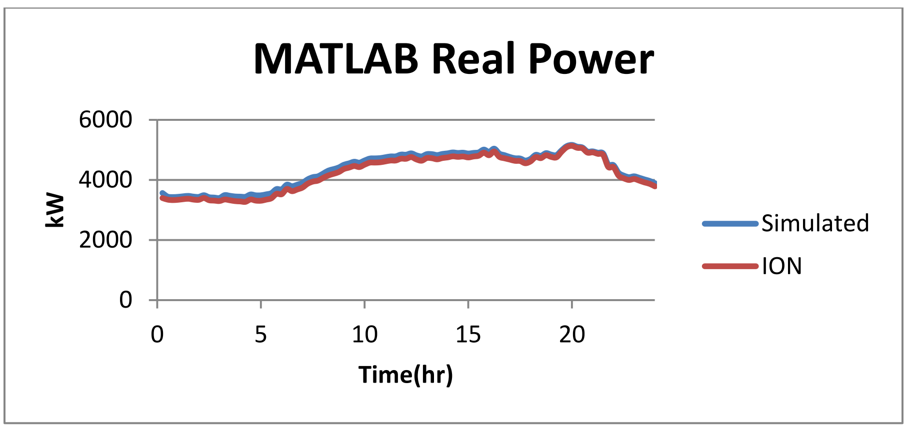


Figure 12: Real Power with new power factor

ETAP was used in the beginning to correct the power factor and at the time only one point in time could be simulated so it wasn't very useful in simulating a whole day. Later on we moved into using the ETAP Real time feature, which allows for one to connect directly to meters and acquire data while running the simulations. Since not all the meters at UCI were working an approach for estimating metered data was accomplished that will be described below.

### 4.2.1 REAL-TIME MODELING

The UCI Microgrid is a unique system that needs to be analyzed using a load flow model for steady state performance characteristics and scenario evaluation. The Real-Time feature of ETAP was used to model the microgrid. A microgrid configuration file, received from UCI Facilities Management, was converted using the ETAP load flow software. The circuits and loads were verified by comparing the results to UCI electrical measurements. Figure 13 is a workflow chart showing how the ETAP model was used.

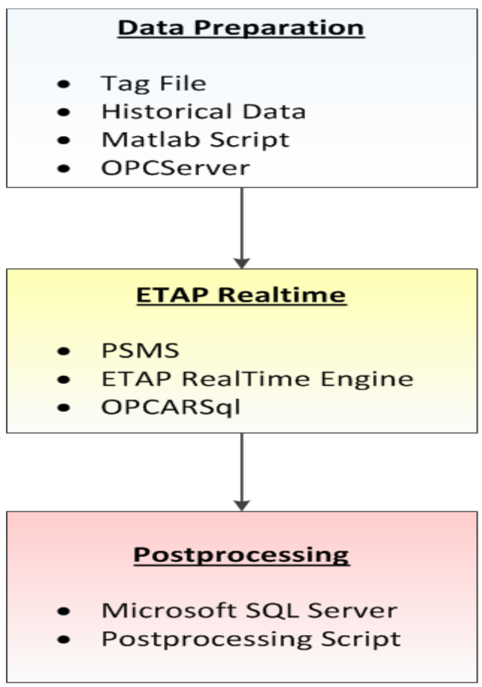


Figure 13: ETAP model workflow

In order to run the model using the ETAP Real Time feature, an input file had to be created. To create the data file, load information for the transformers and a tag file created in ETAP were used in order to link the circuit components in the model to the data. The UCI campus has over 140 building loads 32 of which have meters. The data for the measured loads were obtained from UCI Facilities Management. The remaining loads were estimated. Originally the square footage and building type were used to estimate the unknown loads. However, ETAP has a feature called the State Load Estimator (SLE) that simulates the unknown loads. Those two files were processed in MATLAB using a script that created the input file that was used in ETAP.

The ETAP load flow software performs voltage drop calculations and a power flow analysis. It does this by calculating the bus voltages, branch power factors, currents, and power flows throughout the system. The equations used for these calculations can be found in the voltage drop section of the thesis. An input file created in MATLAB was put into the ETAP Real-Time model that used this load flow analysis and the output data were sent to an SQL server. Another script was written to analyze the data in a usable form. Figure 14 is a screenshot of the output simulation running. Three transformers, T-55, T-56, and T-57 are associated with building, Engineering Gateway. The red in the figure represents the information that are inputted. The green are the data that the ETAP software estimates (voltage, real and reactive power).

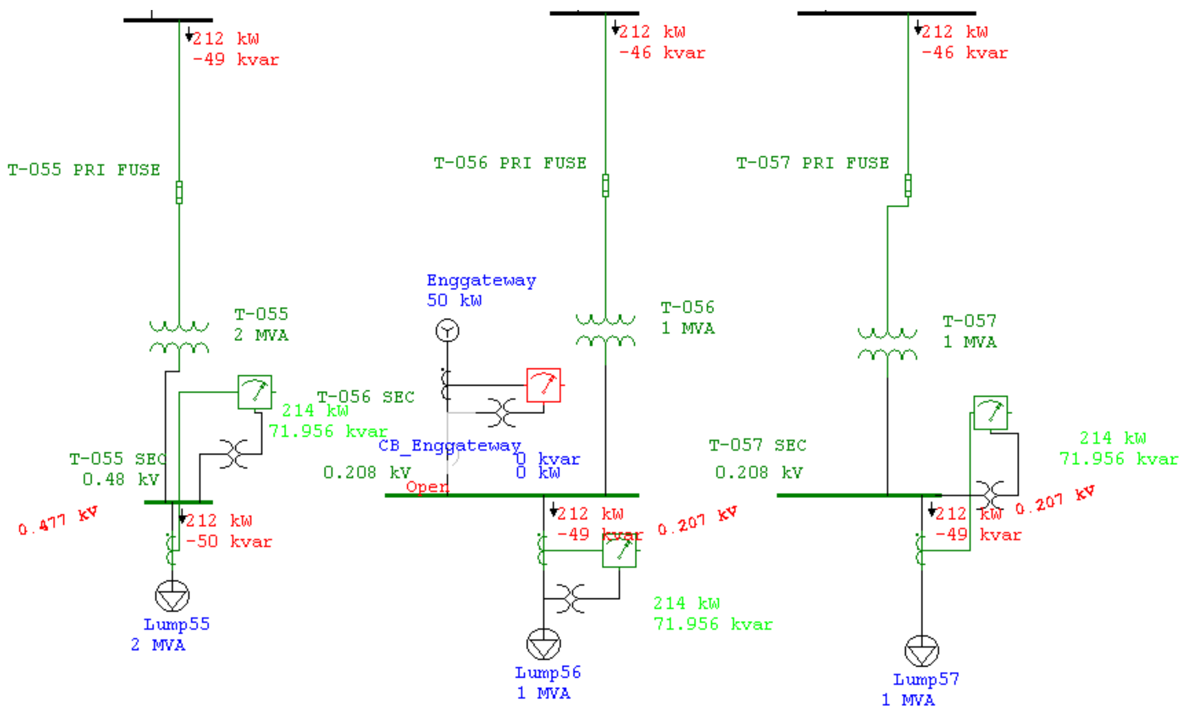


Figure 14: ETAP output of Engineering Gateway

The campus is powered by power generation received from a Combustion Gas Turbine Generator, Photovoltaic systems, a Steam Turbine Generator, and imports from SCE. Figure 15 shows the baseline data used in the model created in ETAP. Note that the total load of the campus during this one day period is relatively flat and between 13 and 17.5 MW. This relatively flat load is created by the campus use of a thermal energy storage (TES) system that stores cold water that is cooled to 39$^{o}$F during off-peak hours (night-time) using the electric chillers of the central plant. The TES tank uses the principle of a thermocline to store hot return water above the chilled water, storing up to 60,000 ton-hours of chilling when fully charged (Brendan P. Shaffer 2013).

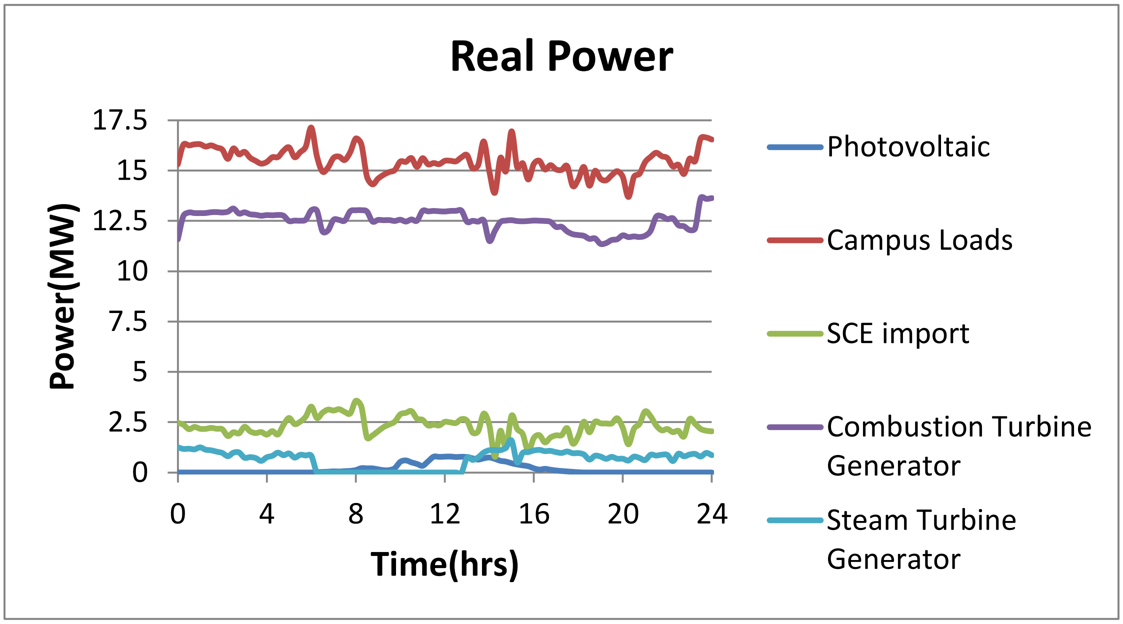


Figure 15: Real Power of the UCI campus

## 4.3 MODELING PLATFORM COMPARISON DEVELOPMENT

In addition to ETAP, MATLAB/Simulink was also utilized to build circuit models for the UCI Microgrid. The initial MATLAB/Simulink model, developed by a previous APEP researcher Dr. Allie Auld, was designed as a dynamic model (capturing waveform level of detail) of a multi-bus radial circuit system (A. E. Auld 2010). The model included load currents and bus voltages as inputs for each of the nine circuits. The model was able to simulate inverters and active power filters, and to create the outputs which were the line voltages as well as the real and reactive power in the microgrid circuits. While the MATLAB/Simulink model is computationally intensive, the capability provides a valuable tool for dynamic insights and quality control, and is a good complement to ETAP.

ETAP was selected as the principal modeling platform. The most challenging part of configuring ETAP for the Car Shade project simulation was the development of a 4-port inverter model. A DC to DC converter was created in order to model that inverter. In contrast to the MATLAB/Simulink model, the ETAP UCI Microgrid model runs in a matter of seconds, an attribute that is particularly attractive for steady-state analyses.

# 5 TASK 2: ANALYZE DATA RECEIVED FROM SOUTHERN CALIFORNIA EDISON

To evaluate the model performance, the Car Shade system data acquired by SCE were analyzed for consistency and accuracy, and then was used as appropriate to evaluate deficiencies and inaccuracies in the simulation results. Two sets of data were used:

- First Set: April 8, 2014
- Second Set: June 17, 2014

Examples of plug-in electric vehicles using the Car Shade chargers during this period include:

- The Chevy Volt
- The Nissan Leaf
- The Toyota Prius

## 5.1 FIRST SET OF DATA

The following is an analysis made of one week (April 6, 2014 until April 12, 2014) of BESS and grid power data provided by SCE in fifteen minute increments. Figure 16 shows the total power received for an entire day. The BESS has a maximum power of 100kW and as the figure shows it reaches a peak of about 36kW between 11am and 12pm.

As described in the introduction, the BESS is charged by the PV power. The BESS and PV are connected to two ports of the inverter. This power is shown as the grid data in the figures mentioned later on in this section. The grid data do not mean that the power is being imported from the grid but it means that it is the export of the combination between the BESS and the PV.  Because the PV power is charging the battery and excess power is being exported, Figure 17 is the inverse of Figure 16.

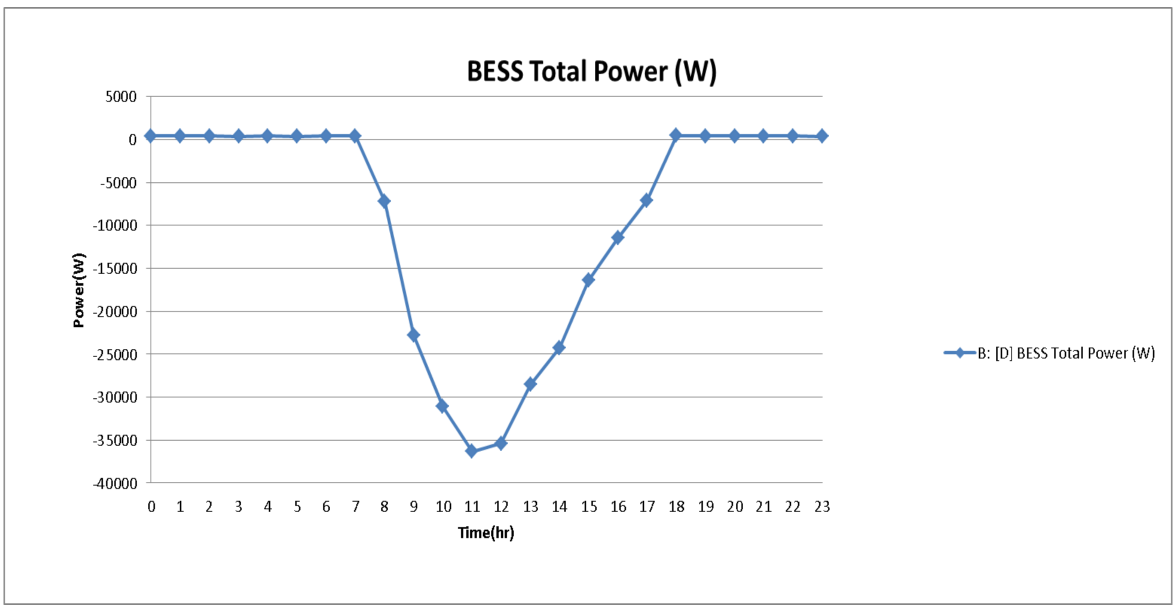


Figure 16: BESS Total Power for April 7, 2014 (Southern California Edison 2014)

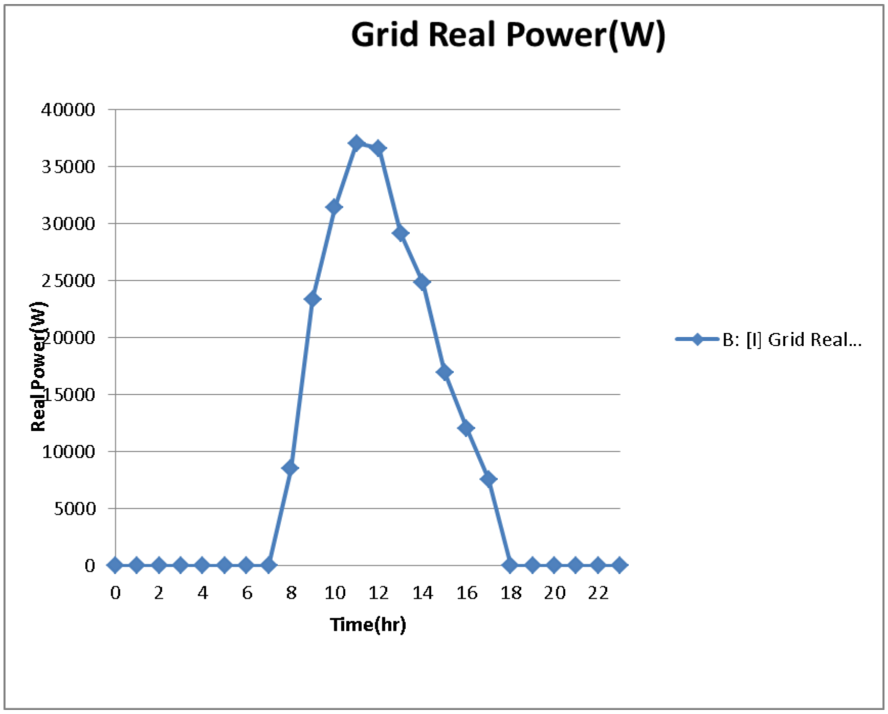


Figure 17: Grid Power for April 7, 2014 (Southern California Edison 2014)

### 5.1.1 Summer time data (July 14, 2014)

The data from July 14, 2014, is presented to describe the performance of the various components of the Car Shade system during the summer. The data from Figure 18 shows that between 2pm and 4pm the solar power is at its maximum. It is likely that limited cloud coverage was in effect before this time since the power has a small dip.

The data from Figure 19 represent the export from the BESS that goes into the EVSE chargers. Figure 20 shows the total power that is consumed from the 20 electric vehicle chargers. It reaches a maximum around 10am and you start to see the number of cars charging decrease as the day goes on. Around 5pm there is a peak in the data and that corresponds to cars beginning to charge at that time.

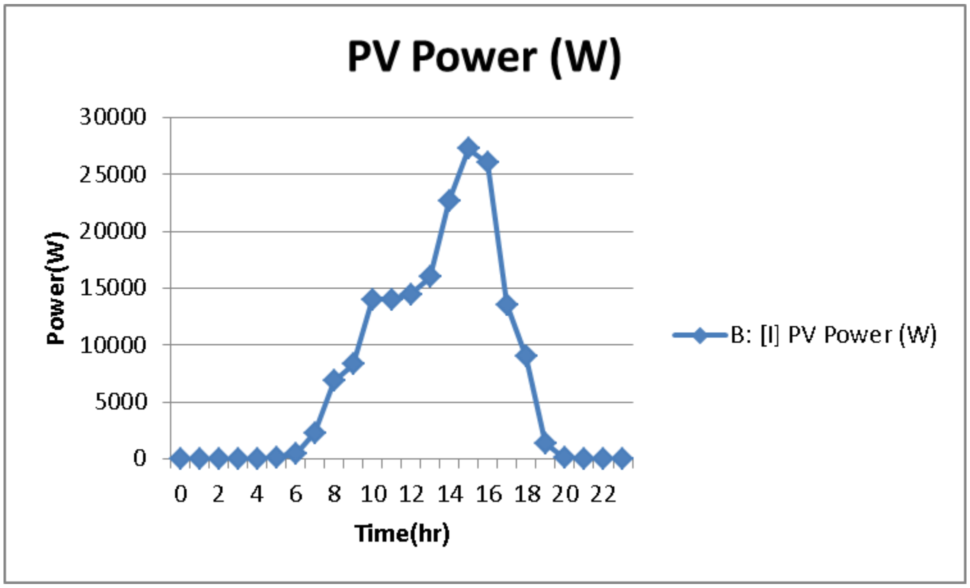


Figure 18: PV power for July 14, 2014 (Southern California Edison 2014)

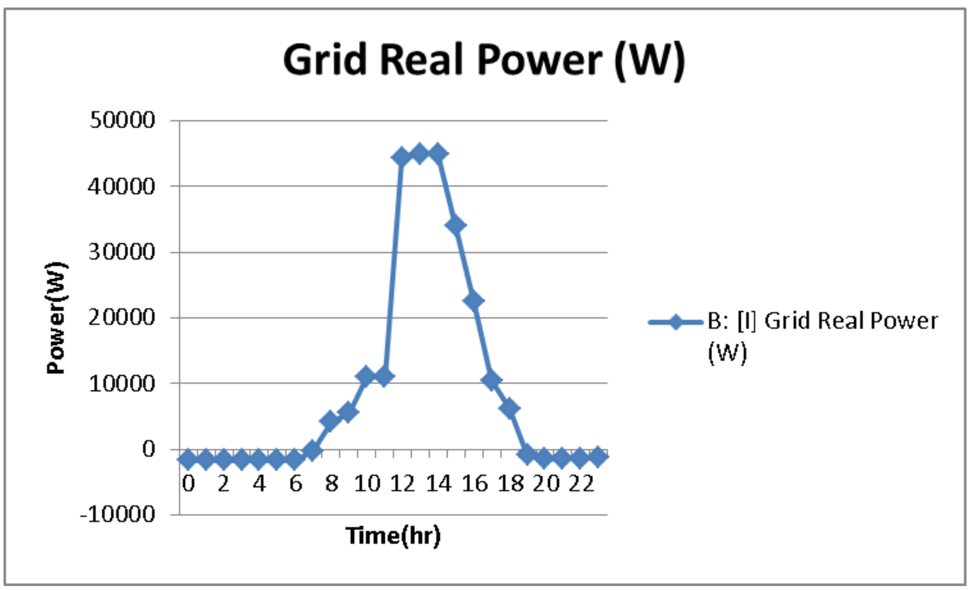


Figure 19: Grid Real Power July 14, 2014 (Southern California Edison 2014)

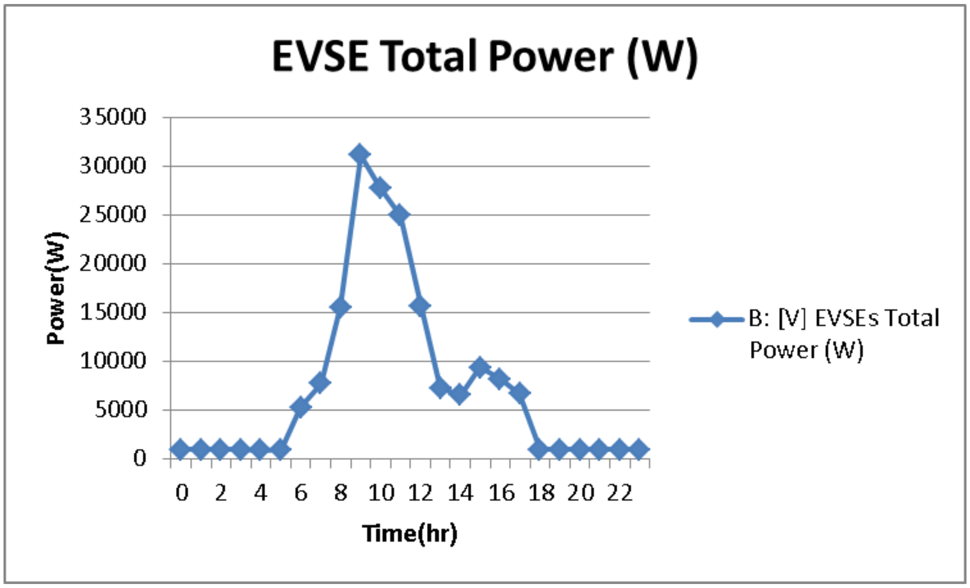


Figure 20: EVSE Total Power for July 14, 2014 (Southern California Edison 2014)

## 5.2 SECOND SET OF DATA

The data presented below are for June 17, 2014.

| Time (PDT) | Temp. | Conditions |
|---|---|---|
| 12:53 AM | 66.9 °F | Clear |
| 1:53 AM | 66.0 °F | Clear |
| 2:53 AM | 66.0 °F | Clear |
| 3:17 AM | 66.2 °F | Mostly Cloudy |
| 3:53 AM | 66.0 °F | Overcast |
| 4:53 AM | 66.0 °F | Overcast |
| 5:53 AM | 66.0 °F | Mostly Cloudy |
| 6:53 AM | 66.9 °F | Mostly Cloudy |
| 7:53 AM | 68.0 °F | Mostly Cloudy |
| 8:53 AM | 70.0 °F | Scattered Clouds |
| 9:00 AM | 69.8 °F | Mostly Cloudy |
| 9:23 AM | 71.6 °F | Scattered Clouds |
| 9:53 AM | 72.0 °F | Scattered Clouds |
| 10:53 AM | 73.0 °F | Scattered Clouds |
| 11:53 AM | 73.9 °F | Scattered Clouds |
| 12:53 PM | 73.9 °F | Scattered Clouds |
| 1:53 PM | 75.0 °F | Partly Cloudy |
| 2:53 PM | 75.0 °F | Partly Cloudy |
| 3:53 PM | 73.0 °F | Partly Cloudy |
| 4:53 PM | 72.0 °F | Partly Cloudy |
| 5:53 PM | 71.1 °F | Partly Cloudy |
| 6:53 PM | 69.1 °F | Partly Cloudy |
| 7:53 PM | 66.9 °F | Partly Cloudy |

Table 3 shows the temperature as well as cloud coverage for June 17, 2014 in Irvine. These data provide some insights into the rooftop solar generation, and enable a qualitative association of power drops with cloud coverage. Figure 21 shows a representation of the inputs and outputs that correspond to the Car Shade system.

| Time (PDT) | Temp. | Conditions |
|---|---|---|
| 12:53 AM | 66.9 °F | Clear |
| 1:53 AM | 66.0 °F | Clear |
| 2:53 AM | 66.0 °F | Clear |
| 3:17 AM | 66.2 °F | Mostly Cloudy |
| 3:53 AM | 66.0 °F | Overcast |
| 4:53 AM | 66.0 °F | Overcast |
| 5:53 AM | 66.0 °F | Mostly Cloudy |
| 6:53 AM | 66.9 °F | Mostly Cloudy |
| 7:53 AM | 68.0 °F | Mostly Cloudy |
| 8:53 AM | 70.0 °F | Scattered Clouds |
| 9:00 AM | 69.8 °F | Mostly Cloudy |
| 9:23 AM | 71.6 °F | Scattered Clouds |
| 9:53 AM | 72.0 °F | Scattered Clouds |
| 10:53 AM | 73.0 °F | Scattered Clouds |
| 11:53 AM | 73.9 °F | Scattered Clouds |
| 12:53 PM | 73.9 °F | Scattered Clouds |
| 1:53 PM | 75.0 °F | Partly Cloudy |
| 2:53 PM | 75.0 °F | Partly Cloudy |
| 3:53 PM | 73.0 °F | Partly Cloudy |
| 4:53 PM | 72.0 °F | Partly Cloudy |
| 5:53 PM | 71.1 °F | Partly Cloudy |
| 6:53 PM | 69.1 °F | Partly Cloudy |
| 7:53 PM | 66.9 °F | Partly Cloudy |

**Table 3: Weather Information (Wunderground 2014)**

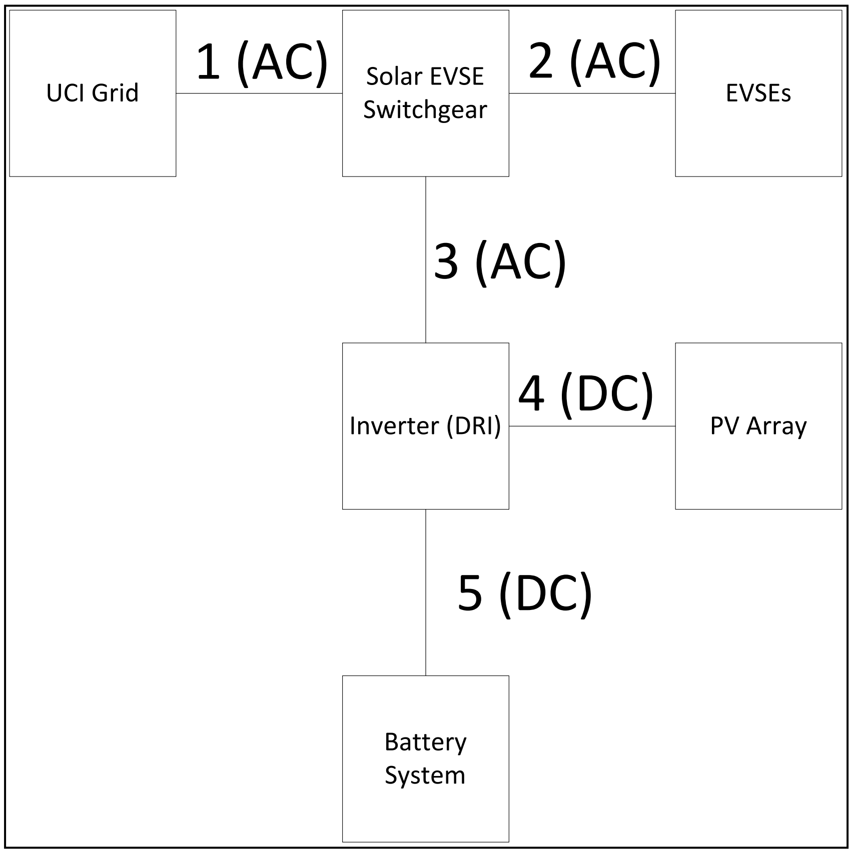


Figure 21: Car shade diagram showing five (5) measurement points.

### 5.2.1 DC Measurements

#### 5.2.1.1 BESS Measurements

**Error! Reference source not found.** and Figure 23 correspond to point number 5 of Figure 21, which is the DC side of the figure prior to the inverter. **Error! Reference source not found.** shows a drop in voltage between midnight and 6:00am that is associated with the battery being charged by the grid. The voltage increases exponentially between 6:00am and

12:00pm consistent with the PV and EVSE voltages shown in the figures below. Between 12:00pm and 8:00pm the BESS starts to discharge due to the EVSE using the battery power. From 8:00pm to midnight the BESS goes into a PLS dispatch that is concurrent with the current and power in Figure 23 and Figure 24 for that same range of time.

Figure 23 shows that from midnight to 6:00am the battery is being powered by the grid. From 6:00am to 12:00pm the battery power and current are zero which is associated to the PV and grid being the primary sources of power for the EVSE and the battery being in PLS mode. The dip at 1pm is associated with the EVSE using the battery's power and it starts to go up slowly since PV is on, the spike around 7pm is associated with the PLS mode turning on which leads to the current going back to zero is the result of **Error! Reference source not found.** and Figure 23 that can be calculated using Equation 2.

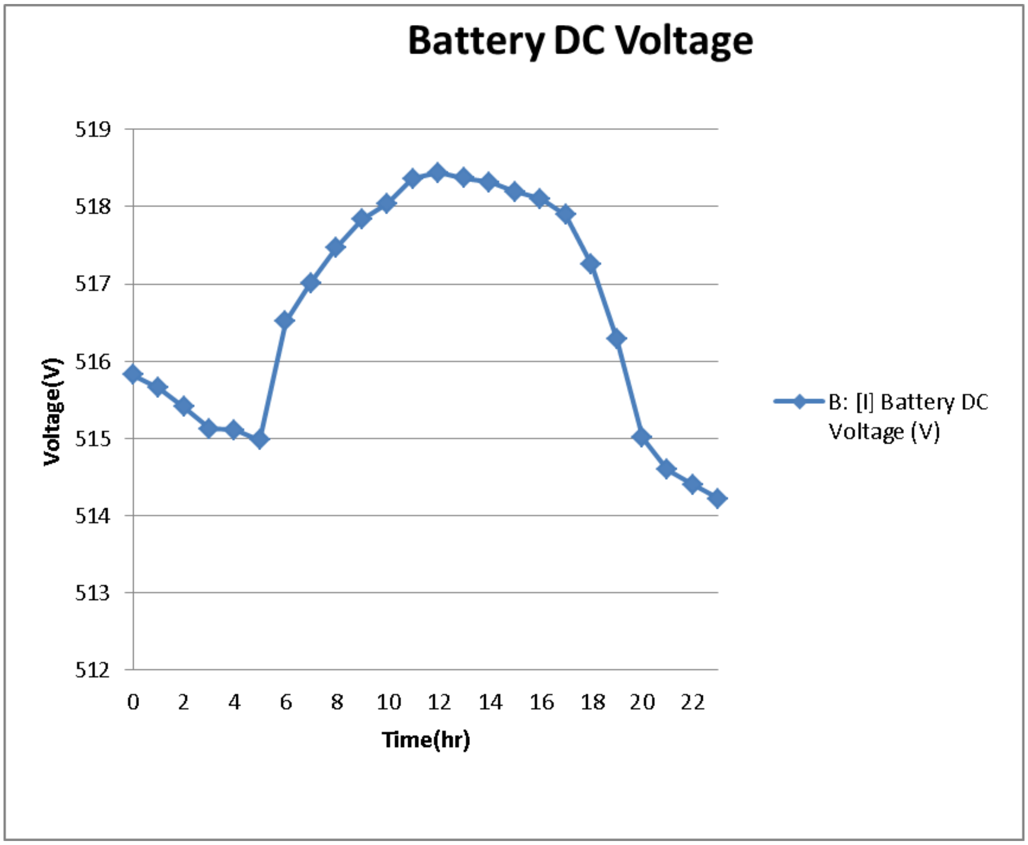


Figure 22: BESS DC Voltage

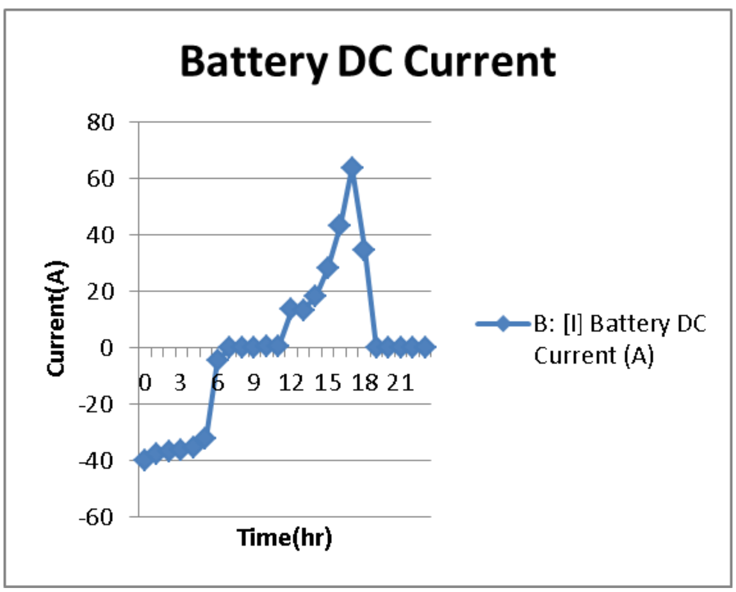


Figure 23: BESS DC Current (Southern California Edison 2014)

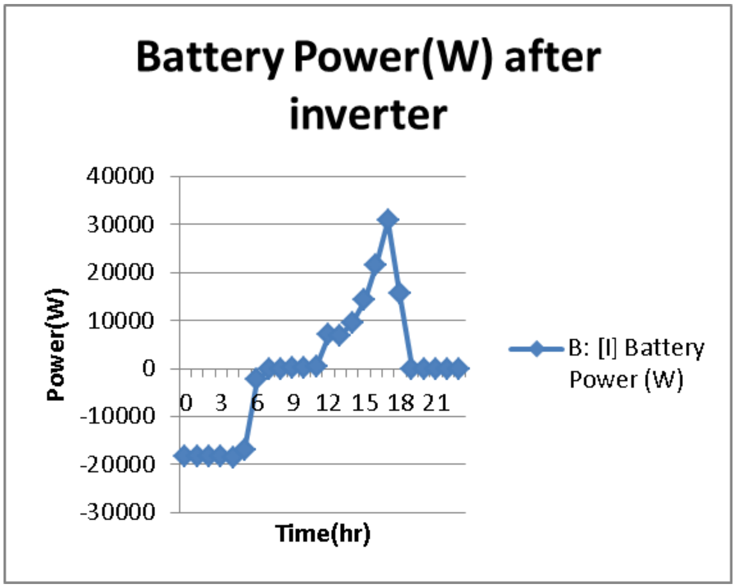


Figure 24: BESS power before the inverter (Southern California Edison 2014)

#### 5.2.1.2 PV measurements

The current and voltage inputs associated with the photovoltaic panels, required for point measurement 4 of the Car Shade diagram (Figure 21), are presented in Figure 25 and Figure 26. In measurement 3 of Figure 21, the DC components go into the inverter. This produces the AC current measurements seen in Figure 33 that go into the grid. From midnight to 6:00am there is an average of 25A coming from the grid to charge the battery. Between 6:00am and 8:00am the grid is providing 10A and then it switches direction as can be seen in Figure 35 at 6:00am. The switching of the direction means that the grid is taking power out of the BESS, the current between 8:00am and 12:00pm is only coming from the PV and at 12:00pm there is a summation of current coming from the BESS and the PV. The current starts to drop after 8pm and stays at a constant 10A due to the BESS going into the PLS mode.

Due to the cloud coverage in the morning the current and voltage take a dip between 7:00am and 9:00am. Other than that small dip the solar current looks ideal. The voltage is mostly flat between 9:00am and 8:00pm and an ideal voltage plot with no losses would have a completely flat line. Around noon, when the solar radiation is highest, the PV generation reaches a peak of 43kW. The panels have a maximum rated capacity of 45kW.

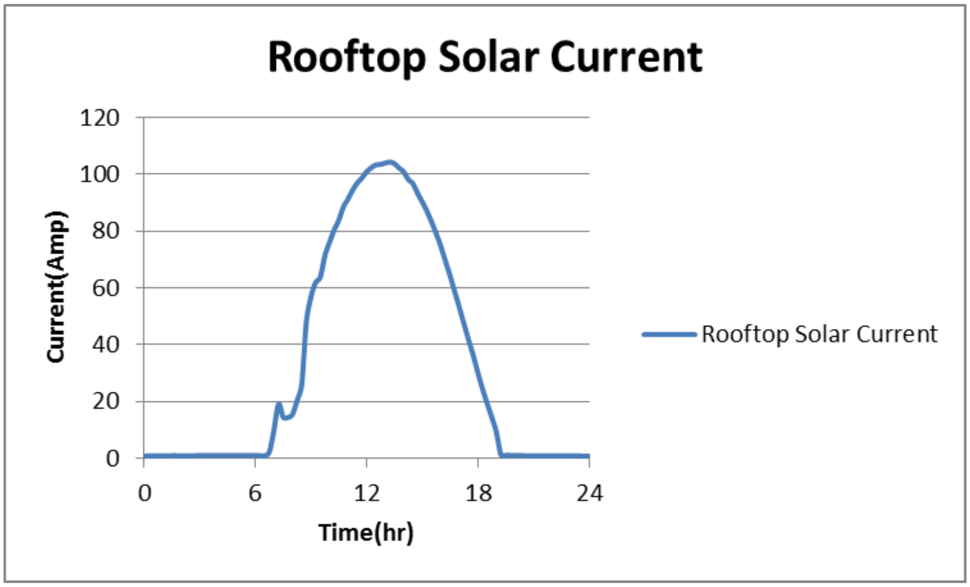


Figure 25: DC PV current

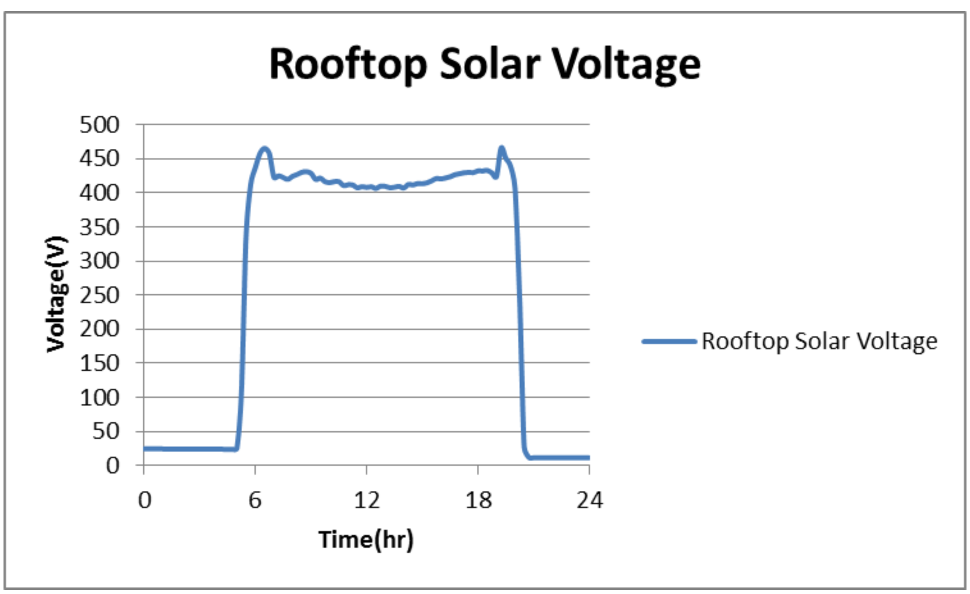


Figure 26: DC Voltage for PV

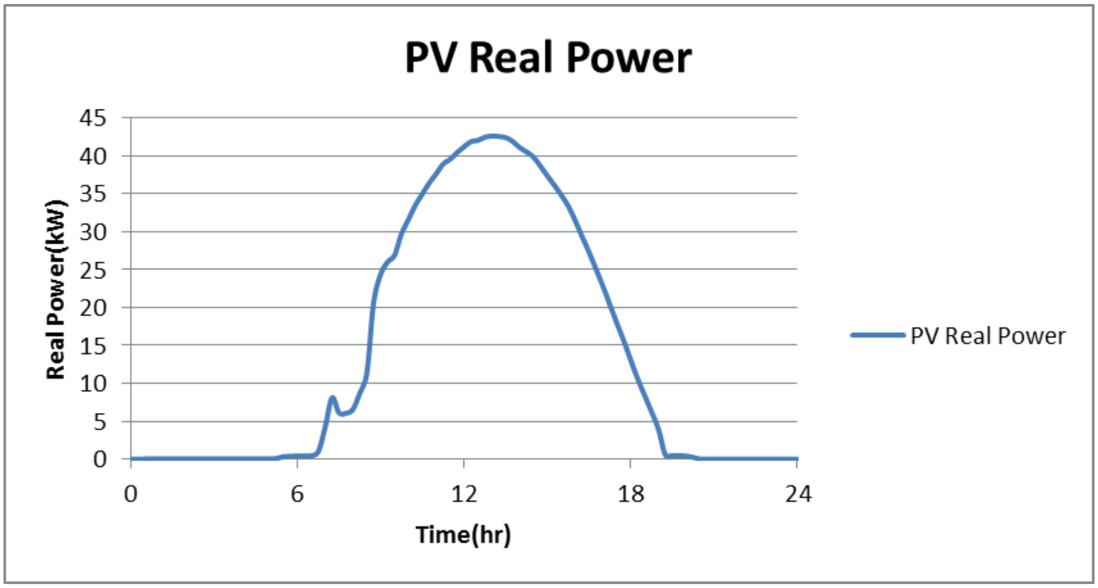


Figure 27: PV Power

The morning of June 17, 2014 was slightly cloudy as shown in Table 3, this can be seen in Figure 27 between 7:00am and 9:00am as a rapid change in the power production.. Around noon, when the solar radiation is highest, the PV generation reaches a peak of 43kW. The panels have a maximum rated capacity of 45kW. On an occasion where there is no cloud coverage, a completely smooth PV output curve can be produced. This can result in up to an 80% loss of power output in seconds. Cloud coverage poses a threat to grid stability at high penetrations.

### 5.2.2 AC Measurements

#### 5.2.2.1 BESS measurements

Figure 28 and Figure 29 represent the data acquired at measurement point number 3 from Figure 21. The values are in AC since they are measured after the inverter.

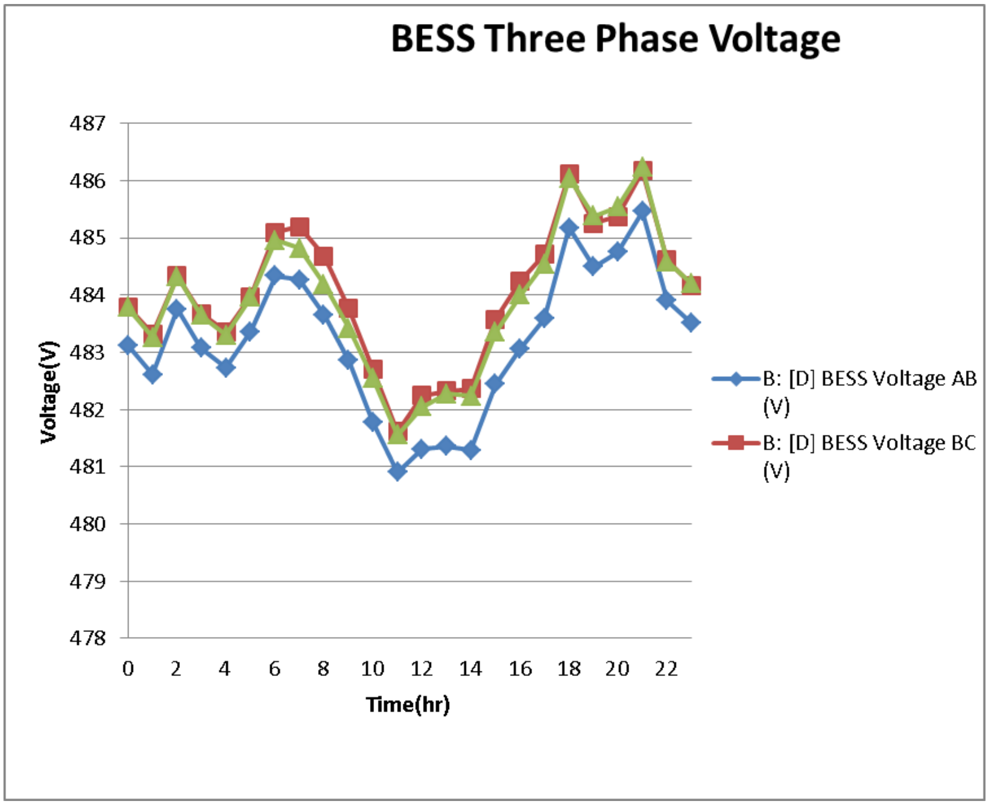


Figure 28: BESS AC Voltage (Southern California Edison 2014)

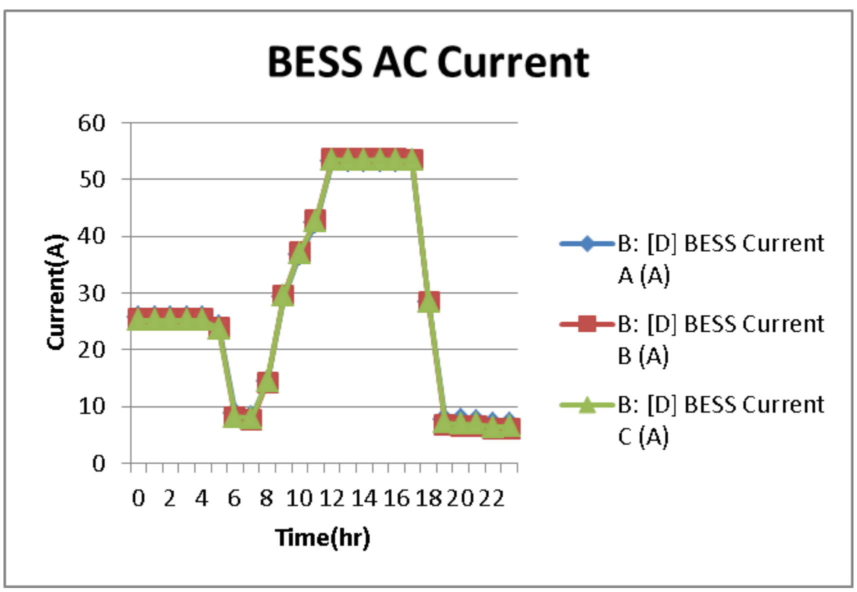


Figure 29: BESS AC Current (Southern California Edison 2014)

The BESS voltage is relatively constant between midnight and 6:00am since it is being charged at 20kW as presented in Figure 31 for that same time period. Between 6:00am and

12:00pm the voltage starts to drop since the battery power isn't being used to charge the EVSE. After 12:00pm the voltage starts to increase and this is due to the combined discharging of the battery and the PV power in order to charge the electric vehicles. After 8:00pm the battery goes back into the PLS mode giving it a more variable voltage. Figure 29 shows that it is in PLS operating mode from 8:00pm to 5:00am which gives the constant current average of 25A. Between 6:00am and 12:00pm the battery's state of charge is at 100% as can be seen in Figure 30 and during that time the PV and the grid are used to charge the EVSE that are shown in Figure 36. The smooth curve that we get between 6:00am and 12:00pm is the result of the summation of the solar and EV chargers. Between 12:00pm and 8:00pm the battery is switched back into the PLS operating mode resulting in a constant current.

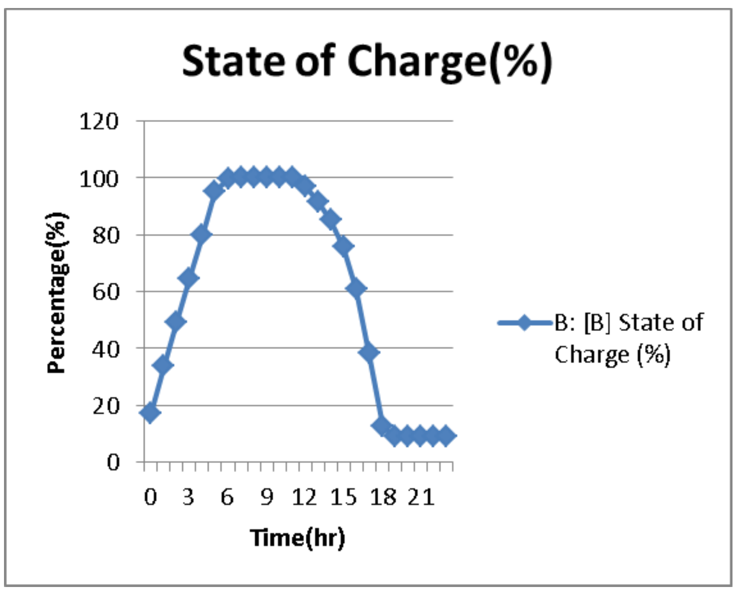


Figure 30: BESS State of Charge (Southern California Edison 2014)

A constant discharge strategy is used in Figure 30 known as the PLC operation mode; this is used to extend the length of time the battery is available to provide power to the EVSE. Applying this constant power discharge strategy helps in reducing the steep ramp that occurs between 12:00pm and 8:00pm.From midnight to 6:00am the battery is charged by the grid. Between 6:00am and 12:00pm the battery stays at 100% state of charge because the PV is providing all the power to the EVSE so you don't need to discharge the battery. The amount of power needed for the EVSE goes down at noon as can be seen in Figure 36. This means that the battery goes into PLS dispatch at noon to conserve the power. The battery then begins to discharge is part of the EVSE since it is using the battery power.

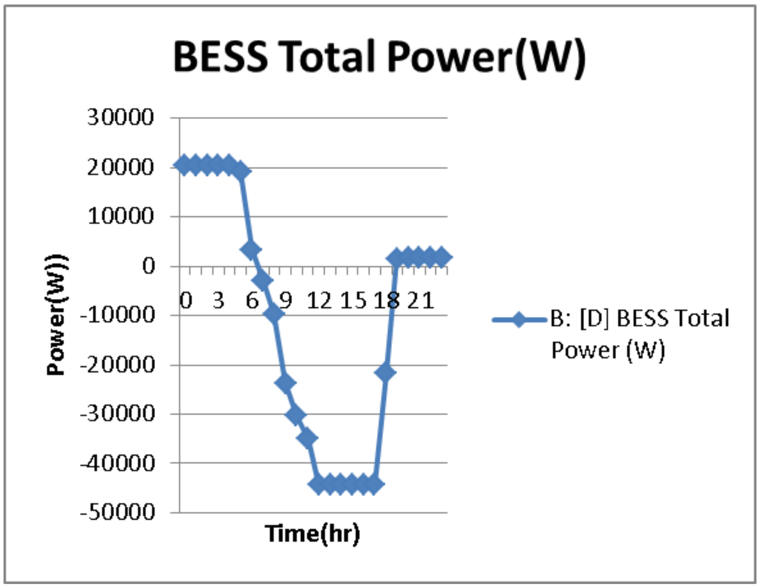


Figure 31: BESS Total Power after the inverter (Southern California Edison 2014)

Figure 31 and Figure 32 represent the real and reactive power of the BESS after the inverter. Figure 31 shows a correlation with the state of charge percentage represented in Figure 30. Power is going into the battery between midnight and 6:00am and this correlates with Figure 30 as it shows that the battery starts to charge during that same time period. From 6:00am to 8:00am is starts heading to 0 which means that it is in a state of fully charge. Some of the power is leaving the BESS mainly from the solar until you get to 12:00pm, after that you see an additional amount being dispatched by the battery.  The dispatch from the system is coming from the PV and after noon it's a combination of the PV and the battery.

Figure 32 shows that the BESS operates at a constant reactive power level of about 600 VAR from midnight to 7:00am when power is going into the battery. It operates  at an average of  between 6000-7000 VAR when the PV is on before it drops back to down to 600VAR when it enters the PLS mode.

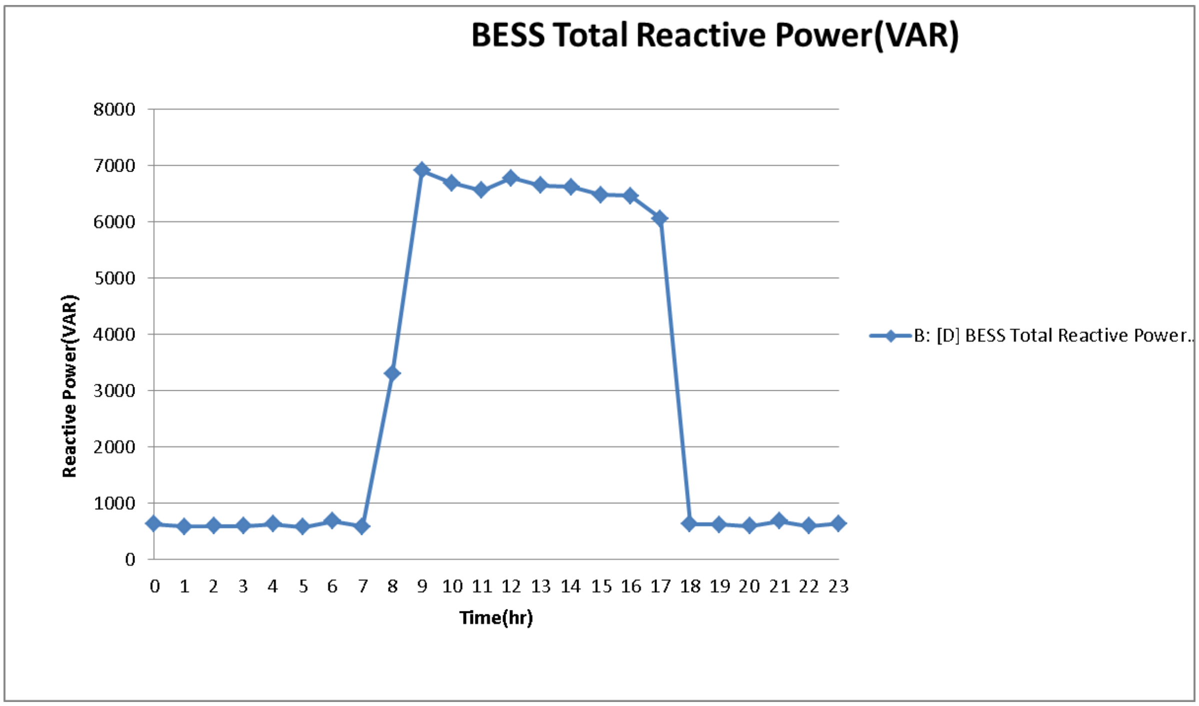


Figure 32: Reactive Power after the inverter (Southern California Edison 2014)

### 5.2.2.2 Grid Measurements

In measurement 3 of Figure 21, the DC components go into the inverter. This produces the AC current measurements seen in Figure 33 that go into the grid. From midnight to 6:00am there is an average of 25A coming from the grid to charge the battery. Between 6:00am and

8:00am the grid is providing 10A and then it switches direction as can be seen in Figure 35 at 6:00am. The switching of the direction means that the grid is taking power out of the BESS, the current between 8:00am and 12:00pm is only coming from the PV and at 12:00pm there is a summation of current coming from the BESS and the PV. The current starts to drop after 8pm and stays at a constant 10A due to the BESS going into the PLS mode.

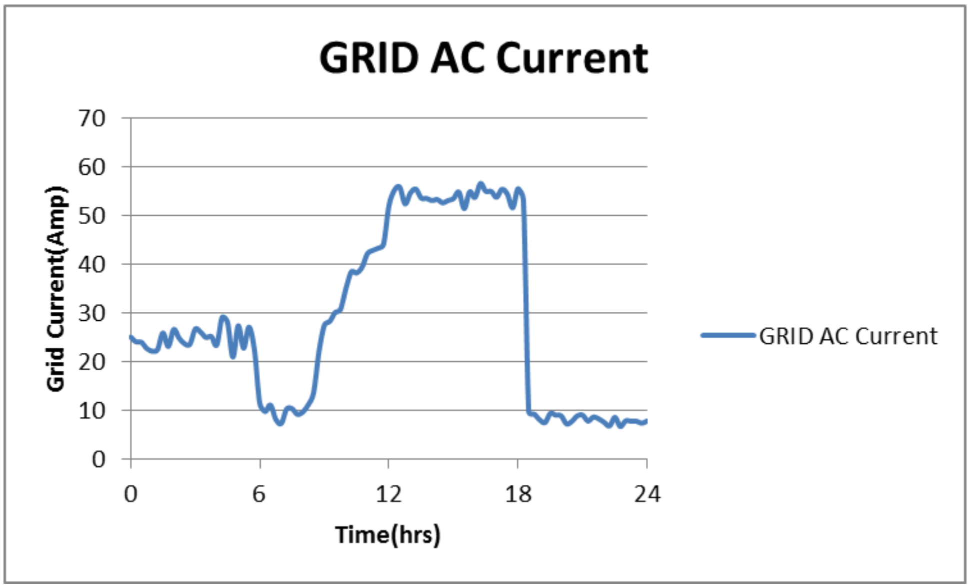


Figure 33: AC Grid current

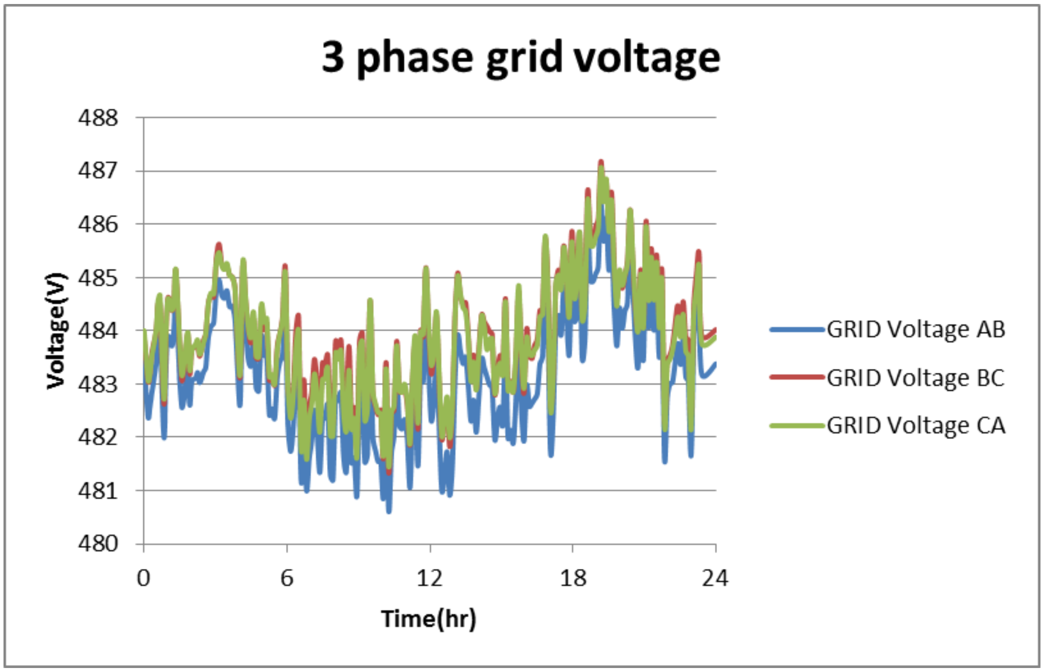


Figure 34: AC voltage to the grid

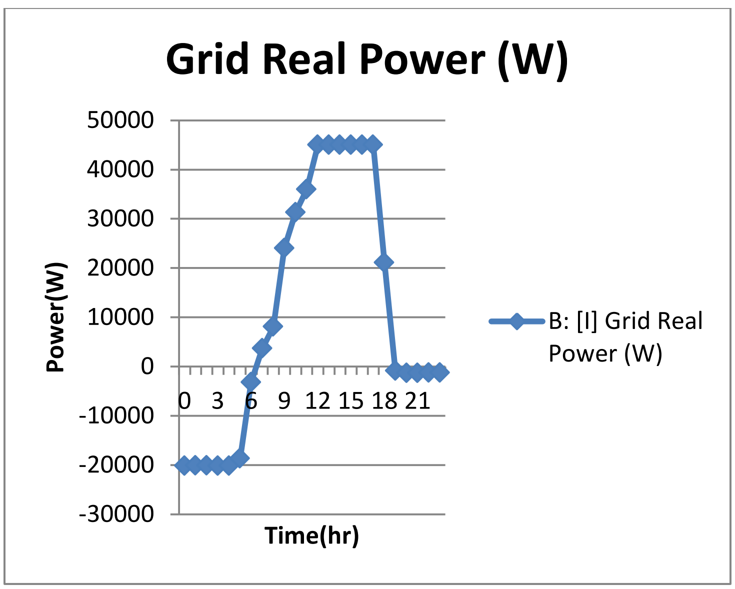


Figure 35: Real Power coming from the inverter to the grid

Figure 34 shows a relatively constant voltage at about 484V between midnight and 6:00am that corresponds to the grid powering the battery during that time period. Between 6:00am and 9:00pm the voltage starts to slowly increase, this is due to the discharging of the battery in order to charge the electric vehicles. It then starts to drop as the battery goes into PLS mode.

Between midnight and 6:00am the grid powers the battery at 20kW. Between 6am and 9am there is a small increase in power that is associated with the EVSE total power during the same points in time. Between 9:00 am and 12:00pm the grid power is showing the PV that is being used to charge the EVSE as seen in Figure 36 . Between 12:00pm and 8:00pm the BESS power that was stored is being used to charge the rest of the remaining EVSE vehicles during that time period along with the remaining solar power. After 8:00pm the grid shows a value of zero due to the BESS being in PLS mode.

#### 5.2.2.3 EVSE Measurements

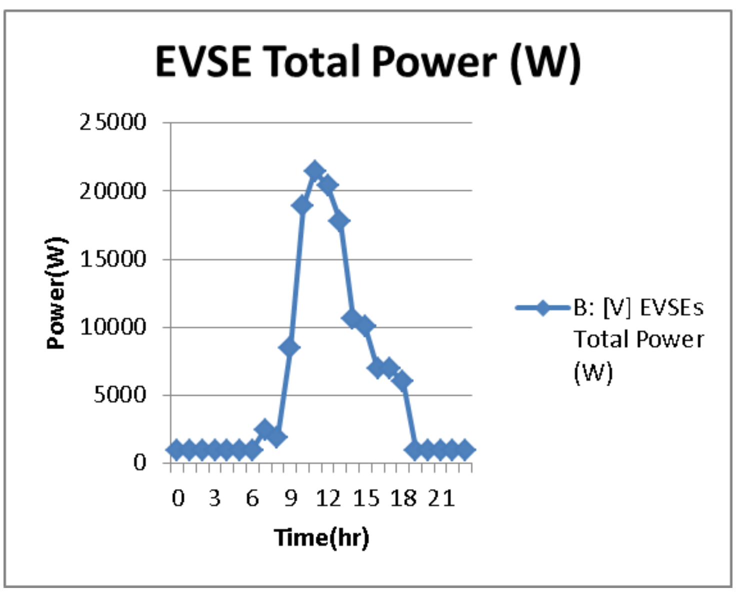


Figure 36: EVSE Total Real Power (Southern California Edison 2014)

The EV's are primarily charged from the solar and the grid between 6:00am and 12:00pm. After 12:00pm the BESS starts to discharge due to the EV's using the power. At

8:00pm there are no more EV's in the parking lot so the BESS switches to PLS mode. The reactive power is steady from midnight until about 9:00am, after that it starts to sporadically spike up and down and this is due to the various cars plugging in and out of the charging station. The reactive power dips down between 12:00pm and 3:00pm which is when the most power was being used to power the vehicles. After 8:00pm the reactive power goes back to a minimum level and the BESS switches to PLS mode.

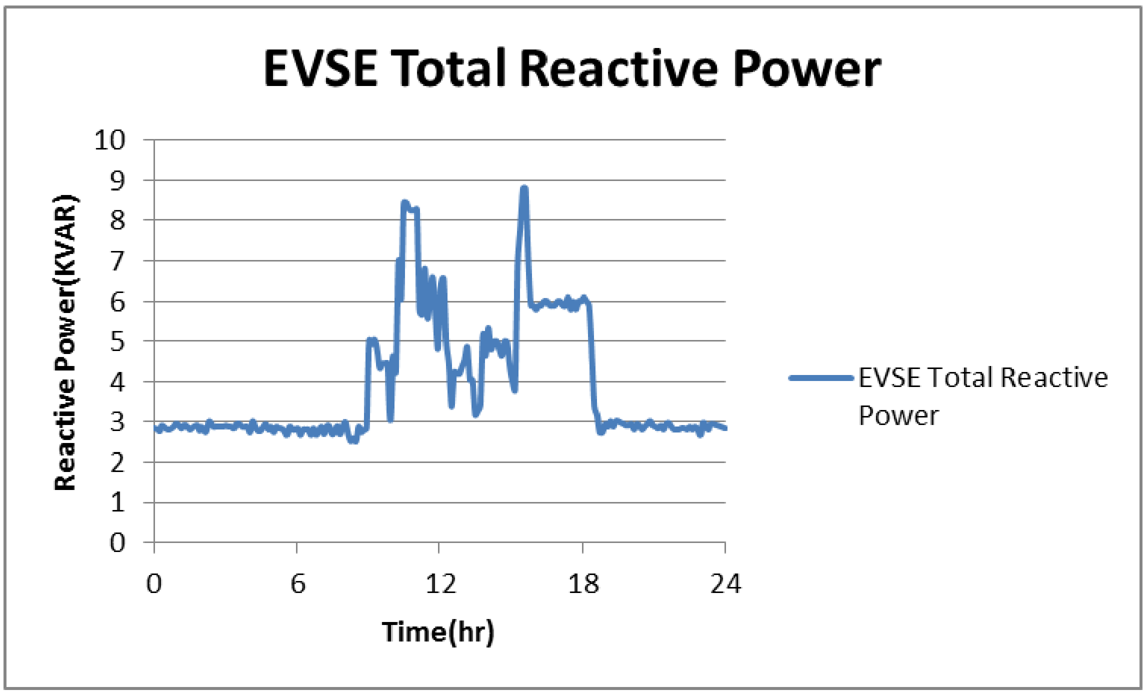


Figure 37: EVSE Total Reactive Power

# 6 TASK 3: MODEL VERIFICATION

## 6.1 INITIAL MODEL VERIFICATION

In Figure 38, the generation on campus along with the total campus load and Southern California Edison import for April 16, 2012 are presented. The total load for the campus is approximately 15MW. In order to sustain the load, the two 24/7 generators on campus are used to provide power along with the photovoltaic. The figure shows that the photovoltaic power is higher in the afternoon and drops to zero in the morning and in the evening. The Southern California Edison import is used to provide the extra power needed to support the load.

Figure 39 shows the UC-9 data from the ION metering system compared to the ETAP UC-9 real power simulation. The ETAP simulation results used ION input data from the buildings in the UC-9 circuit as well as estimated values. Note, that the Amonix panels are installed on UC-9. Since the ION measurements did not include power generation from the Amonix panels, the ETAP predicted real power is lower than that of the ION measurements in the period when Amonix solar power is produced.

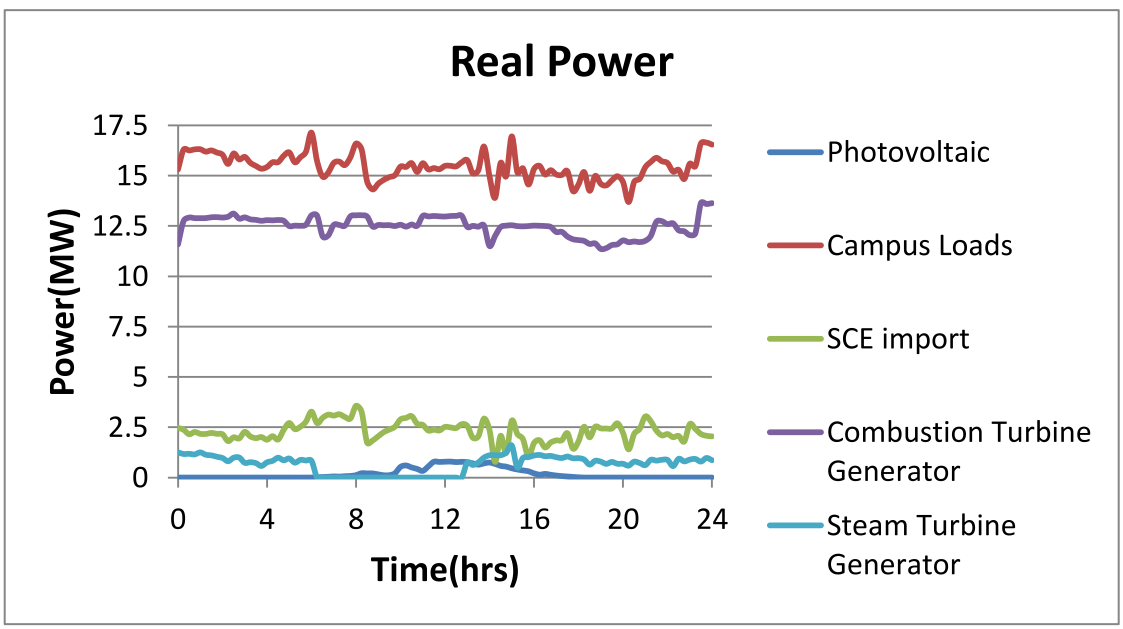

Figure 38: Real Power of the UCI campus

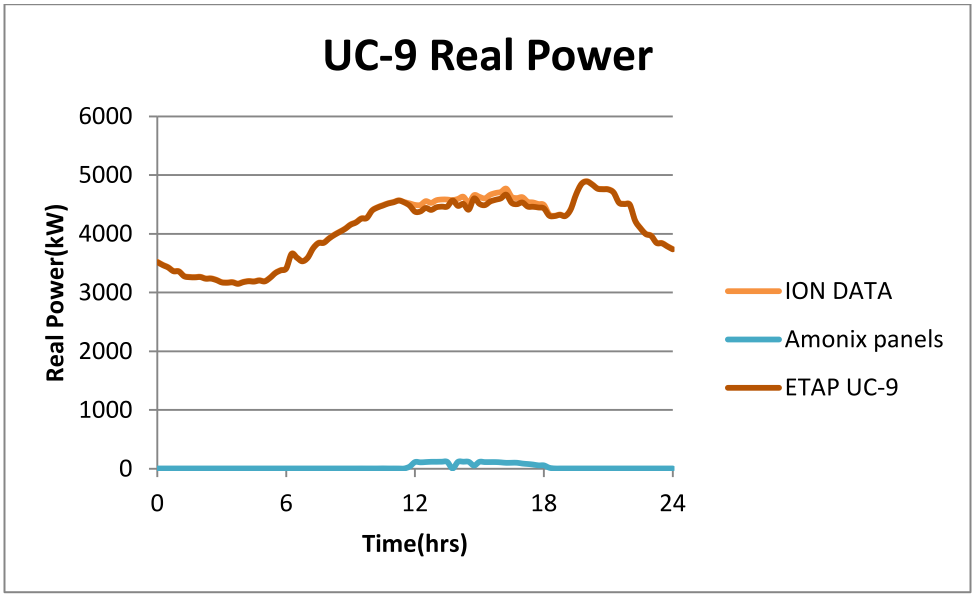


Figure 39: UC-9 Real power comparisons

## 6.2 BASELINE MODEL VERIFICATION

The ETAP load flow module was used to create and verify the model that includes the entire UCI microgrid along with the Car Shade components. The analysis calculates the bus voltages, currents, branch power factors, and power flows throughout the entire electrical system. For the purpose of the scenarios that will be described later on, the warnings that the analysis gives for possible transformer overloads is very helpful. The power flow can also be calculated and used to evaluate the system performance (ETAP 2009).

The model converges by running the load flow analysis and generating an output report that is presented in Figure 60, located in the Appendix. This output report shows the load flow for the circuit and the percentage that the voltage differs between the measurement and the simulation. The voltage difference was found to be less than 2% at all measurement locations (as shown in Table 4 of the Appendix). From this result it was concluded that the model was verified.

## 6.3 BASELINE MODEL RESULTS

Figure 40 presents a section of the Car Shade model. T-131 PRIMARY is the bus that connects to the transformer serving the Anteater Parking Structure. Bus42 is the section that serves the loads in the building adjacent to and integrated into the parking structure. The Car Shade system is also connected to Bus 42 and then is broken down according to the Car Shade one-line diagram representation shown in Figure 40.

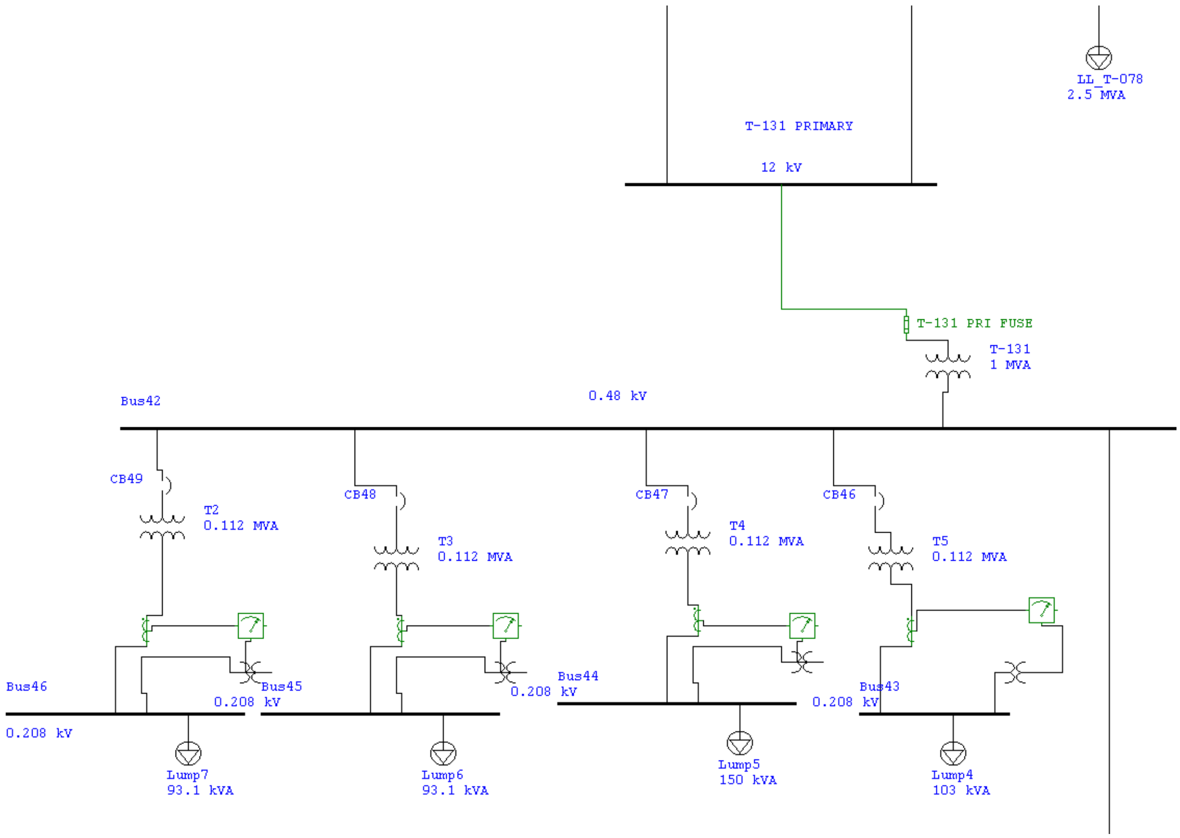


Figure 40: Section of ETAP model corresponding to the buses of interest

## Load profile for Anteater Parking Structure and AIRB

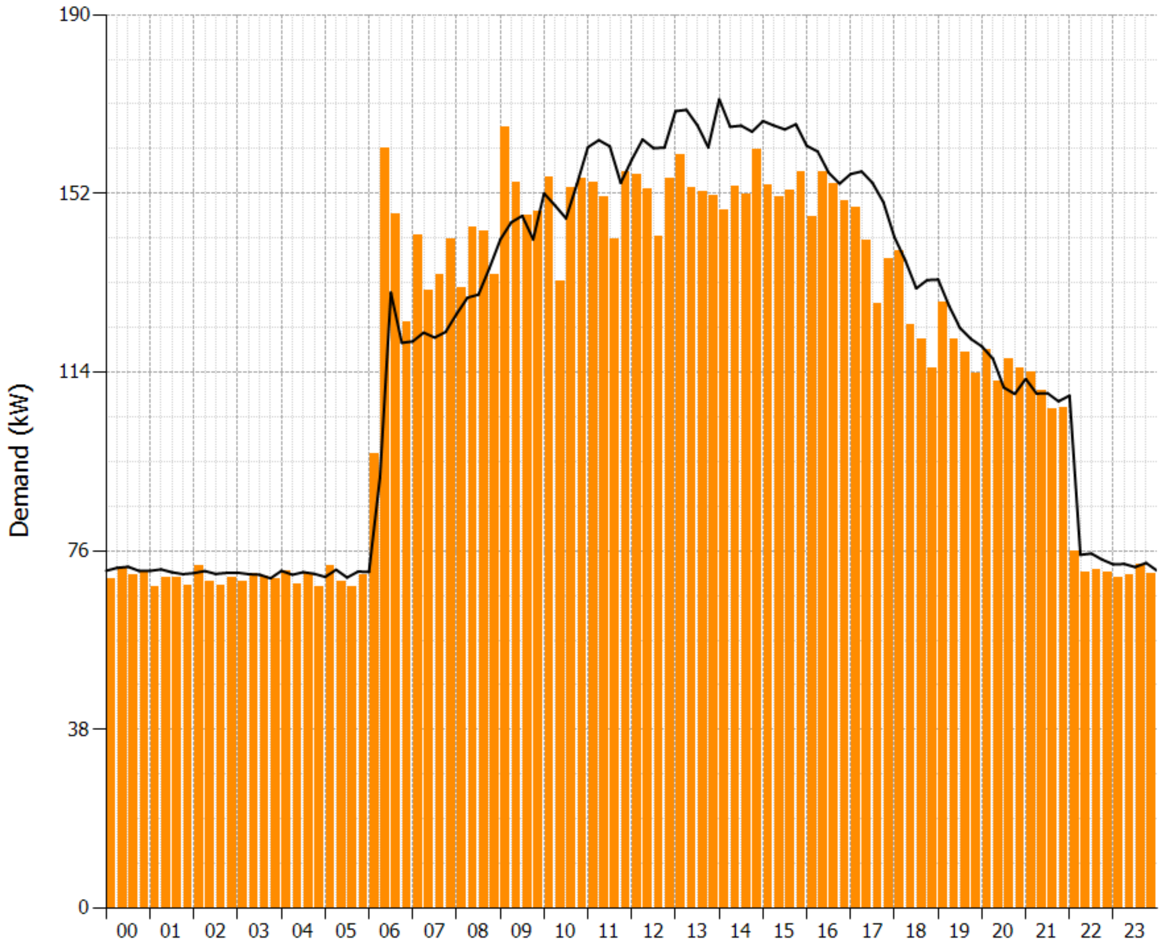


Figure 41: Load profile for the parking structure without car shade components (MelRok 2014)

The load in Figure 41 is representative of all the power that comes from the transformers connected to Bus 42. The bars represent the loads at each fifteen minute interval and the line throughout it is the average within the day. These data also includes the loads in the adjacent building which is called the anteater instruction and research building (AIRB).

Figure 42 is a comparison of the output voltage calculated by the ETAP Car Shade model and the actual data. This voltage is of interest since it is affected when a change in the magnitude of the battery or PV power occurs. Currently the voltage is stable it is only off from the actual data by less than 5%.

The voltage comparisons in Figure **43** correspond to the section that is not a part of the Car Shade infrastructure. This voltage provides insights in seeing if the elements of the Car Shade system are the source of fluctuations in the rest of the system. Figure 44 shows the starting point of the model that starts at the 66kV substation. Figure 45 presents the output voltage comparisons from the model and the actual data. The transformer can only go up to 66kV and this comparison shows that the measured data do not alter too drastically but the voltage does drop.

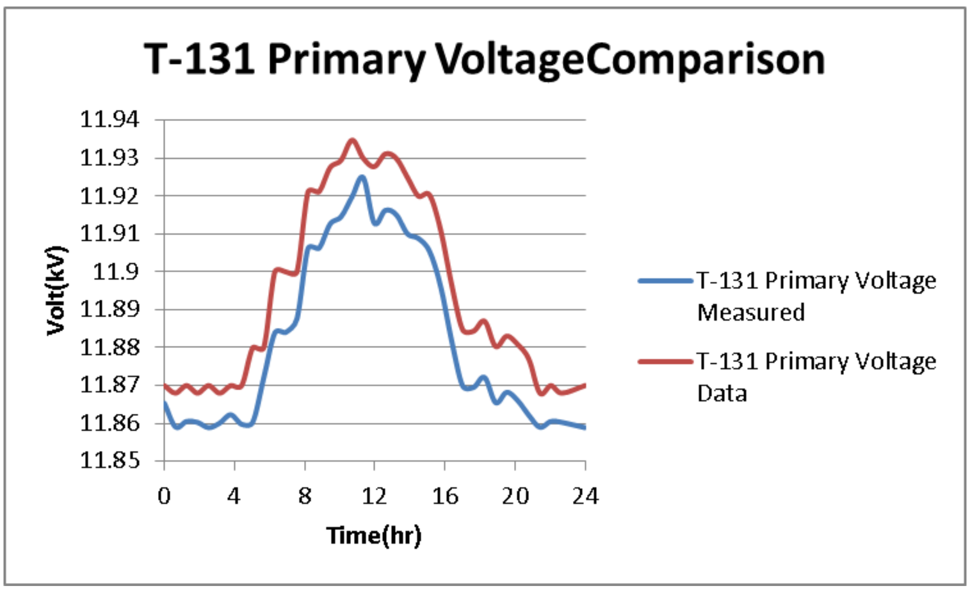


Figure 42: T-131 Primary voltage

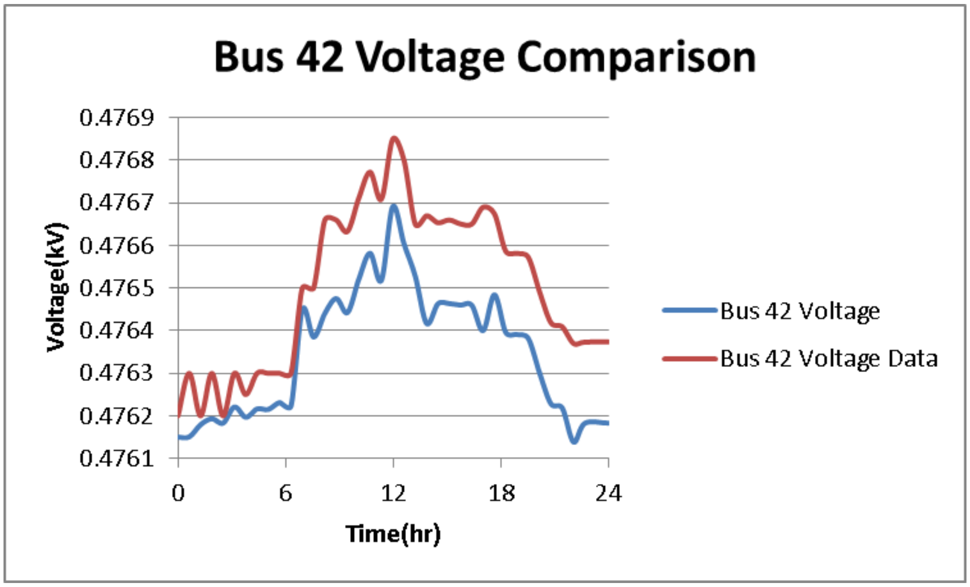


Figure 43: Bus 42 AC voltage

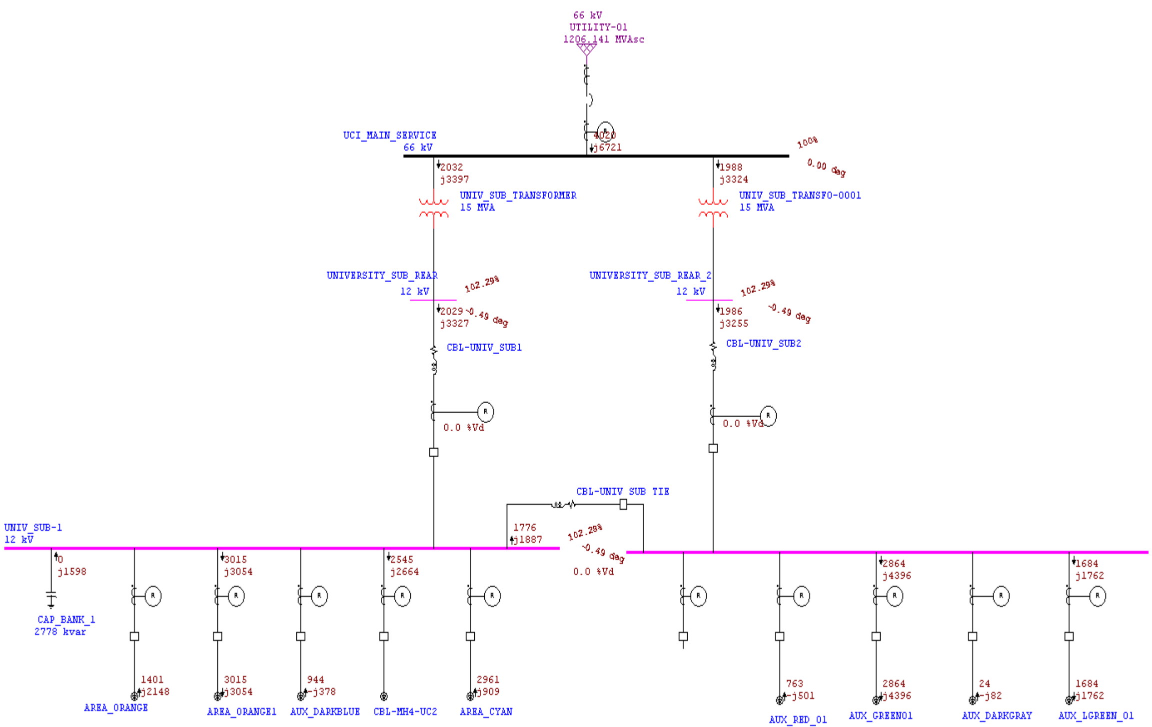


Figure 44: UCI model start point

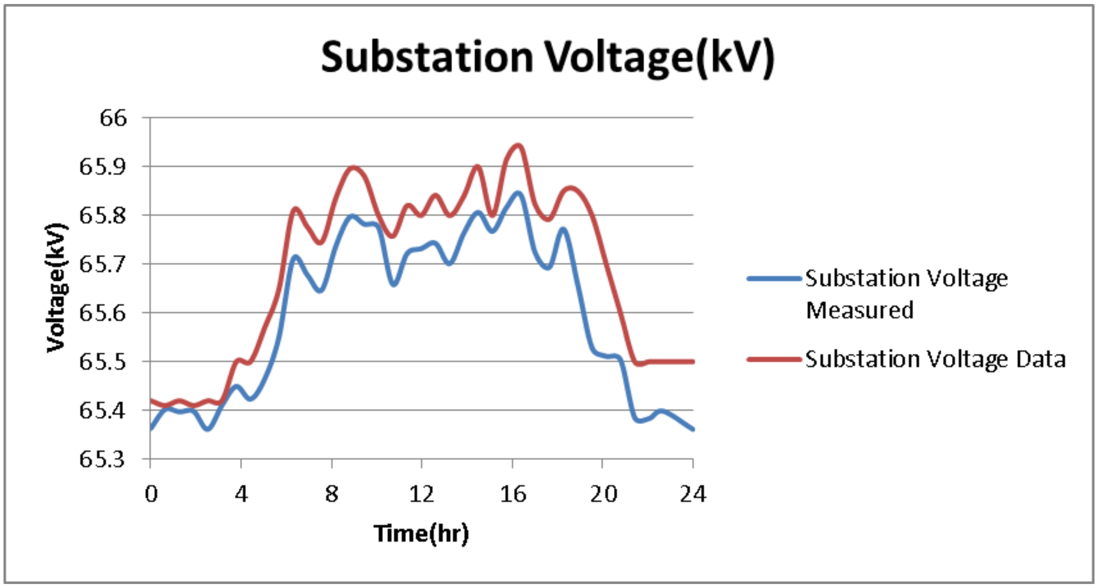


Figure 45: Voltage output from ETAP at the substation

# 7 TASK 4: SCENARIOS

## 7.1 FIRST ELECTRIC VEHICLE SCENARIO

Before the battery, rooftop PV, and chargers were installed, a scenario was created using data obtained by the researcher Li Zhang (Zhang 2010). The first scenario modeled included an electric vehicle (EV) profile that only had ten percent of the cars in the parking structure being electric vehicles. The parking structure has 2026 spaces in total. The data set includes 292 vehicles and the charging time for 100 points per hour during an entire day.

More details on the use of the data and the steps taken to create the EV charging demand plots used in the model are listed below.

1. Use the car in and car out times determined by Li Zhang for the electric vehicles going or leaving the structure as the begin and end times for charging

2. Start with the car entering time data

    i. Create a count equation that counts all the cars going in before a certain time and subtract those that entered before

    ii. Evaluate in a 24hr period

    i.e., Count all the cars that entered on/before 6:00am and subtract by all cars that entered before5:00am in order to provide the cars resident between 5:00am to 6:00am. This resulted in a profile for cars is as shown in Figure 46.

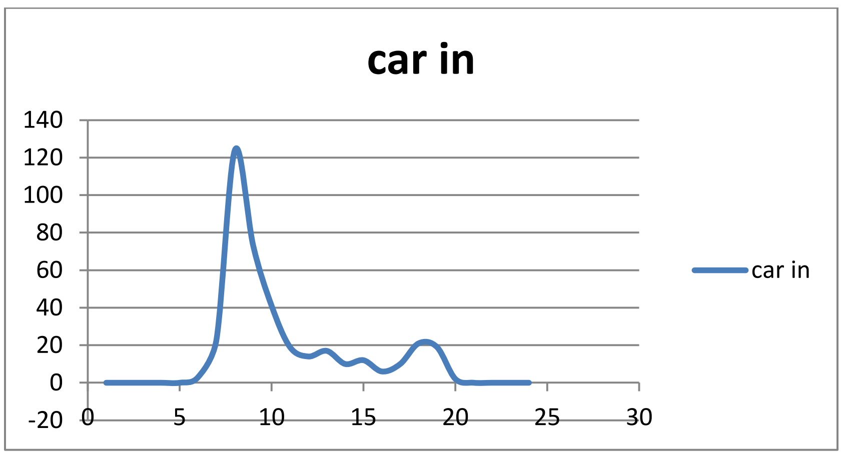


Figure 46: Cars going into the structure

3. The same procedure was applied for all cars out resulting in the profile shown in Figure 47.

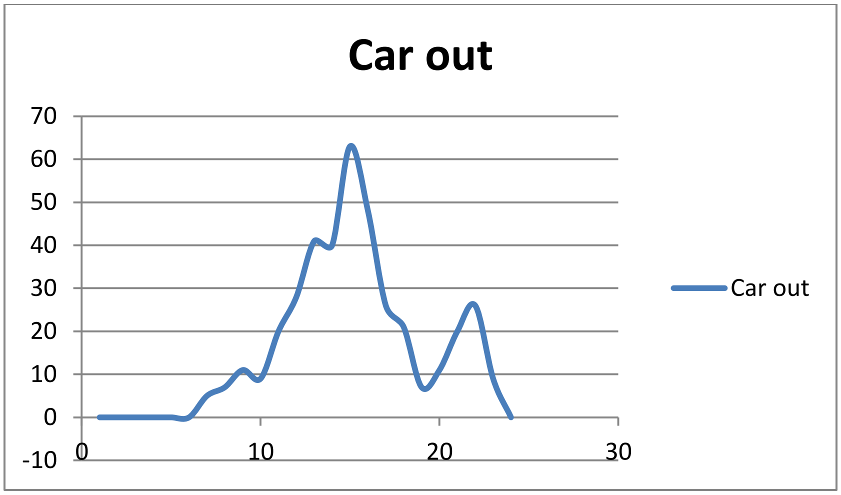


Figure 47: Cars leaving the structure

Once the amount of cars in and cars out are known, the number of cars resident in the lot throughout a 24-hour period can be determined.

4. Subtracted cars out and add to the previous value. For example:

5:00am to 6:00am (Car in – Car out)

6:00am to 7:00am (Car in – Car out) + 5:00am to 6:00am (Car in – Car out)

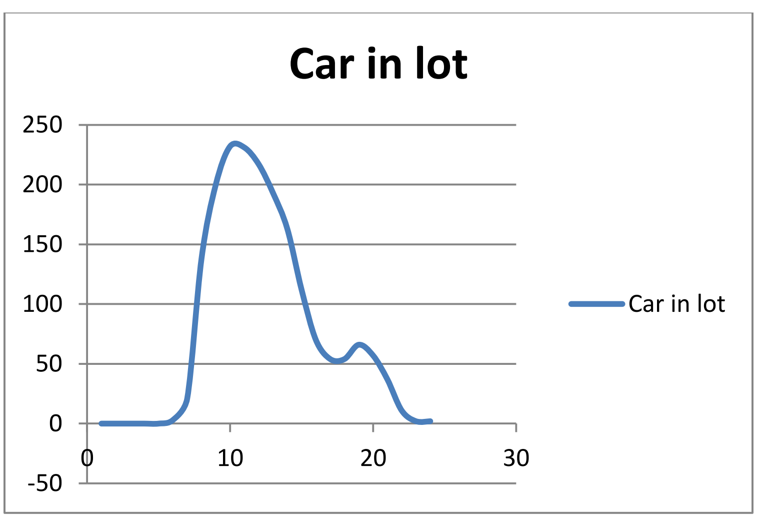


Figure 48: Cars in the structure

i. Create a profile of the cars in the lot in 24 hours and change to 15 min intervals throughout the 24 hours in order to match the model.

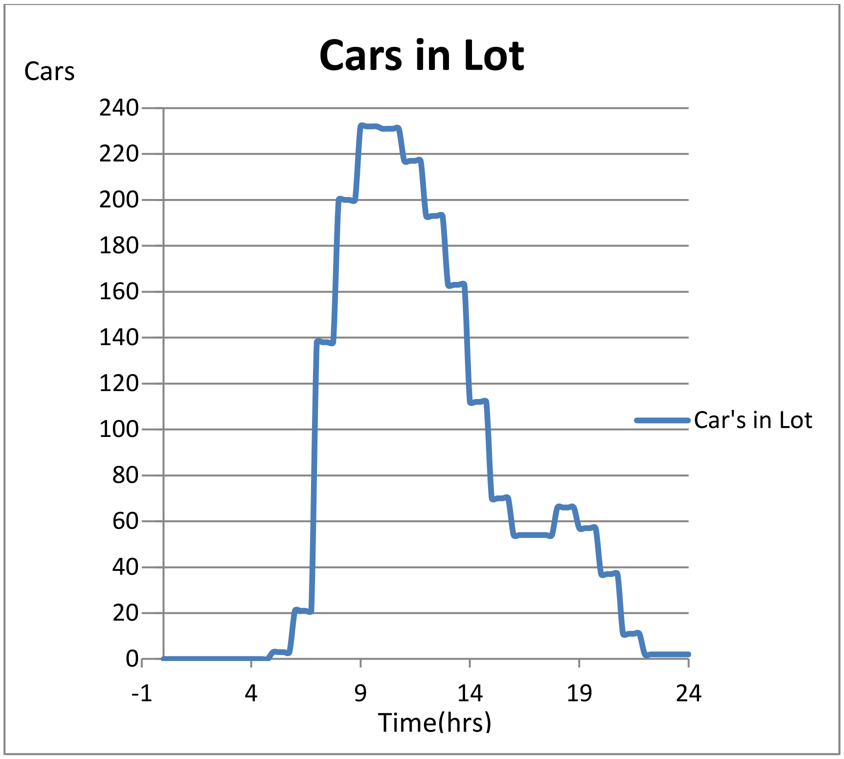


Figure 49: Cars in the structure for 24 hours

5. Insert the excel data in MATLAB, with the time in one column and the number of cars in the structure in another column

    i. Create a block in the model with the EV information, add to the Anteater Parking Structure and multiply by 7.48kW which is the charging power for schools received from a survey (Zhang, charging time survey 2008)

    ii. Process the model with the added block

iii. Run another model with the same block but with a pf=.95.

The vehicles were charged with Level 1 chargers which is 1.44kW. Since the data had 100 points per hour, every 25 points were averaged in order to generate 15 min interval data. In order to generate the data to resemble 10% EV, the following formula was used.

$$10\ percent\ of\ the\ vehicles\ in\ the\ parking\ lot: 2026 * .1 = 202.6$$

**Equation 7: 10 percent of the vehicles in the lot**

$$Ratio\ of\ 10\ percent = \frac{202.6}{292} = 0.693836$$

**Equation 8: Rate of 10 percent**

The number received from the ratio (0.693) is multiplied by the charging time from 0 to 24 hrs in order to generate the data for the 10% electric vehicles. The following figures represent the 10 percent immediate EV charging.

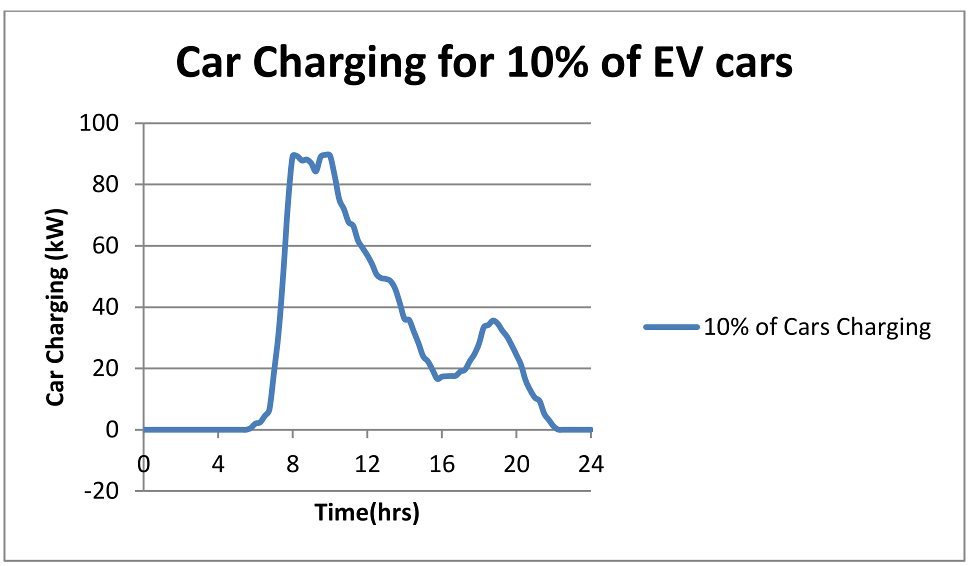


**Figure 50: 10% of cars charging in a 15 minute interval for 24 hrs.**

At 9am there are 23 cars in the lot since only 10% of the total cars is being used from Figure 49.

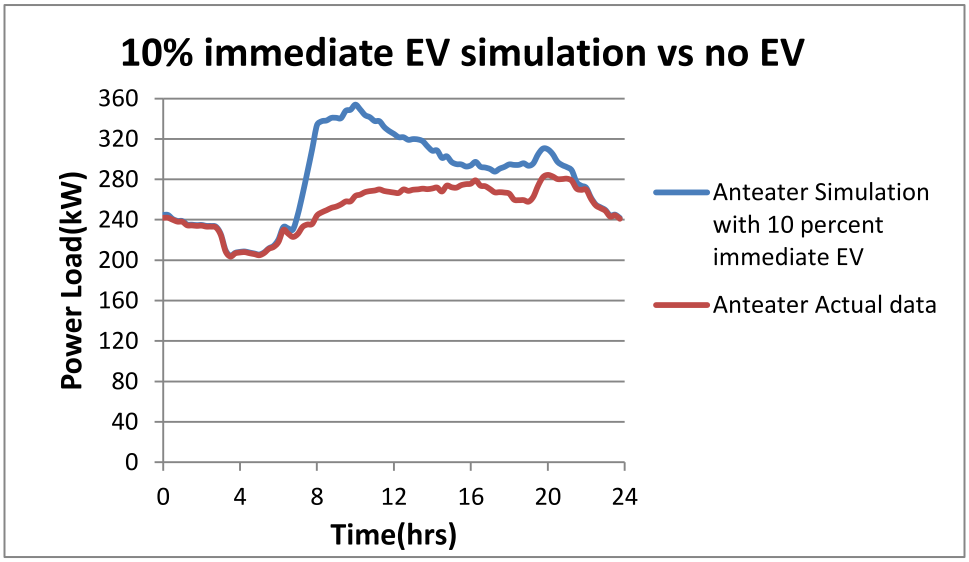


Figure 51: EV simulation vs. the case with no EVs

For the 10 percent delayed EV charging, the same approach was used as the first scenario. All the steps of the first scenario were used except with the change of adding the delayed EV information for vehicles charged at Level 1.

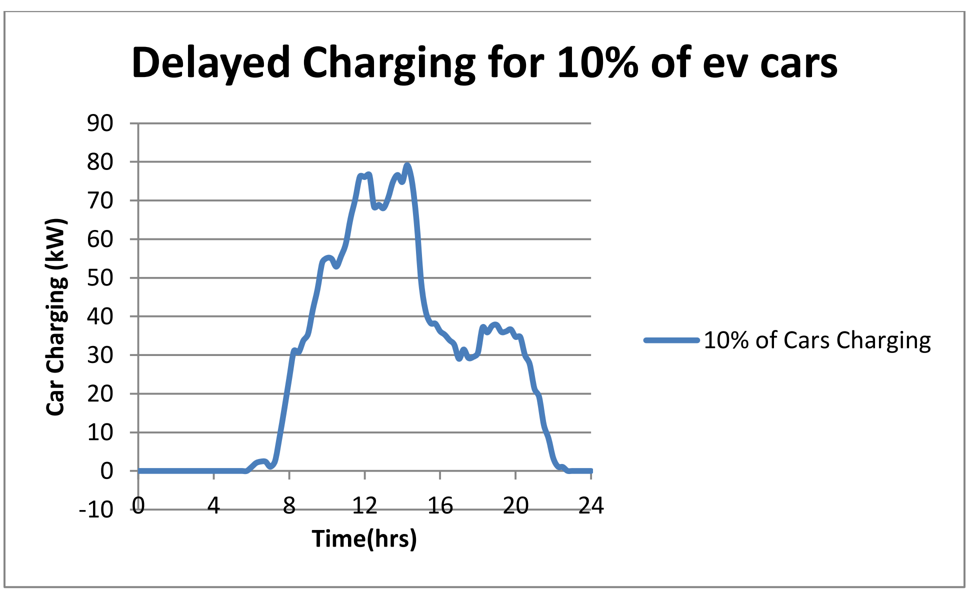


Figure 52: Delayed charging for 10% EV

To compare the voltage between 10 percent delayed charging and no charging, the simulation power loads, actual power loads, and power flow for sub circuit ES5 were analyzed. Figure 53 shows a comparison of the VPU for the 10% delayed charging and the circuit without any electric vehicles. This result shows in an average of .12% increase that was calculated by comparing both of the VPU measurements.

Figure 54 shows a comparison of the measured load at the anteater parking lot without any EV and the parking with 100% of the 230 case study cars from the survey being used. This would result in 2MW of power.

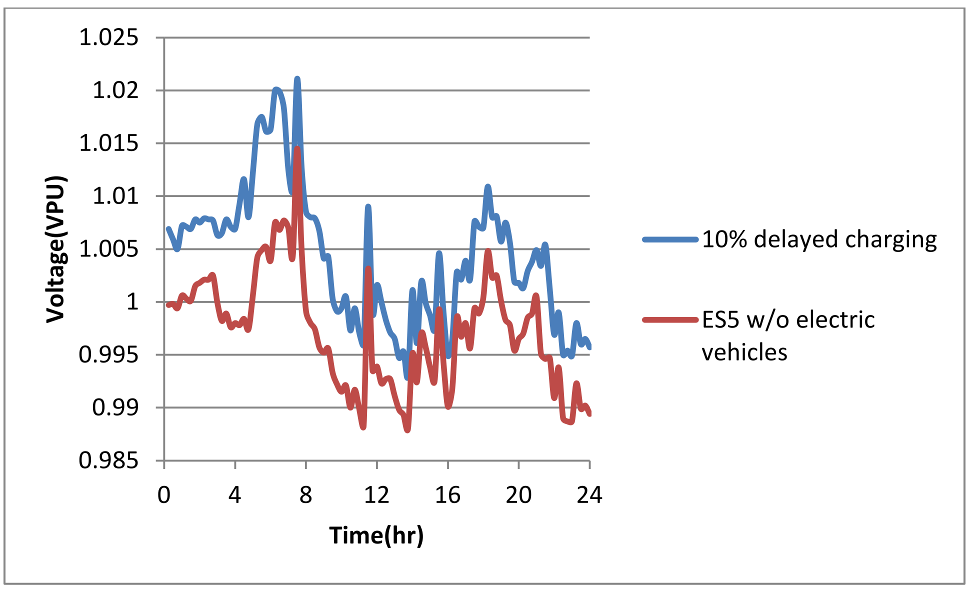


Figure 53: 10% delayed charging EV simulation

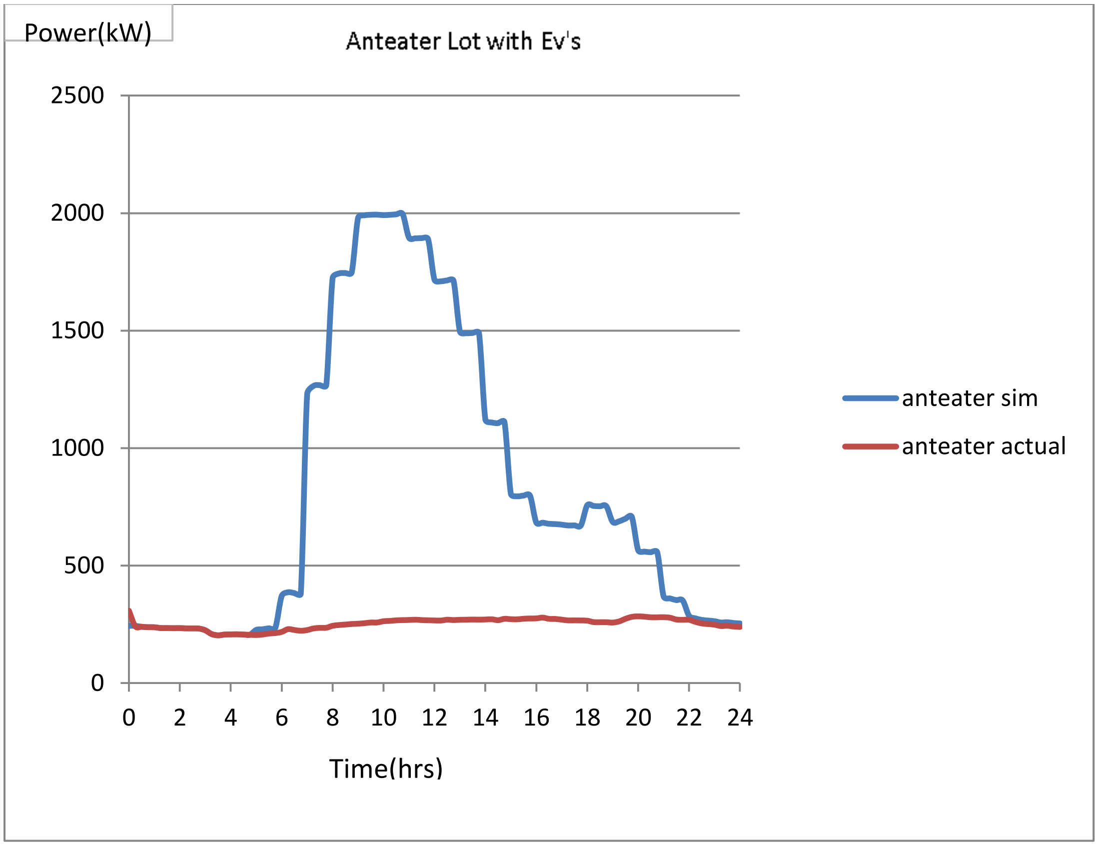


Figure 54: EV simulation comparison

## 7.2 INCREASE IN PV AND BESS GENERATION SCENARIO

Due to the setup of the model, the output from the inverter is a combination of the solar and the BESS. The PV and BESS were multiplied by 5 to evaluate the effect on the voltage. Load profiles for the PV, BESS, and the inverter output are presented in Figure 55Figure 57.

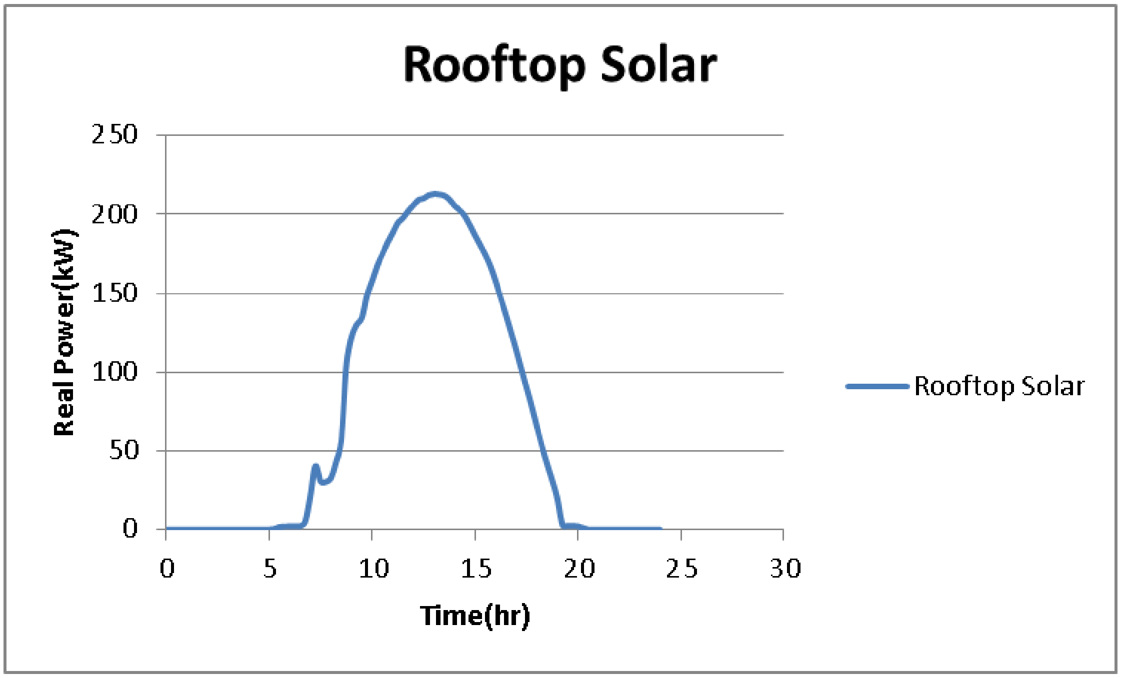


Figure 55: Increase in PV

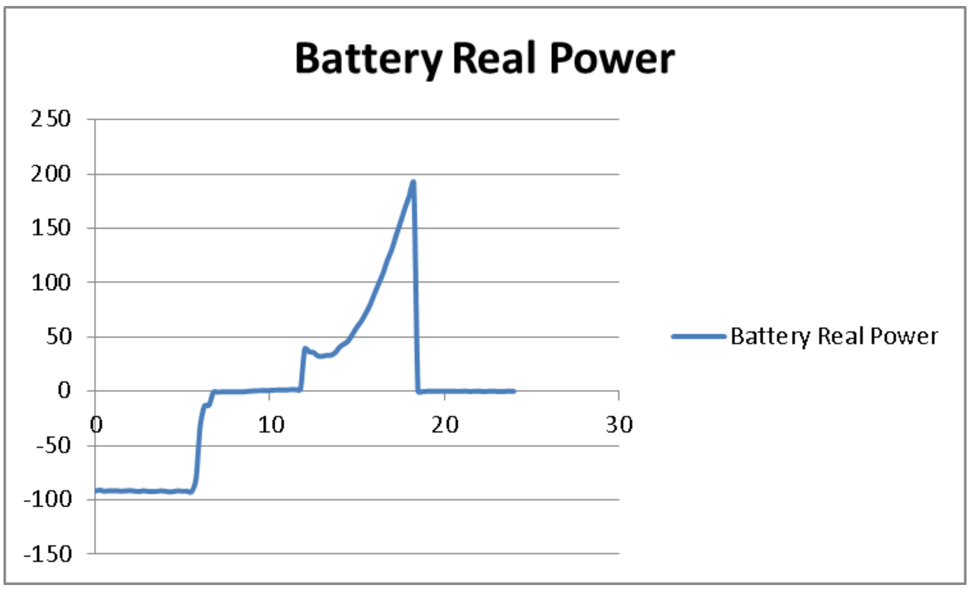


Figure 56: Increase in Battery Stored Power

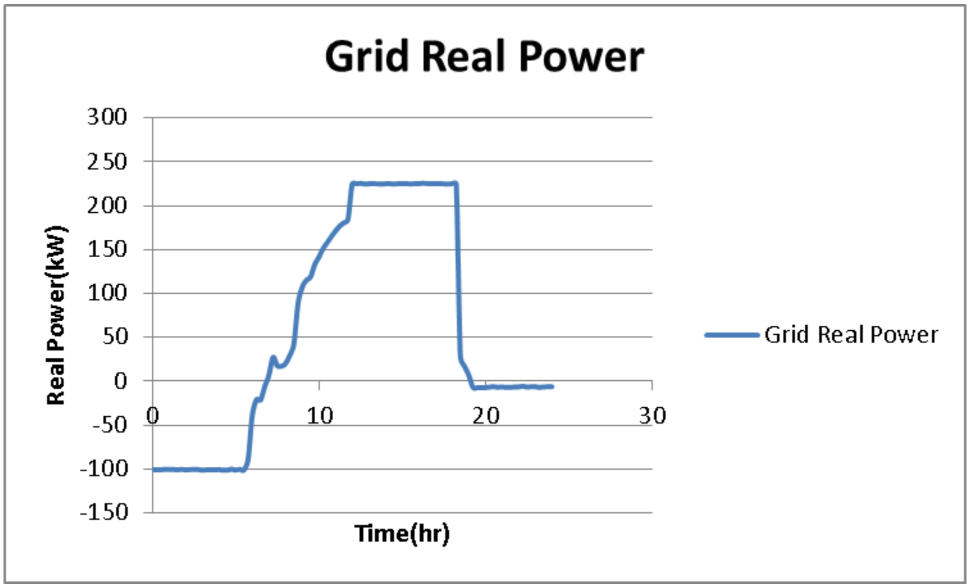


Figure 57: Inverter Output for increase in BESS and PV generation

Figure 58 shows that, as the generation is increased, the voltage starts to drop and a higher dip occurs in the same time window where the cars started coming into the parking lot. The voltage has a smooth increase and decrease during the times that the solar is active.

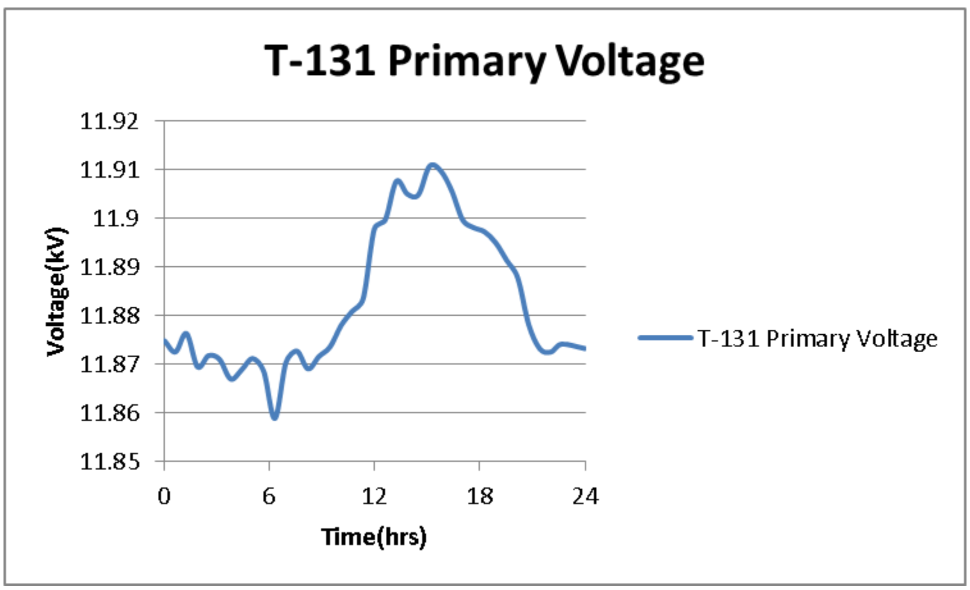


Figure 58: T-131 Primary voltage with increase generation

The load in parallel with the Car Shade project was also affected by the increase in voltage. As seen in Figure 59, the voltage begins to increase during the peak time (7:00am and 2:00pm) and drops after 2pm, in direct correlation with the amount of EV's in Figure 36.

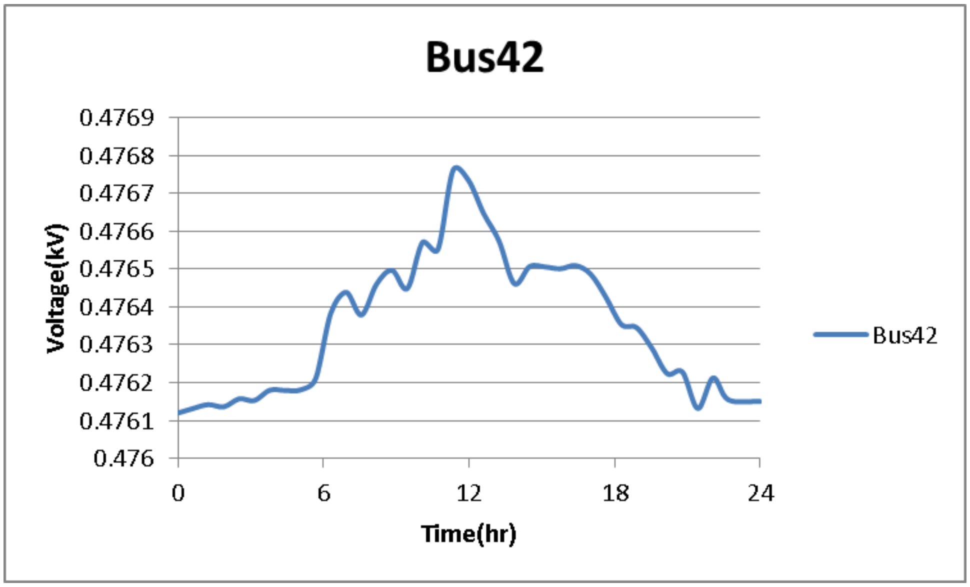


Figure 59: Bus 42 with increased generation

# 8 SUMMARY AND CONCLUSIONS

## 8.1 SUMMARY

Substantial progress has been made in the past 10 years in grid modernization, and an era where all grids should aspire to become a microgrid or smart grid is emerging. As renewables are added to the grid, the current grid is challenged with instabilities and inefficiencies. A microgrid system can facilitate the utilization of intermittent renewables through power management, energy storage, and smart electric vehicle charging.

This thesis addressed the development and simulation of integrating power generation and charging into a secondary circuit. The UCI Microgrid and Car Shade system were selected as an experimental platform. A simulation model developed in ETAP was evaluated against a MATLAB/Simulink model and experimental data obtained from the Car Shade system. The ETAP model was successfully verified against a baseline scenario, and then applied to two scenarios to establish the maximum and minimum amounts of distributed generation that the current circuits can manage.

## 8.2 CONCLUSIONS

Based on the work herein, the following conclusions are drawn

- **The size of the battery and PV system should be increased to accommodate more EV charging.**During the current evaluation (in simulations and measurements), the rooftop solar PV system reached a maximum of 41kW in the daytime during a time when the BESS energy total reached 45kWhr of generation being exported. The EVSE total real power consumed reached 36kW. Each station can only charge up to 6.6kW of power. If all 20 chargers were in use at the same time, a total of 132kWhr would be needed from the battery in order to not import power from the current grid. With the current infrastructure, the battery can dispatch only up to 100kWhr.

- **The addition of a battery energy storage system, rooftop solar PV, and electric vehicle chargers can affect the voltage on an existing microgrid circuit.**

  The 100kW battery stores any excess rooftop solar PV generation that has not been used during the day. This energy is then used to charge the electric vehicles during the evening. The battery has a demand response inverter that allows for the integration of rooftop solar PV, trimming back loads during the grid's peak usage time, energy storage, as well as voltage and frequency regulations. The battery has been running on PLS (Permanent load-shifting) mode. The data shown presented in the thesis are associated with the PLS mode. From the scenarios investigated, the voltage was found to substantially depend upon the power flow throughout the Car Shade system. The scenarios reveal that the data do not exceed the limit and that a higher capacity of solar can be added as long as there is a larger battery that can store the energy. Otherwise the chargers will use power from the grid.

- **Simulation and operation data can help to understand the impacts of solar power, energy storage, and EV charging on secondary circuits.**

  Detailed circuit information regarding the UCI Microgrid such as impedances, cable distances, bus voltages, and a variety of other sources were used to create the model. Load information received from SCE as well as from high-resolution MelRok meters played a crucial role in addressing the impacts of the solar power, energy storage, and EV charging of the Car Shade project has on the UC-9 secondary circuit operation.

## 8.3 RECOMMENDATIONS AND FUTURE WORK

For the purpose of this research, areas that would be useful in conducting future work include:

- Monitor charging events such as when a car plugs in and when a car plugs out
- Establish loading scenarios for different types of electric vehicles to compare to the charging data
- Monitor the types of cars charging

Possible areas of interest if research is continued would include:

- Use battery test data for the different modes as inputs into the model in order to properly model each of the modes
- Consider adding additional Car Shade installations in other parking lots in order to evaluate the performance on a portfolio of circuits

# 9 REFERENCES


Julia Layton. 2006. "How Wind Power Works." Accessed 2014. http://science.howstuffworks.com/environmental/green-science/wind-power2.htm.

U.S.-Canada Power System Outage Task Force. 2014. "Final Report on the August 14, 2003 Blackout in the United States and Canada: Causes and Recomendations." http://www.ferc.gov/industries/electric/indus-act/reliability/blackout/ch1-3.pdf.

A. E. Auld, J. Brouwer, K. M. Smedley, and S. Samuelsen. 2010. "“Effects of Distributed Generation on Voltage Levels ." *Journal of Fuel Cell Science and Technology* 7 (6): 061011–8. Accessed 2013.

A. Ipakchi and F. Albuyeh. 2009. *“Grid of the future.* Vol. 7, 52-62. IEEE power and energy magazine. Accessed 2014.

A. P. Johnson. 2010. "The history of the Smart Grid evolution at Southern California Edison." 1-3. Innovative Smart Grid Technologies.

American National Standards Institute (ANSI). 2007. "Overview of the U.S. Standardization System. Voluntary Consensus Standards and Conf ormity Assessment ."

Bailey, John. 2012. "Workplace charging Bailey Presentation." http://www.workplacecharging.com/uploads/workplacecharging-bailey-presentation.pdf.

Barr, Robert. 2011. "China surpasses US as top energy consumer." *NBCNEWS.* June 8. http://www.nbcnews.com/id/43327793/ns/business-oil_and_energy/t/china-surpasses-us-top-energy-consumer/#.VD2tDGNN0XV.

Bindeshwar Singh, N.K Sharma. 2011. "Applications of phasor measurement units(PMUs) in electric power system networks incorporated with FACTS controllers." *International Journal of Engineering, Science and Technology* 19.

Brendan P. Shaffer. 2013. *UCI Microgrid White Paper.* 7 17. Accessed January 2014. http://www.apep.uci.edu/3/research/pdf/UCIMicrogridWhitePaper_FINAL_071713.pdf.

Burke, John. 2010. "Co Generation gets Thumbs Up from Germany." *Sun Earth Energy.* December 1. Accessed January 2014. http://sun-earth-energy.blogspot.com/2010/12/co-generation-gets-thumbs-up-from.html.

2013. "Center for Sustainable Systems." *University of Michigan.* October. Accessed December 2013. http://css.snre.umich.edu/css_doc/CSS03-12.pdf.

Central Research Institute of Electric Power Industry. 2009. "System Engineering Research Laboratory: Electric Power Systems." Accessed January 2014. http://criepi.denken.or.jp/en/system/unit/01/index.html.

CNET. n.d. "Energy-efficient Smart Grids on the Cheap?" *CNET.* Accessed January 2014. http://news.cnet.com/8301-.

Coleman, Daryl. 2013. *Princeton Power Systems Battery Energy Storage System Laboratory Test Report.* SCE.

Commonwealth Edison Company. 2013. "ComEd's Smart Meter Benefits." https://www.comed.com/Documents/technology/What%20is%20a%20Smart%20Meter.pdf.

Dan Wu, Fen Tang, Tomislav Dragicevic. 2013. "Coordinated Primary and Secondary Control with Frequency-Bus-Signaling for Distributed Generation and Storage in Islanded Microgrids." *IEEE* 7140 - 7145. http://ieeexplore.ieee.org/stamp/stamp.jsp?tp=&arnumber=6700319&tag=1.&tag=1.

Dohn, Robert Liam. 2011. "The business case for microgrids." *Siemens.* http://w3.usa.siemens.com/smartgrid/us/en/microgrid/Documents/The%20business%20case%20for%20microgrids_Siemens%20white%20paper.pdf.

Energy Buddy. n.d. "Welcome to Energybuddy | the home energy monitoring and management system (HEMs) from ." *Energy Buddy.* Accessed 2014. http://www.energy-buddy.com/.

n.d. "Energy Home." *Energy Education.* http://www.energyeducation.tx.gov/renewables/section_3/topics/photovoltaic_cells/c.html.

2013. *Energy in Brief.* August 1. Accessed September 2013. http://www.eia.gov/energy_in_brief/article/major_energy_sources_and_users.cfm.

Energy Tower. 2014. "Compressed Air Wind Electrical Generation System." *Energy Tower.* http://www.energytower.org/cawegs.html.

Energy Independence and Security Act of 2007. 2007. 310.

2007. "Energy Independence and Security Act of 2007." 310.

Environmental Defense Fund. 2011. "What Consumers Need to Know About the Smart Grid and Smart Meters." *Sensus.*

Accessed 2014.
http://sensus.com/documents/10287/58847/EDFFactSheetSmartMeters.pdf.
EPA. 2013. "What Is Asthma?" *EPA.* May. http://www.epa.gov/asthma/about.html.
ETAP. 2009. "Load flow analysis." *ETAP.* Operation Technology, Inc.
http://etap.com/training/tutorials/pdfs/Load-Flow-Analysis.pdf.
Federal Energy Management Program. 1998. "Parabolicc-Trough Solar Water Heating." *Federal Energy Management Program.* April. Accessed February 2014.
Http://www1.eere.energy.gov/femp/pdfs/FTA_para_trough.pdf.
Galvin Electricity Initiative. 2014. *What are the benefits of the smart microgrid approach?* Accessed 2014. http://www.galvinpower.org/resources/microgrid-hub/smart-microgrids-faq/benfits.
Galvin Power. 2014. *Galvin Electricity Initiative.* January.
http://www.galvinpower.org/sites/default/files/documents/Understanding%20Microgrids%20FINAL.pdf.
Green Optimistic. 2009.
"“Flywheel Energy Storage: a Much Greener, 90% Efficient Battery - The Green Optimistic." *Green Optimistic.* Accessed January 2014.
http://www.greenoptimistic.com/2009/04/08/flywheel-energy-storage-a-much-greener-90-.
GreenTech Media. 2013. "The Smart Grid Consumer State of the Union : Greentech Media." *GreenTech Media.* January 28. Accessed February 2014.
http://www.greentechmedia.com/articles/read/the-smart-grid-consumer-state-of-.
Guohung Wu, Shunnosuke Kodama, Yoshiyuki Ono. n.d. "Hybrid microgrid System Including Renewable Power Generations and Energy Storages for supplying both the DC and AC loads." *IEEE.* http://ieeexplore.ieee.org/stamp/stamp.jsp?tp=&arnumber=6477373.
2013. "Highway Wind Energy." *Florida International University.* November 21. Accessed 2014.
http://www.mme.fiu.edu/wp-content/uploads/2013/12/F13-SR-T-2.pdf.
Hong Kong Engineer. n.d. "Is CSP the solution to global warming and climate change? ." *Hong Kong Engineer.*
http://www.hkengineer.org.hk/program/home/articlelist.php?cat=Env&volid=79.
Hyper-Librarian, WTEC. 1997. "Chapter 2: Magnetic Energy Storage Efforts in Japan." Chap. 2.
http://www.wtec.org/loyola/scpa/02_06.htm.
Itron Inc. Jan.2010. "“Impacts of Distribted Generation, Final Report."
J. Mamoh. 2012. *Smart Grid - Fundamentals of Design and Analysis.* Hoboken, New Jersey, New Jersey: Wiley - IEEE Press.
Jenkins, N., Allan, R, Kirschen, D. , Strbac, G. n.d. "Embedded Generation." *Instituion of Electrical Engineers.*
Jenkins, N., Allan, R, Kirschen, D. , Strbac, G. 1995. "Embedded Generation." *Power Engineering Journal* 9 (3): 145-150.
Joshua Meyer, Encorp and Jim Peedin, Honeywell. 2003. *A Microgrid Worth "Bragging" About.* http://www.power-eng.com/articles/print/volume-107/issue-5/dg-update/a-microgrid-worth-bragging-about.html.

Kakigano, Hiroaki. n.d. "DC Micro-grid for Super High Quality Distribution-System Configuration and Control of Distributed Generations and Energy Storage Devices-." *IEEE* 7. http://ieeexplore.ieee.org/stamp/stamp.jsp?tp=&arnumber=1712250.

Kakigano, Hiroaki. 2006. "DC Micro-grid for Super High Quality Distribution-System Configuration and Control of Distributed Generations and Energy Storage Devices-." *IEEE* 7. http://ieeexplore.ieee.org/stamp/stamp.jsp?tp=&arnumber=1712250.

LaMonica, Martin. 2008. "Energy-efficient Smart Grids on the Cheap?" *CNET.* April 3. Accessed January 2014. http://www.cnet.com/news/energy-efficient-smart-grids-on-the-cheap/.

Lawrence Berkeley National Laboratory. 2014. *Microgrids at Berkeley Lab.* Accessed 2014. http://der.lbl.gov/microgrid-concept.

Meier, Alexandra Von. 2006. *Electric power systems a conceptual introduction.* Jon Wiley & Sons Inc.

MelRok. 2014. *Plot created in MelRok system on September 2014.*

National Energy Technology Laboratory . 2010. "Understanding the Benefits of the Smart Grid." *National Energy Technology Laboratory .* June 18. http://www.netl.doe.gov/File%20Library/research/energy%20efficiency/smart%20grid/whitepapers/06-18-2010_Understanding-Smart-Grid-Benefits.pdf.

NETL. n.d. "Understanding the Benefits of the Smart Grid." *NETL.* http://www.netl.doe.gov/smartgrid/referenceshelf/whitepapers/06.18.2010_Understanding%20Smart%20G.

New Home Wind Power. 2012. "The A-Z of wind power generators." *New Home Wind Power.* Accessed 2014. http://www.newhomewindpower.com/wind-power-generators.html.

2011. "Oil Peak." *End of Crude Oil.* June 30. Accessed January 2014. http://www.endofcrudeoil.com/2011/06/renewable-energys-share-of.html.

2010. "Parabolic Trough Solar Field Technology." *NREL.* January 28. Accessed 2014. http://www.nrel.gov/csp/troughnet/solar_field.html.

PG&E. 2014. "SmartMeter Benefits." *PG&E.* http://www.pge.com/en/myhome/customerservice/smartmeter/benefits/index.page.

PricewaterhouseCoopers. 2012. "The Future of Microgrids Their Promise and Challenges." *PWC.* July. http://www.pwc.com/en_US/us/technology/publications/cleantech-perspectives/pdfs/pwc-cleantech-the-future-of-microgrids.pdf.

R. Wiser, C. Namovicz, M. Gielecki, and R. Smith. 2007. "Renewables portfolio standards: A factual introduction to ." 19. Accessed 2014. http://emp.lbl.gov/sites/all/files/lbnl%20-%2062569.pdf.

Reyes, Karina. 2014. "Photograph taken by KReyes on February 11, 2014." February 11.

Rockland, Orange &. 2013. *Power Factor.* Accessed November 2013. http://www.oru.com/energyandsafety/electricdelivery/powerfactor/calculatingpowerfactor.html.

Sensus. n.d. "What Consumers Need to Know About the Smart Grid and Smart Meters." *Sensus.* Accessed 2014. http://sensus.com/documents/10287/58847/EDFFactSheetSmartMeters.pdf.

Sivanagaraju, S. 2008. *Electric Power Transmission and Distribution.* Pearson Education India. http://my.safaribooksonline.com/book/electrical-engineering/9789332503410/14-distribution-systems/head14_6_xhtml.

2011. *Smart Grid, Building on the Grid.* Vol. 2, in *The National Electrical Manufacturers Association*.

Southern California Edison. 2014. "Car Shade Project data." April 7.

The Economist. 2012. "Energy storage: Packing some power | The Economist." *The Economist.* March 31. Accessed 2014. http://www.economist.com/node/21548495?frsc=dg%7Ca.

Toby Considine, William Cox,Edward G. Cazalet. 2012. "Understanding Microgrids as the Essential Architecture of Smart Energy." *GridWiseAC.* http://www.gridwiseac.org/pdfs/forum_papers12/considine_paper_gi12.pdf.

TreeHugger. n.d. "More Pumped Hydro Storage Could Help Wind & Solar Power : TreeHugger." *TreeHugger.* Accessed 2014. http://www.treehugger.com/renewable-energy/more-pumped-hydro-storage-could-help-wind-solar-.

U.S. Department of Energy, Office of Electricity Delivery & Energy Reliability. 2008. "The Smart Grid: An ."

Wunderground. 2014. *Wunderground.* http://www.wunderground.com/history/airport/KSNA/2014/6/17/DailyHistory.html?

Zhang, Li. 2008. "charging time survey." July.

—. 2010. *EV Survey Data.*

## 10 Appendix: Load Flow Report

Below is the load flow report produced by ETAP. The report is separated into six different columns: bus, voltage, generation, load, load flow, and transformer. Bus represents the node name given in the ETAP model. Voltage is divided into three sections: the rated kV, percentage of error, and the difference in the angle. The generation represents any solar data bring produced for that particular segment. The load, which is one of the most important sections, shows the load being simulated in the model as well as the as the load flowing from that bus. Table 4 and Table 5 show a clearer representation of the data that were developed in the load flow report shown in Figure 60. The tables compare the actual voltage to the voltage simulated by ETAP as well as the error percentage.

| Circuit | Primary Voltage | Load Flow Report Voltage % | Load Flow Report Name |
|---|---|---|---|
| UC-1 | 12kV | 102.397 | AUX_CYAN |
| UC-2 | 12kV | 102.397 | AUX_ORANGE |
| UC-3 | 12kV | 102.397 | AUX_ORANGE1 |
| UC-4 | 12kV | 101.811 | AUX_BLUE01 |
| UC-5 | 12kV | 101.812 | AUX_BLUE02 |
| UC-6 | 12kV | 102.041 | AUX_DARKBLUE |
| UC-8 | 12kV | 102.394 | AUX_DARKGRAY |
| UC-9 | 12kV | 102.394 | AUX_GREEN01 |
| UC-10 | 12kV | 1102.397 | AUX_RED_01 |

**Table 4: Explanation of the Primary Voltages for the load flow report**

| Secondary Voltage | Load Flow Report Name | Load Flow Report Voltage % | Load Flow Report Secondary Voltage |
|---|---|---|---|
| .280kV | Bus10 | 98.109 | .277kV |
| .280kV | Bus11 | 102.397 | 277kV |
| .480kV | Bus18 | 100.367 | .480kV |

**Table 5: Explanation of the Secondary Voltages for the load flow report**

## LOAD FLOW REPORT

| Bus | | Voltage | | Generation | | Load | | Load Flow | | | | | XFMR |
|---|---|---|---|---|---|---|---|---|---|---|---|---|---|
| ID | kV | % | Ang. | MW | Mvar | MW | Mvar | ID | MW | Mvar | Amp | %PF | %Tap |
| AREA_CYAN | 12.000 | 102.397 | -0.4 | 0 | 0 | 0 | 0 | BUS-0077 | -2.716 | -0.875 | 134.1 | 95.2 | |
| | | | | | | | | UNIV_SUB-1 | 2.716 | 0.875 | 134.1 | 95.2 | |
| AREA_ORANGE | 12.000 | 102.397 | -0.4 | 0 | 0 | 0 | 0 | COGEN REACTOR | -1.267 | -1.998 | 111.2 | 53.5 | |
| | | | | | | | | UNIV_SUB-1 | 1.267 | 1.998 | 111.2 | 53.5 | |
| AREA_ORANGE1 | 12.000 | 102.397 | -0.4 | 0 | 0 | 0 | 0 | SF6-62 | 2.747 | 2.827 | 185.2 | 69.7 | |
| | | | | | | | | UNIV_SUB-1 | -2.747 | -2.827 | 185.2 | 69.7 | |
| AUX_BLUE01 | 12.000 | 101.811 | -0.5 | 0 | 0 | 0 | 0 | SF6-65 | -2.169 | -1.921 | 136.9 | 74.9 | |
| | | | | | | | | SF6-24 | 2.169 | 1.921 | 136.9 | 74.9 | |
| Aux_Blue1 | 12.000 | 102.041 | -0.5 | 0 | 0 | 0 | 0 | OS-08 | 0.000 | 0.000 | 0.0 | 0.0 | |
| Aux_Blue02 | 12.000 | 102.098 | -0.5 | 0 | 0 | 0 | 0 | PB206-1 | 0.217 | 0.960 | 46.4 | 22.1 | |
| | | | | | | | | SF6-50 | -0.217 | -0.960 | 46.4 | 22.1 | |
| AUX_BLUE02 | 12.000 | 101.812 | -0.5 | 0 | 0 | 0 | 0 | SF6-64 | -2.188 | -1.890 | 136.6 | 75.7 | |
| | | | | | | | | SF6-25 | 2.188 | 1.890 | 136.6 | 75.7 | |
| Aux_Blue03 | 12.000 | 102.098 | -0.5 | 0 | 0 | 0 | 0 | PB206-2 | 0.288 | 1.010 | 49.5 | 27.5 | |
| | | | | | | | | SF6-50 | -0.288 | -1.010 | 49.5 | 27.5 | |
| AUX_DARKBLUE | 12.000 | 102.397 | -0.4 | 0 | 0 | 0 | 0 | CP2 MAIN SWGR | -0.876 | 0.319 | 43.8 | -94.0 | |
| | | | | | | | | UNIV_SUB-1 | 0.876 | -0.319 | 43.8 | -94.0 | |
| AUX_DARKGRAY | 12.000 | 102.396 | -0.4 | 0 | 0 | 0 | 0 | SF6-61 | -0.017 | 0.084 | 4.0 | -20.2 | |
| | | | | | | | | UNIV_SUB-2 | 0.017 | -0.084 | 4.0 | -20.2 | |
| AUX_GREEN01 | 12.000 | 102.396 | -0.4 | 0 | 0 | 0 | 0 | SF6-72 | 2.609 | 4.135 | 229.7 | 53.4 | |
| | | | | | | | | UNIV_SUB-2 | -2.609 | -4.135 | 229.7 | 53.4 | |
| Aux_Green_01 | 12.000 | 101.923 | -0.5 | 0 | 0 | 0 | 0 | SF6-20 | 2.612 | 1.998 | 155.2 | 79.4 | |
| | | | | | | | | SF6-14 | -2.612 | -1.998 | 155.2 | 79.4 | |
| Aux_Green_02 | 12.000 | 101.923 | -0.5 | 0 | 0 | 0 | 0 | SF6-21 | 2.589 | 1.982 | 153.9 | 79.4 | |
| | | | | | | | | SF6-15 | -2.589 | -1.982 | 153.9 | 79.4 | |
| AUX_LGREEN_01 | 12.000 | 102.396 | -0.4 | 0 | 0 | 0 | 0 | ES SWGR | 1.537 | 1.642 | 105.7 | 68.3 | |
| | | | | | | | | UNIV_SUB-2 | -1.537 | -1.642 | 105.7 | 68.3 | |
| AUX_RED_01 | 12.000 | 102.396 | -0.4 | 0 | 0 | 0 | 0 | CP1 MAIN SWGR | -0.710 | 0.434 | 39.1 | -85.3 | |
| | | | | | | | | UNIV_SUB-2 | 0.710 | -0.434 | 39.1 | -85.3 | |
| BIO SCI II SWGR 1 | 12.000 | 102.016 | -0.5 | 0 | 0 | 0 | 0 | OS-08 | -1.011 | -0.540 | 54.1 | 88.2 | |
| | | | | | | | | T-046 PRIMARY | 0.274 | 0.060 | 13.2 | 97.7 | |
| | | | | | | | | T-050 PRIMARY | 0.737 | 0.480 | 41.5 | 83.8 | |
| Bus1 | 0.480 | 100.283 | -1.6 | 0 | 0 | 0.319 | 0.198 | T-062_PRIMARY | -0.319 | -0.198 | 450.3 | 85.0 | |
| Bus1-1 | 0.480 | 100.367 | -0.9 | 0 | 0 | 0 | 0 | Bus42 | 0.000 | 0.000 | 0.0 | 0.0 | |
| Bus2 | 12.000 | 102.098 | -0.5 | 0 | 0 | 0 | 0 | MH4-UC2 | -1.232 | -1.634 | 96.4 | 60.2 | |
| | | | | | | | | SF6-50 | 1.232 | 1.634 | 96.4 | 60.2 | |

| Project: | | ETAP | Page: | 2 |
|---|---|---|---|---|
| Location: | | 12.5.0T | Date: | 09-17-2014 |
| Contract: | | | SN: | TRL-APUCI1 |
| Engineer: | | Study Case: LF | Revision: | Base |
| Filename: | UCI_Model | | Config.: | Normal |

| Bus | | Voltage | | Generation | | Load | | Load Flow | | | | | XFMR |
|---|---|---|---|---|---|---|---|---|---|---|---|---|---|
| ID | kV | % | Ang. | MW | Mvar | MW | Mvar | ID | MW | Mvar | Amp | %PF | %Tap |
| Bus10 | 0.277 | 98.109 | -2.3 | 0 | 0 | 0.004 | 0.002 | T-078 SEC7 | -0.004 | -0.002 | 9.2 | 85.0 | |
| Bus11 | 0.277 | 98.109 | -2.3 | 0 | 0 | 0.004 | 0.002 | T-078 SEC7 | -0.004 | -0.002 | 9.2 | 85.0 | |
| Bus18 | 0.480 | 100.367 | -0.9 | 0 | 0 | 0 | 0 | T-078 SEC7 | 0.037 | 0.024 | 52.9 | 83.7 | |
| | | | | | | | | T-078 SEC8 | 0.037 | 0.024 | 52.9 | 83.7 | |
| | | | | | | | | Bus42 | -0.074 | -0.048 | 105.8 | 83.7 | |
| BUS-0026 | 4.160 | 101.545 | -1.3 | 0 | 0 | 0 | 0 | T-128 SEC SWGR | 1.215 | 0.761 | 196.0 | 84.8 | |
| | | | | | | | | T-128 PRIMARY | -1.215 | -0.761 | 196.0 | 84.8 | |
| Bus42 | 0.480 | 100.367 | -0.9 | 0 | 0 | 0 | 0 | Bus46 | 0.011 | 0.042 | 52.2 | 25.6 | |
| | | | | | | | | Bus45 | 0.011 | 0.042 | 52.2 | 25.6 | |
| | | | | | | | | Bus44 | 0.055 | 0.044 | 84.5 | 78.1 | |
| | | | | | | | | Bus43 | 0.023 | 0.042 | 57.7 | 47.7 | |
| | | | | | | | | T-131 PRIMARY | -0.174 | -0.219 | 335.2 | 62.3 | |
| | | | | | | | | Bus1-1 | 0.000 | 0.000 | 0.0 | 0.0 | |
| | | | | | | | | Bus18 | 0.074 | 0.048 | 105.8 | 83.7 | |
| Bus43 | 0.208 | 97.207 | -1.5 | 0 | 0 | 0.023 | 0.041 | Bus42 | -0.023 | -0.041 | 133.3 | 48.6 | |
| Bus44 | 0.208 | 96.679 | -2.7 | 0 | 0 | 0.054 | 0.041 | Bus42 | -0.054 | -0.041 | 195.0 | 80.0 | |
| Bus45 | 0.208 | 97.389 | -1.0 | 0 | 0 | 0.011 | 0.041 | Bus42 | -0.011 | -0.041 | 120.4 | 25.8 | |
| Bus46 | 0.208 | 97.389 | -1.0 | 0 | 0 | 0.011 | 0.041 | Bus42 | -0.011 | -0.041 | 120.4 | 25.8 | |
| Bus49 | 0.277 | 98.109 | -2.3 | 0 | 0 | 0.004 | 0.002 | T-078 SEC7 | -0.004 | -0.002 | 9.2 | 85.0 | |
| Bus50 | 0.277 | 98.109 | -2.3 | 0 | 0 | 0.004 | 0.002 | T-078 SEC7 | -0.004 | -0.002 | 9.2 | 85.0 | |
| Bus52 | 0.277 | 98.109 | -2.3 | 0 | 0 | 0.004 | 0.002 | T-078 SEC8 | -0.004 | -0.002 | 9.2 | 85.0 | |
| Bus53 | 0.277 | 98.109 | -2.3 | 0 | 0 | 0.004 | 0.002 | T-078 SEC8 | -0.004 | -0.002 | 9.2 | 85.0 | |
| Bus54 | 0.277 | 98.109 | -2.3 | 0 | 0 | 0.004 | 0.002 | T-078 SEC8 | -0.004 | -0.002 | 9.2 | 85.0 | |
| Bus55 | 0.277 | 98.109 | -2.3 | 0 | 0 | 0.004 | 0.002 | T-078 SEC8 | -0.004 | -0.002 | 9.2 | 85.0 | |
| Bus56 | 0.277 | 98.109 | -2.3 | 0 | 0 | 0.004 | 0.002 | T-078 SEC8 | -0.004 | -0.002 | 9.2 | 85.0 | |
| Bus57 | 0.277 | 98.109 | -2.3 | 0 | 0 | 0.004 | 0.002 | T-078 SEC8 | -0.004 | -0.002 | 9.2 | 85.0 | |
| BUS-0058 | 12.000 | 103.630 | 0.0 | 0 | 0 | 0 | 0 | COGEN SWGR-MV-01-1 | -1.267 | -2.032 | 111.2 | 52.9 | |
| | | | | | | | | COGEN REACTOR | 1.267 | 2.032 | 111.2 | 52.9 | |
| Bus58 | 0.277 | 98.109 | -2.3 | 0 | 0 | 0.004 | 0.002 | T-078 SEC8 | -0.004 | -0.002 | 9.2 | 85.0 | |
| Bus59 | 0.277 | 98.109 | -2.3 | 0 | 0 | 0.004 | 0.002 | T-078 SEC8 | -0.004 | -0.002 | 9.2 | 85.0 | |
| Bus60 | 0.277 | 98.109 | -2.3 | 0 | 0 | 0.004 | 0.002 | T-078 SEC8 | -0.004 | -0.002 | 9.2 | 85.0 | |
| Bus61 | 0.277 | 98.109 | -2.3 | 0 | 0 | 0.004 | 0.002 | T-078 SEC8 | -0.004 | -0.002 | 9.2 | 85.0 | |
| Bus63 | 0.277 | 98.109 | -2.3 | 0 | 0 | 0.004 | 0.002 | T-078 SEC7 | -0.004 | -0.002 | 9.2 | 85.0 | |
| Bus64 | 0.277 | 98.109 | -2.3 | 0 | 0 | 0.004 | 0.002 | T-078 SEC7 | -0.004 | -0.002 | 9.2 | 85.0 | |
| Bus65 | 0.277 | 98.109 | -2.3 | 0 | 0 | 0.004 | 0.002 | T-078 SEC7 | -0.004 | -0.002 | 9.2 | 85.0 | |
| Bus68 | 0.277 | 98.109 | -2.3 | 0 | 0 | 0.004 | 0.002 | T-078 SEC7 | -0.004 | -0.002 | 9.2 | 85.0 | |
| Bus69 | 0.277 | 98.109 | -2.3 | 0 | 0 | 0.004 | 0.002 | T-078 SEC7 | -0.004 | -0.002 | 9.2 | 85.0 | |
| BUS-0070 | 4.160 | 103.238 | -0.5 | 0 | 0 | 0 | 0 | CP-SWGR-MV-03 | 0.508 | 0.273 | 77.5 | 88.1 | |
| | | | | | | | | CP-XFMR-CHL-01 | -0.508 | -0.273 | 77.5 | 88.1 | |

Figure 60: Load Flow Report produced by ETAP